Hydrogeologic Modelling to Assess Conditions Related to OPG's Proposed Deep Geologic Repository in Tiverton, Ontario

by

Eric A. Sykes

A thesis
presented to the University of Waterloo
in fulfillment of the
thesis requirement for the degree of
Master of Science
in
Earth Sciences

Waterloo, Ontario, Canada, 2007

I hereby declare that I am the sole author of this thesis. This is a true copy of the thesis, including any required final revisions, as accepted by my examiners.
I understand that my thesis may be made electronically available to the public.

Abstract

A Deep Geologic Repository (DGR) for Low and Intermediate Level (L&IL) Radioactive Waste has been proposed by Ontario Power Generation for the Bruce Nuclear site in Ontario Canada. The DGR is to be constructed at a depth of about 660 m below ground surface within the argillaceous Ordovician limestone of the Cobourg Formation. The objective of this thesis is to develop a regional-scale geologic conceptual model for the DGR site and to describe modelling using FRAC3DVS-OPG that provides a basis for the assembly and integration of site-specific geoscientific data. The numerical model is used to explain and illustrate the influence of conceptual model, parameter and scenario uncertainty on predicted long-term geosphere barrier performance. The modelling also provides a framework for hydrogeologic and geochemical investigations of the DGR, serves as a basis for exploring potential anthropogenic and natural perturbations to the DGR system, and demonstrates the long-term stability of the deep system.

In the geologic framework of the Province of Ontario, the Bruce DGR is located west of the Algonquin Arch within the Bruce Mega-Block at the eastern edge of the Michigan Basin. Well logs have been used to define the structural contours at the regional and site scale of the up to 37 units that may be present above the Precambrian crystalline basement rock. The regional scale domain is restricted to a region extending from Lake Huron to Georgian Bay. While the selection of a larger domain might decrease the contribution of boundary condition uncertainty to any uncertainty in any site-scale performance measure, it significantly increases the contribution of the uncertainty in the spatial characterization to the uncertainty of the selected measure. From a hydrogeologic perspective, the domain can be subdivided into three horizons: a shallow zone characterized by the units of the Devonian; an intermediate zone comprised of the low permeability units of the Silurian and the shale units of the upper Ordovician; and a deep groundwater domain or zone characterized by units, such as the Cobourg formation, with stagnant water having high total dissolved solids concentrations that can exceed 200g/l. Hence, the conceptual model of the Bruce DGR site required the development of constitutive models that relate the fluid density and viscosity to the fluid total dissolved solids (TDS), temperature and pressure.

The regional-scale hydrogeologic modelling will help demonstrate that at the proposed repository horizons, there are low energy gradients and that the combination of the low permeabilities and gradients will result in diffusional groundwater systems with favourable retardation properties.

Acknowledgements

There are many people who deserve thanks for the help they provided over the course of my masters thesis. Firstly, I would like to extend my thanks to Ed Sudicky for accepting me as a Masters candidate and for the help and guidance he provided as my supervisor. I would also like to thank Shaun Frape for geological and geochemical insights he gave me, which were greatly beneficial. Stefano Normani, Young-Jin Park and Rob McLaren also deserve great thanks for the immense help they provided for the many technical problems I ran into during the two years. I would also like to thank my friends who helped me stay well caffeinated. Lastly, I would like to thank my mother and especially my father for all of the support and encouragement they gave me over the 2 years.

Thanks and recognition are also extended to Mark Jensen and OPG for proposing this excellent project, aswell as the providing the funding with which to carry it out.

Contents

List of Tables

List of Figures

Chapter 1

Introduction

A Deep Geologic Repository (DGR) for Low and Intermediate Level (L&IL) radioactive waste has been proposed by Ontario Power Generation (OPG) for the Bruce site on the shore of Lake Huron near Tiverton, Ontario (Figure 1.1). The DGR is to be excavated at a depth of approximately 660 m within the argillaceous limestone of the Ordovician Cobourg Formation (Figure 1.2). In order to reasonably assure safety of the radioactive waste at the site and better understand the geochemistry and hydrogeology of the formations surrounding the proposed DGR, a regional-scale numerical modeling study is completed, as reported herein. This numerical modeling study provides a framework to investigate the regional groundwater flow system as it applies and potentially affects the safety and long-term performance of the DGR.

In order to capture and recreate the regional groundwater system, in both near-surface and deep environments, a groundwater model is developed for a fully three-dimensional realization of the bedrock stratigraphy within a portion of South-Western Ontario centred on the Bruce DGR site. From a hydrogeologic perspective, the domain can be subdivided into three hypothetical horizons: a shallow zone characterized by the units of the Devonian that have higher permeability and groundwater composition with a relatively low total dissolved solids content; an intermediate zone comprised of the low permeability units of the Silurian and the formations above the upper Ordovician shales; and a deep groundwater domain or zone characterized by the Ordovician carbonate and shale formations with stagnant water having high total dissolved solids (TDS) concentration that can exceed 200 $\mathrm{g/L}$ with a corresponding specific gravity of 1.2 for the fluids. This deep zone is comprised of the Ordovician, the Cambrian where present and the Precam-

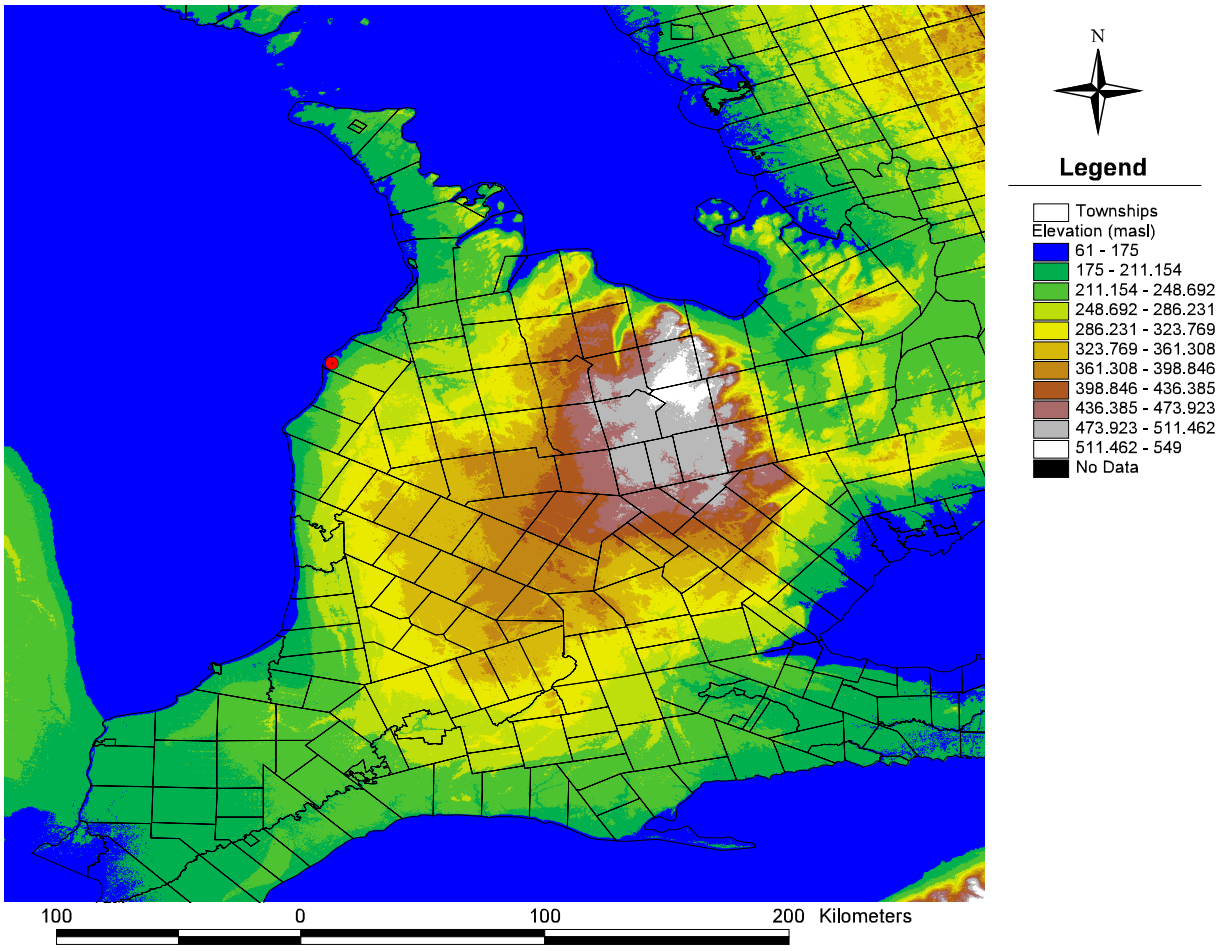

Figure 1.1: Location of proposed DGR site.

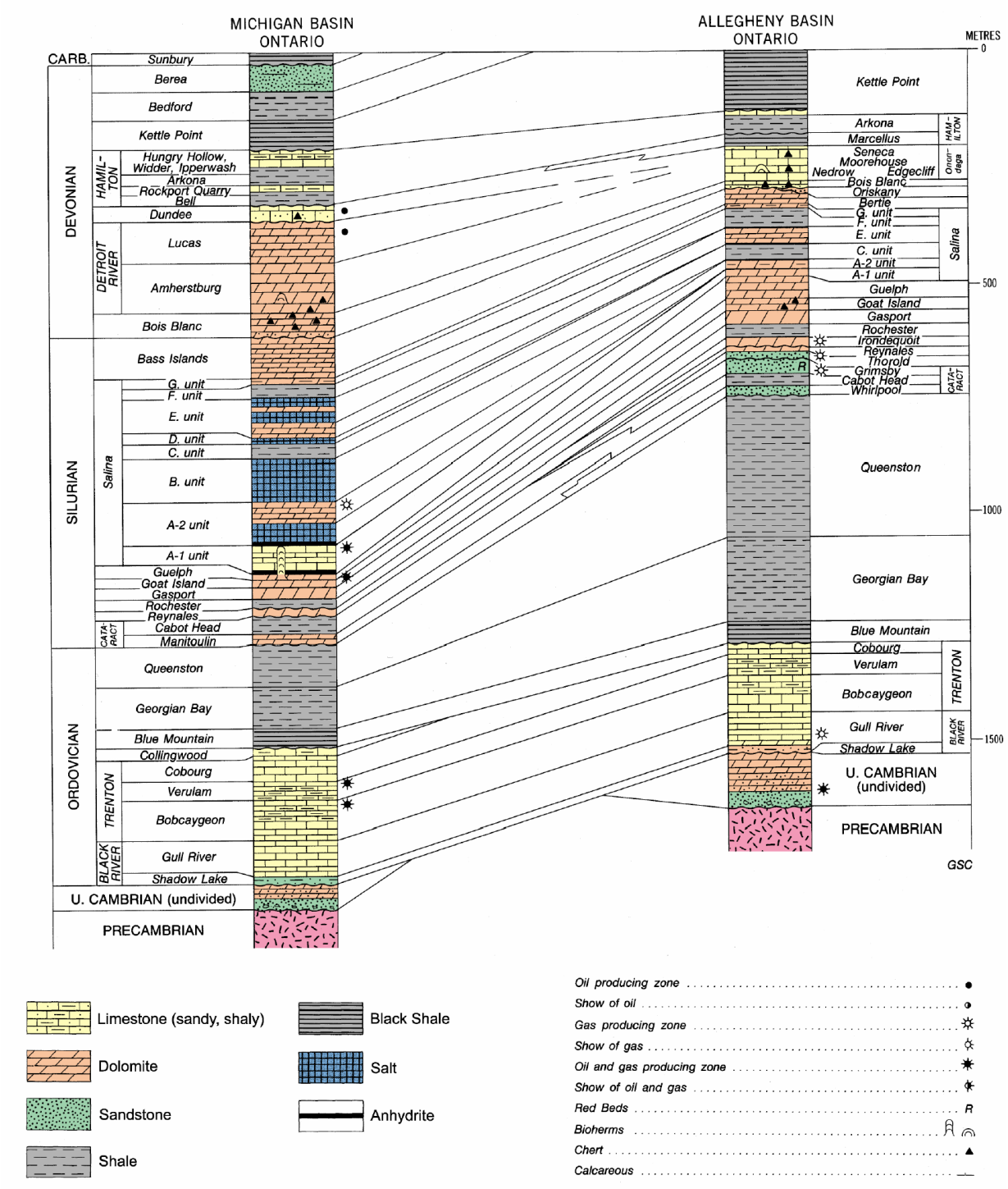

Figure 1.2: Composite stratigraphic columns of southern Ontario from *Mazurek* [2004]

brian (Figure 1.2). The direction of groundwater flow in the shallow zone is strongly influenced by topography thus concurring with the theory of *Toth* [1963] while the low-permeability intermediate zone isolates the deep groundwater domain from the influence of local scale topographic changes. Flow in the deep domain, as it may occur, most likely will be controlled by basin wide topography and potential formational facies changes and balanced by fluid density gradients. As a consequence, any horizontal gradients that govern flow in the deep domain are expected to be low resulting in diffusion dominated flow.

The regional-scale modelling was accomplished using FRAC3DVS-OPG. Developed from FRAC3DVS [*Therrien et al.*, 2004], the model provides a solution of three-dimensional density-dependent groundwater flow and solute transport in porous and discretely-fractured media.

The modelling process requires a large computational effort for this horizontally layered geological sequence. Pre- and post-processors are essential for data interpretation, synthesis, manipulation, management and visualization. ArcGIS is an important tool for data visualization.

1.1 Geologic Framework

The Michigan Basin is a sedimentary geological feature found in the Southern peninsula of Michigan, Southern Ontario as well as a few states surrounding Michigan (Figure 1.3). The northern edge of the Michigan Basin rim is defined as the areas where the depositionally continuous basal Paleozoic sediments come in contact with older rocks of Precambrian age [*Stonehouse*, 1969]. In Southern Ontario, the Michigan Basin is bounded to the east by the Algonquin Arch. The Algonquin Arch is a feature in the crystalline basement rock that trends NE-SW [*Mazurek*, 2004]. The Algonquin Arch ranges in elevation from approximately 300 m where it outcrops to -1000 m at the Chatham Sag. South of the Chatham Sag, the Michigan Basin is bounded by the Findlay Arch [*Ellis*, 1969]. The Findlay Arch is the southern continuation of the Algonquin Arch.

In general, Southern Ontario can be divided into two separate fracture systems, or megablocks [*Sanford et al.*, 1985]. The Megablocks have been named the Niagara Megablock and the Bruce Megablock (Figure 1.4) and are divided by the Algonquin Arch. The proposed location for the DGR places it in the Bruce Megablock. One of the primary differences between the Bruce and Niagara Megablocks is the fracture lineament patterns. The Bruce Megablock has a less

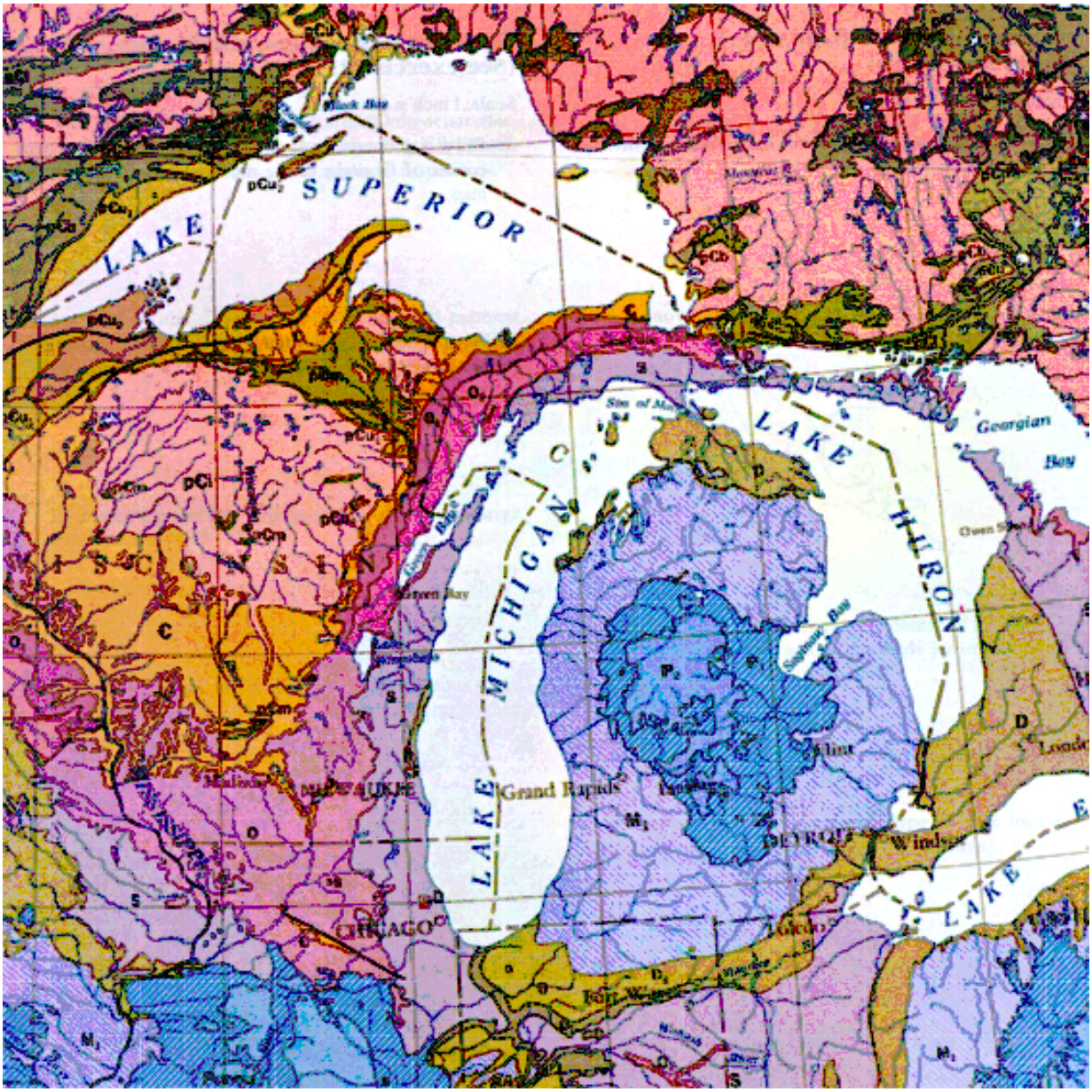

Figure 1.3: Spatial extent of Michigan Basin.

dense lineament pattern for the fractures than that of the Niagara Megablock. In the Niagara Megblock, the intersection of the fracture lineaments act as oil traps and are frequently found to contain petroleum and natural gas reserves; however, borehole tests indicate that the Bruce Megablock is devoid of natural gas or petroleum products.

The suitability of a sedimentary formation as a horizon for a potential repository depends on many criteria, such as a low energy gradient with this being the sum of the flow energy or pressure gradient and a potential energy gradient. The potential energy gradient is given in terms of a density gradient and a gravitational gradient. Other criteria include sufficient depth below surface in a geologic unit with thickness, lateral contiguity and simple internal homogeneity and favourable retardation properties [*Mazurek*, 2004]. The regional-scale hydrogeologic modelling will help demonstrate that at the proposed repository horizons, there are low energy gradients and that the combination of the low permeabilities and gradients will result in diffusional groundwater systems with favourable retardation properties.

1.2 Regional-Scale Conceptual Model

The regional-scale groundwater model can be described as having an upper and lower flow regime separated by the intermediate regime. The upper flow regime is restricted to units above the Salina Formation. This is because the low hydraulic conductivity of the Salina Formation restricts near surface groundwater from penetrating to greater depths. The upper flow regime therefore mimics the topography according to *Toth* [1963], flowing from the highlands of the Niagara Escarpment to Lake Huron.

The lower flow regime is found beneath the Silurian sediments. Based on the conceptual model used in this study, there is little hydraulic connection between the deep geologic formations with the near-surface units. The horizontal energy gradients at depth are expected to be very low. The only location for groundwater recharge into the rocks of the lower flow regime will be where they outcrop because the intermediate regime, where present, acts as an aquaclude, preventing connection to surface recharge.

In order to determine the maximum energy gradient found in the deeper units, the lake elevations (Figure 1.5) must be studied. The highest possible elevation gradient throughout the Great Lakes region would be between Lake Superior and Lake Ontario, which have a difference in

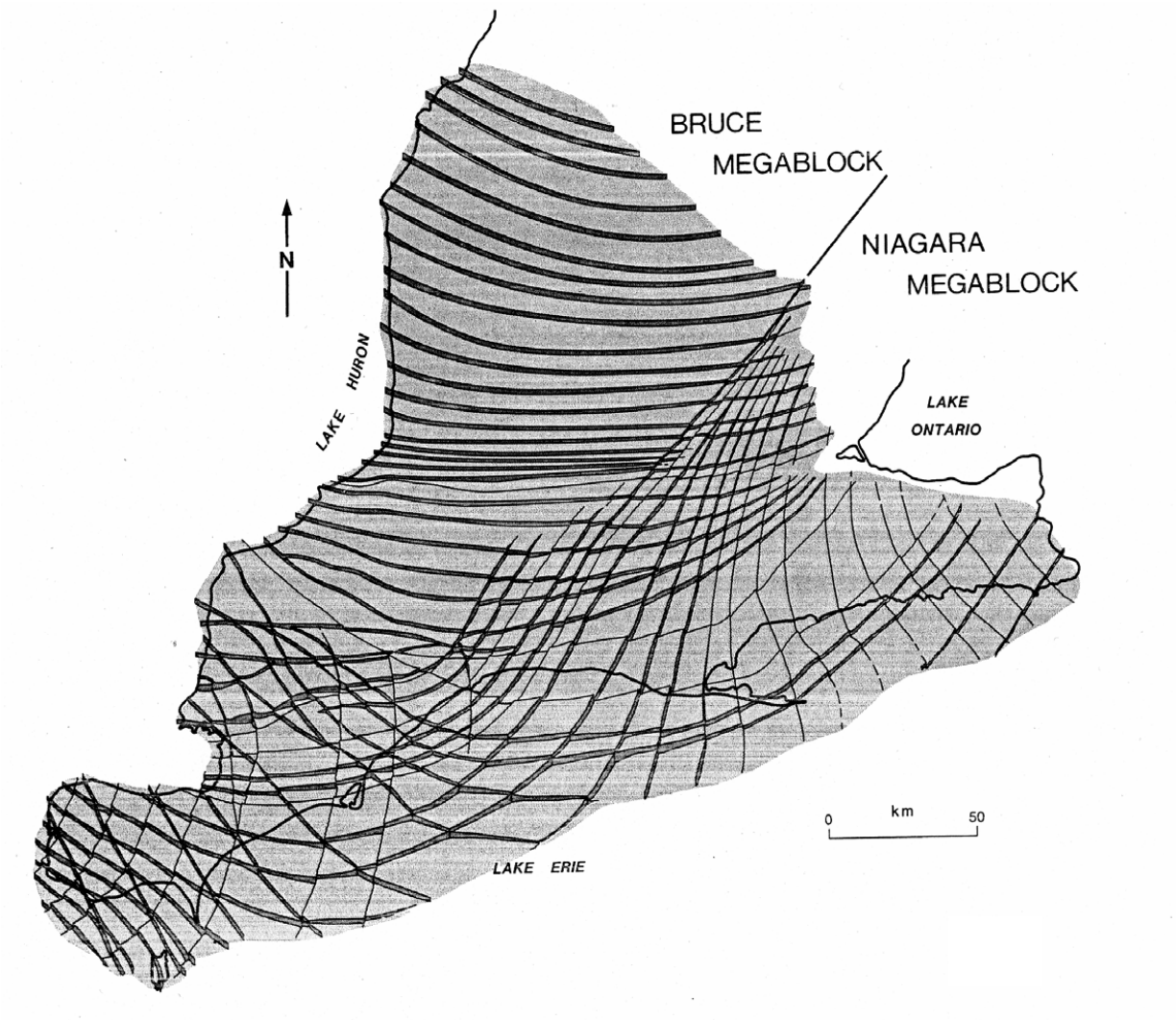

Figure 1.4: Bruce and Niagara megablocks with fracture lineaments [*Sanford et al.*, 1985].

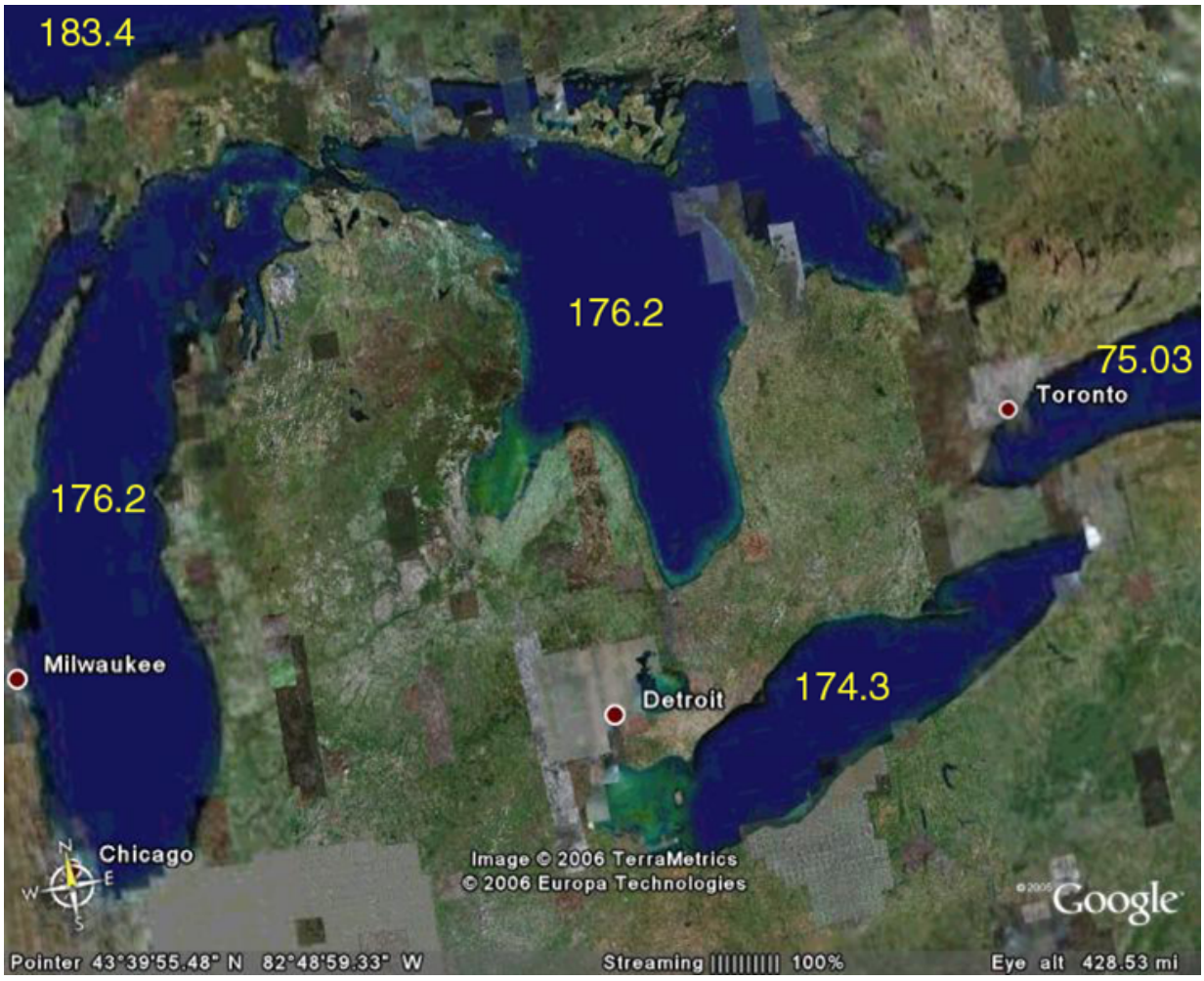

Figure 1.5: Lake elevations (m)

elevation of approximately 108 m. Although the head difference between these lakes is considerable, the substantial distance between them would result in a negligible potential energy gradient. When assessing the possible gradient between Lake Michigan and Lake Huron, the identical surface water elevation would prevent any gravity potential energy gradient from occurring between them.

The negligible potential energy gradients that occur between the Great Lakes surrounding the Michigan Basin, will be reduced due to the presence of the dense saline groundwater found within the formations of the lower flow regime. Where these units outcrop at recharge areas, there will be a potential for fresh water to infiltrate the geologic units and displace higher density water until there is a balance between the elevation gradient and the density gradient. At this equilibrium point, the energy gradient will approach zero. With the dense brines, there will be associated higher viscosities which will act to further impede flow. The combination of the negligible horizontal energy gradients with the dense brines and low permeabilities in the lower groundwater regime will then force the system at depth to become diffusion dominated.

On the basis of the negligible energy gradients expected within the lower flow regime, it is then possible to limit the spatial extent that will be modelled to include a section of the Michigan Basin, as opposed to the basin as a whole. The stagnant flow regime can be replicated independent of the extent of the spatial domain provided that the domain includes appropriate recharge zones for the units that have high total dissolved solids concentrations.

The boundaries of the conceptual model (Figure 1.6) were defined using the following criteria. The south-eastern portion of the conceptual model boundary lies such that it follows the regional surface water divides surrounding the Bruce site. The surface water divide was determined by using a DEM derived from data from NASA's Shuttle Radar Topography Mission (SRTM) and a river maps in ArcGIS (Figure 1.6). With the assumption that the groundwater system is a subdued reflection of topography, the divide boundary conditions would only apply to the upper groundwater regime. The domain includes the local topographic high in Southern Ontario. The model domain extends to the deepest portion of both Lake Huron and Georgian Bay. The bathymetric map was used to define the model boundaries in these areas. The eastern boundary of the domain is west of the Algonquin Arch.

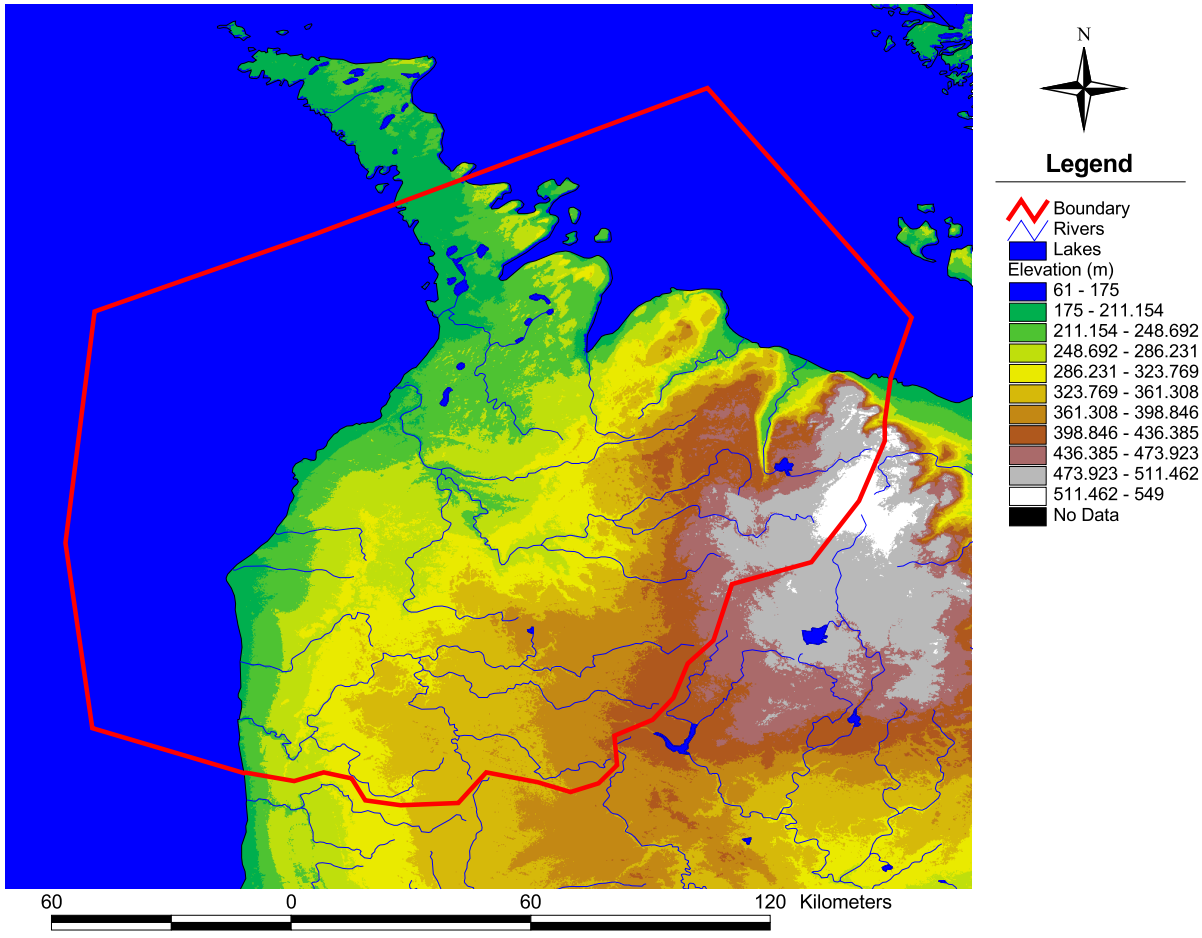

Figure 1.6: Regional scale elevations and river courses

1.3 Scope and Objectives

The objective of the regional-scale groundwater modelling study as part of the geosynthesis program and site characterization is to assist in presenting the safety case for the proposed Bruce Deep Geologic Repository. This assistance is provided by characterizing and analyzing the groundwater flow system in the deep geologic formations by creating a robust numerical groundwater model. In order to properly characterize the flow in the deep geological units, it is especially pertinent to ensure that the basis for the numerical model is developed from sound geologic interpretations and models. This will ensure an accurate distribution of unit properties such as permeability for an appropriate realization of the domain geometry. The distribution of permeability is of importance due to the safety case requirement of sufficient thickness and lateral contiguity and predicability of the geologic units that may be potentially impacted by the proposed repository.

Argillaceous media are being considered by many countries as potential host rocks for radioactive waste. Numerical modelling, whether as part of site-characterization, geosynthesis, performance assessment or safety assessment, provides an important tool in the evaluation of the features, events and processes that may be relevant to the long-term safety of a repository. The modelling requires a sound understanding of the basic physical and chemical processes that govern water and solute transport through the host media. A framework that facilitates the evaluation of the suitability of a proposed repository involves the development and the use of FEPCATs, with this being an acronym for "features, events and processes catalogue" [*Mazurek*, 2003]. For the short term concerns of a system hosted in argillaceous media, there are three separate FEPCATs that are relevant to this thesis with these being transport mechanisms, retardation mechanisms and paleohydrogeology. Following *Jensen* [2007], a further description of these concerns is presented in the following paragraphs.

Transport of a radionuclide within and from a deep geologic repository occurs by a number of possible transport mechanisms, and it is counteracted by a number of retardation mechanisms [*Mazurek*, 2003]. Numerical models, laboratory experiments and field experiments are components that are considered in the assessment and resolution of transport and retardation mechanisms. The transport mechanisms and factors or processes that influence it include:

- Stratigraphy/hydrostratigraphy - predictability/homogeneity/bedrock layering (3-D Geom-

etry)

- Hydraulic gradients - gravity, density, anomalous
- Hydraulic conductivities - extremely low; anisotropic, inter-formational/intra-formational
- Hydrogeochemistry - brine viscosity; formation distinct pore fluid compositions (elemental/isotopic), scale dependency (laboratory (cm) vs. field scale (10s m))
- Diffusivities - Cobourg/Ordovician shales (i.e. pore geometry/connectivity, porosity, pore space, anisotropy)
- Structural geology - geometry of regional/local scale discontinuities
- Colloid transport - qualitative statement on principles, process and likelihood

The parameters and features that are relevant in the determination of the retardation mechanisms that counteract transport include:

- Grain size distribution/mineralogy
- Pore water composition (inorganic/organic)
- Dissolution/precipitation of secondary mineral phases
- Matrix diffusion where fracture flow occurs

Numerical modelling at both the regional-scale and the site-scale plays an important role in demonstrating and illustrating the transportation and retardation mechanisms. This thesis will contribute to the assessment of these mechanisms through the use of the model FRAC3DVS-OPG to demonstrate and illustrate:

- Flow, transport or time domain probability estimates of particle residence time in the regional flow system based on estimates of the transport mechanisms of advection, dispersion and diffusion
- Flow system anisotropy at inter-/intra-formational scale

- Influence of variable density flow (i.e. horizontal stratification)
- Influence of basin hydrostratigraphy and geometry on 'absence' of exfiltration zones
- Migration of unretarded/non-decaying environmental isotopes within the subsurface
- Role/implications of sub-vertical transmissive feature in variably dense groundwater flow domain

The evaluation of a feature or process using numerical models can be accomplished using, in part, a sensitivity analysis that estimates the change in a system performance measure to changes in a system parameter. These estimated sensitivity coefficients are local derivatives evaluated in terms of the base case parameters that describe the system. The robustness of the sensitivity coefficients for large changes or perturbations of parameters also can be assessed. The performance measures that can be used to characterize the system can include, but are not restricted to:

- Darcy fluxes and average linear velocities for both steady-state and transient, density-dependant flow
- Salinity and environmental isotope concentrations
- fluid pressures and energy gradients for both steady-state and transient, density-dependant flow
- Time domain probabilities of fluid particle residence times
- Flow system discharge

Regional-scale modelling can provide the framework for the assessment of paleo-hydrogeology. Based on the work of *Peltier* [2002, 2003] it is clear that to credibly address the long-term safety of a deep geologic repository, long-term climate change and in particular a glaciation scenario, needs to be incorporated into performance assessment modelling activities. In addition, by simulating flow system responses to the last Laurentide (North American) glacial episode, insight is gained into the role of significant past stresses (mechanical, thermal and hydrological) on determining the nature of present flow system conditions, and by extension, the likely impact of

similar, future boundary condition changes on long-term flow system stability. The Wisconsinian glacial episode, that occurred over a 120 000 year time period, included at least three cycles of glacial advance and retreat, with maximum ice thickness over the Southern Ontario DGR site reaching more than 2 km. Between glacial episodes were extensive periods of transient, peri-glacial conditions during which permafrost could impact the subsurface to several hundreds of metres. Near the end of a glacial episode, significant basal meltwater production occurred. This thesis will restrict itself to the development of a model domain and parameters that will provide a framework for subsequent assessment of paleo-hydrogeology. This future assessment can include:

- Evaluating the expected flow system perturbation by glacial events (boreal, peri-glacial or ice sheet)
- Assessing the depth of penetration by glacial meltwaters into Palaeozoic formations
- Illustrating numerically the transient influence of glacial event(s) on the Bruce site flow system
- Estimating pore fluid residence times during Quaternary glacial events

The regional-scale modelling of the Bruce DGR site using FRAC3DVS-OPG is restricted to isothermal flow. The extent of the regional domain is defined in Figure 1.6. Analyses include both steady-state, density independent flow and transient flow that couples the density dependent flow equation with the appropriate equation that describes the transport of the total dissolved solids within the system domain. The assessment of the impact of parameter perturbations on system performance measures that can include fluid pressure, fluid velocity, groundwater life expectancy and groundwater age will be accomplished using a sensitivity derivative framework. The base case parameters that describe the regional domain are dependant on the geological and geochemical framework described in Chapter 2. The elements of FRAC3DVS-OPG that are relevant to the regional scale modelling are described in Chapter 3. The regional scale groundwater flow conceptual model is detailed in Chapter 4. The analyses of the regional scale model are developed in Chapter 5 while conclusions are presented in Chapter 6.

Chapter 2

Geological and Geochemical Framework

2.1 Geological History

The depositional sequence observed in Southern Ontario was developed by the accumulation of sediments upon the Precambrian basement rock Figure 1.2. The rocks of Precambrian age that are found in Southern Ontario are predominately granitic gneisses, amphibolite, quartzite, marble and metamorphosed conglomerate [*Winder and Sanford*, 1972]. These rocks are all associated with the Canadian Shield.

The Cambrian rocks are comprised of two formations. The deepest or first Cambrian Formation is the Mount Simon Formation. It consists of grey orthoquartizitic sandstones and arkosic conglomerates towards the base of the formation. The second Cambrian aged formation that is found west of the Algonquin arch is the Eau Claire formation which consists of the shaly and oolitic dolostones [*Winder and Sanford*, 1972]. The Cambrian sediments are not continuous throughout the regional model domain [*Sanford et al.*, 1985].

The Cambrian sandstones and dolostones are succeeded in the stratigraphic sequence by rocks of Ordovician age. When the Cambrian rocks are not present, the Ordovician sediments directly overlay the Precambrian basement rock. The first group of Ordovician age is the Black River Group. This group consists of the Shadow Lake, Gull River and Coboconk Formations. The first formation, Shadow Lake, represents the first deposited in the middle Ordovician [*Sanford*, 1961]. The Shadow Lake Formation in the area of Bruce County consists of red shales, with the red colour being attributed to small amounts of reddish quartz sandstone [*Sanford*, 1961].

The shales of the Shadow Lake Formation also possess limestone interbeds [*Sanford*, 1961]. The Shadow Lake Formation is also absent in some wells.

The second geological formation that comprises the Black River group is the Gull River Formation. The Gull River Formation consists of a brown limestone with finely crystalline dolostone interbedded [*Sanford*, 1961]. At many locations in Ontario, complete dolomitization of the formation has been observed [*Sanford*, 1961]. Cores demonstrate that the Gull River Formation rests upon either the Cambrian units, or in their absences, the Precambrian gneisses [*Sanford*, 1961].

The third and final formation of the Black River Group is the Coboconk Formation. The Coboconk Formation consists of a buff to buff-brown and tan coloured limestone with a finely crystalline to granular texture [*Sanford*, 1961].

Above the Black River Group, the next geological group is the Trenton Group. The Trenton Group includes the Kirkfield, Sherman Fall and the Cobourg Formations. The first formation, found at the base of the Trenton Group is the Kirkfield Formation. The Kirkfield Formation comprises the beds found between the Coboconk Formation of the Black River Group and the Sherman Fall Formation of the Trenton Group [*Sanford*, 1961]. The Kirkfield Formation consists of greyish brown limestone that grades upward to a dark grey shaly limestone. The Kirkfield grades down further to shale at the base of the Formation [*Sanford*, 1961].

The Sherman Fall Formation overlies the Kirkfield Formation in the Trenton Group. The Sherman Fall Formation includes all rock beds found between the Kirkfield and the Cobourg Formations [*Sanford*, 1961]. The Sherman Fall Formation is composed of grey to grey-buff, finely crystalline to fragmented limestone [*Sanford*, 1961]. The limestone contains a high frequency of shale partings and interbedded grey shale.

The upper formation of the Trenton Group is the Cobourg Formation. The Cobourg Formation is defined as being the rock beds that lay upon the grey fragmented limestone of the Sherman Fall Formation and lie beneath the Collingwood Formation [*Sanford*, 1961]. The Cobourg Formation is composed of a brown to dark brown or greyish brown, finely crystalline to subaphanitic limestone that has occasional shale partings [*Sanford*, 1961]. The Cobourg Formation is the proposed horizon for the DGR [*Intera Ltd.*, 2006].

The formation that follows the Cobourg is the late Ordovician age Collingwood Formation and it is described as being dark brownish grey to black, fissile, bituminous and pyritiferous

shale [*Sanford*, 1961]. The Collingwood Formation grades upwards to a dark grey shale with dark brownish grey bituminous shale interbeds [*Sanford*, 1961].

The Georgian Bay Formation lies above the Collingwood. It is composed of grey to dark grey, soft fissile shale containing occasional laminations of grey argillaceous and silty limestone [*Sanford*, 1961]. The Georgian Bay Formation varies in thickness from 14 m to 121 m [*Sanford*, 1961].

The Queenston Formation, containing the youngest Ordovician strata in Southern Ontario, is comprised of red and maroon siltstones and shales [*Winder and Sanford*, 1972]. The Queenston Formation thins northwestward.

The Silurian sediments comprise the intermediate groundwater domain. The first sediments in this regime are comprised of the lower Silurian Manitoulin dolostones and the shales of the Cabot Head Formation. The lower hydrostratigraphic regime is created in part by the low hydraulic conductivities of the the intermediate groundwater domain, specifically the overlying horizontally bedded Salina Formation, .

The middle Silurian consists of gradational dolostones of the Reynales and Fossil Hill formations, the dolomitic shales of the Rochester Formation, the white crinoidal dolostones of the Gasport formation, the cherty dolostones of the Goat Island and the Guelph Formation [*Winder and Sanford*, 1972]. The Guelph Formation consists of thick carbonate rocks that form a reef complex.

The younger Silurian Formations are comprised of the Salina and the Bass Island Formations. These formations consist of sequences of dolostones, limestones, salt anhydrite, gypsum and shale [*Winder and Sanford*, 1972]. The Salina Formation is subdivided into eight members which are in order of succession A-1, A-2, B, C, D, E, F, G. Members B and D are comprised entirely of salt. Members A-1, A-2 and F contain considerable salt interbedded with dolostones. The Bass Island Formation that supersedes the Salina Formation is comprised of dolostone [*Winder and Sanford*, 1972]. The evaporite and shale member beds in the Salina Formation will form a major barrier impeding the vertical hydraulic connection of deeper geologic formations with shallower formations.

Above the Bass Island Formation are the Devonian age formations, the first of which is the Bois Blanc Formation. The Bois Blanc Formation is a blue-grey finely crystalline, silty, granular dolomitic limestone [*Winder and Sanford*, 1972].

The Bois Blanc Formation is then overlain by an alternating series of limestones and dolostones. This succession is what comprises the upper hydrostratigraphic regime. The series begins with the dolostone of the Amherstberg Formation and is followed by microcrystalline dolostone of the Lucas Formation [*Winder and Sanford*, 1972]. Lying atop the Lucas Formation is the Dundee. The Dundee Formation is composed of fine to medium crystalline limestone. The Dundee then lies beneath sequences of glacial deposits.

2.2 Geological Reconstruction

One of the foci of this project was to create a three-dimensional geological framework that will form the basis of the numerical groundwater model. The geological framework consists of a three-dimensional reconstruction of the geology of a portion of Southern Ontario within the range of the computational domain. To facilitate the modelling of the geology, data for more than 50,000 boreholes in Southern Ontario were obtained from the Ontario Oil, Gas and Salt Resource (OGSR) Library in London, Ontario (Figure 2.1). The borehole data consisted of a series of databases that included geologic formation description, contact depth, ground surface elevation as well as the spatial coordinates for each associated borehole. The OGSR data contained some possible inconsistencies. The potential inconsistencies in the borehole data included uncertain ground elevations and locations and alternative interpretations of the presence of various geologic units in certain boreholes. For this study, the raw borehole data was screened and classified. The Microsoft Access relational data base system was used as a tool to facilitate the assessment of the OGSR data. Data from queries were sorted to determine anomalies. The contouring of data using Tecplot facilitated visual inspection. The correlation structure of data such as unit thickness was determined using the Geopack kriging program [*Yates and Yates*, 1989].

Due to the large number of boreholes that were to be included within the geologic reconstruction, only the 10 boreholes proximal to the proposed Bruce DGR site were analyzed in detail to assess the accuracy of the formation contact depths. It was observed that there were instances where units, such as the Cambrian, may not be present in wells that otherwise penetrate the underlying Precambrian surface Figure 2.2. This absence could be attributed to differences in stratigraphic nomenclature conventions used by the technician logging the core. However, the geologic model put forth by *Sanford et al.* [1985]indicates that the Cambrian is absent over the

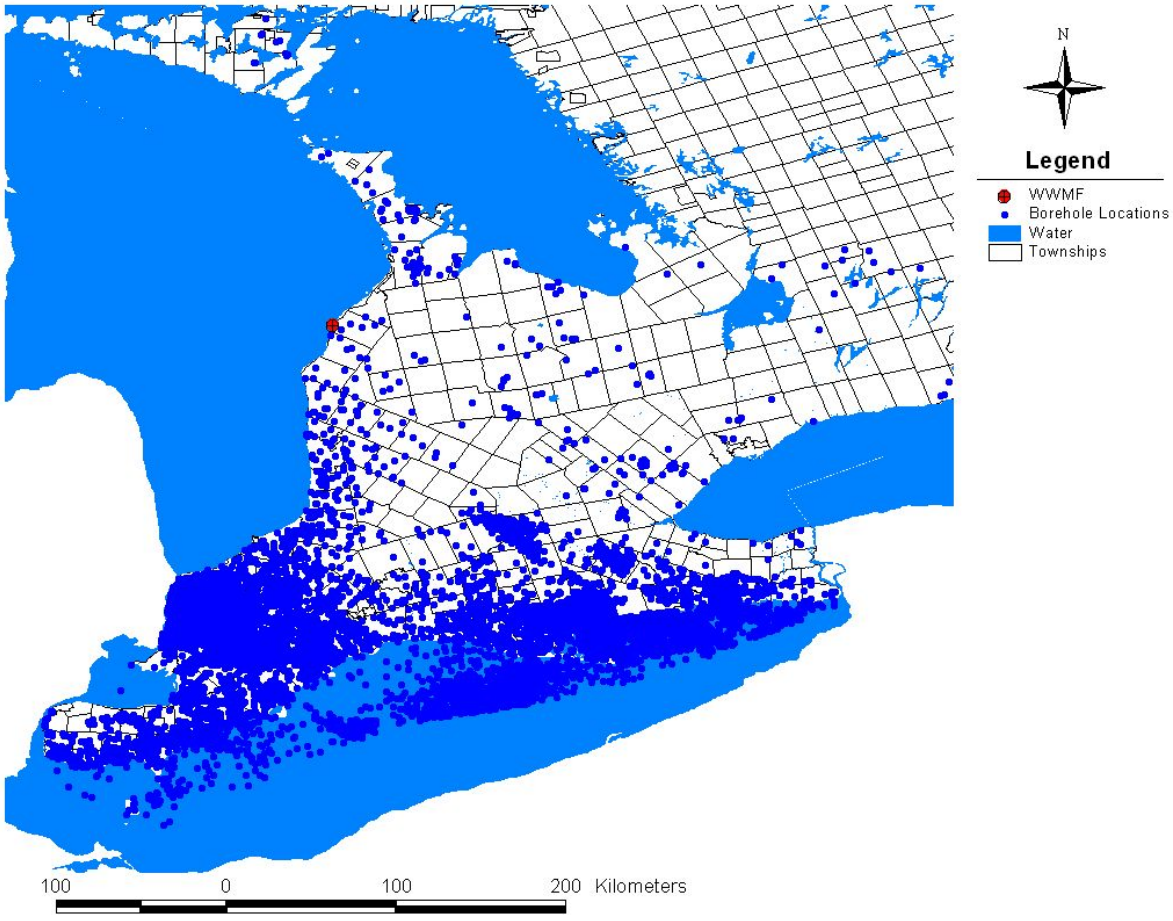

Figure 2.1: Location of OSGR boreholes.

Algonquin Arch.

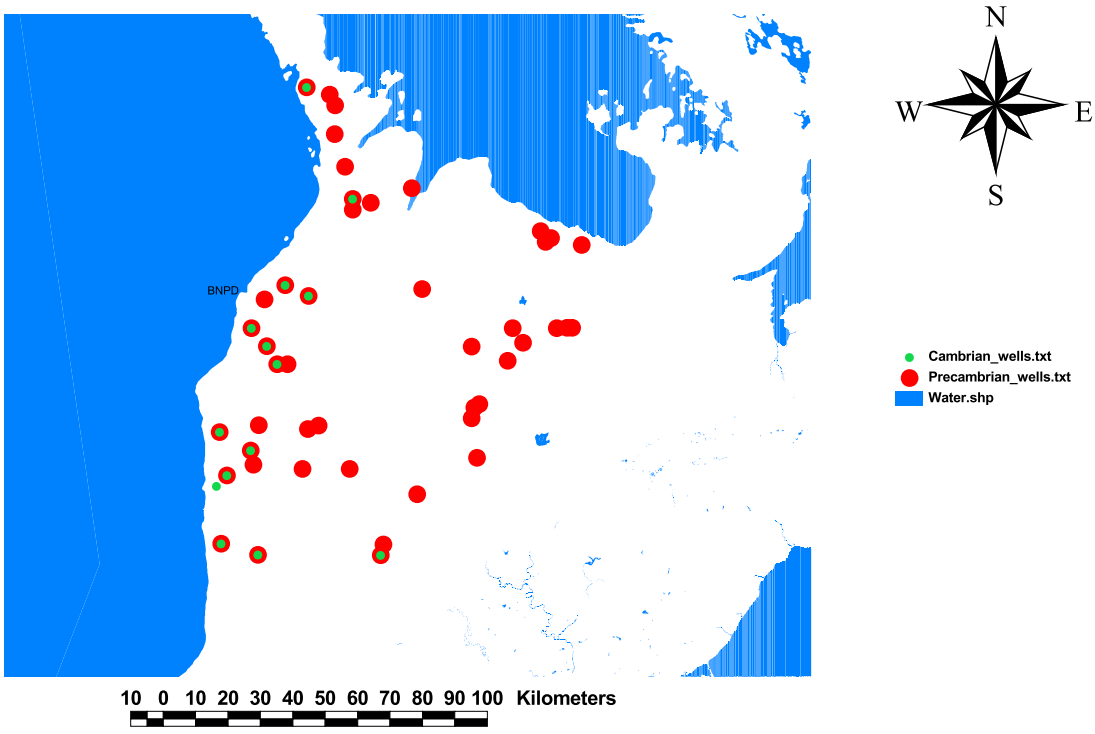

Figure 2.2: Location of wells intersecting Cambrian and Precambrian formations.

Although the structural contacts for only the closest 10 boreholes were rigourously analyzed, it is still possible to obtain a gauge of the data quality by applying a kriging geostatistical analysis of the data. In order to perform this, the Ordovician shales and limestones (key marker beds) were selected. The Ordovician units are continuous across the regional model domain and they are characterized by low permeabilities. As the host geologic unit for the Bruce DGR, the continuity of their properties and characteristics is important. The Queenston, Georgian Bay/Blue Mountain and Collingwood formations comprised the Ordovician shales, while the Cobourg,

Sherman Fall, Kirkfield, Coboconk and Gull River comprised the Ordovician limestones. A separate analysis of the Cobourg was also undertaken. The data for the formation thicknesses were analyzed using Geopack. The steps of the analysis include determination of variograms for thickness, the determination of a model for the variogram, cross-validation to ensure that a best-fit of the model to the variogram data is obtained and finally estimation of the spatial distribution of thickness and variance of thickness over the regional model domain. The use of Microsoft Access facilitated the determination of the statistics for the selected units. The results from this analysis are presented in Table 2.1. The statistics that were calcutated were the mean thickness (m), the standard deviation (m), the minimum thickness (m) and maximum thicknesses (m). Table 2.1 also identifies the type of variogram used, as well as the calculated nugget. A Gaussian semi-variogram model provided a best fit for the Ordovician shale while spherical and linear models provided the best for the Ordovician Limestone and Cobourg unit respectively. The semi-variogram model parameters are nugget, sill nugget and range. The nugget parameter is an estimate of the variance in the data that are separated by small distances. For larger separation distances, the sill nugget provides an estimate of the variance in the data in excess of the nugget. The sill or maximum variance in the model is determined as twice the sum of the nugget and the sill nugget and occurs at the distance given by the range. Data can be considered to be uncorrelated at separation distances greater than the range. Also shown in Table 2.1 are the measured thicknesses of the units from the Bruce DGR field program.

The nugget can be used as a measure of spatial variability between points within the data set. A large nugget implies that for the given dataset, there is a large amount of uncertainty in the ability to predict the thickness of the unit at a given distance from a known location. The Ordovician shales and limestones have nugget effects that vary between 5998 m^2 and 10 877 m^2. This implies that the thickness of the unit is highly variable, and the ability to accurately predict the thickness of the unit between data points is limited. However, while the variance of the thickness of the units at locations between punctual data points can be estimated, the statistics for the units as shown in Table 2.1 indicate that the units are continuous across the model domain. The units are present in all OGSR wells located south-west of the units outcrop. The minimum thicknesses of the units are associated with wells that are located in the vicinity of the outcrop. Wells that are closer to the Bruce DGR were associated with estimates that are close to or exceed the mean thickness for the unit. Thus, the estimate of the minimum thickness and properties

Table 2.1: Statistical properties of the Ordovician shale and limestone units

	Shale	**Ordovician Limestone**	**Cobourg**
Number of Wells	45	37	59
Mean Thickness (m)	183.0 (205.0)*	192.7 (191.8)*	97.4 (43.0)*
Standard Deviation (m)	67.4	49.2	108.7
Minimum Thickness (m)	9.2	133.2	0.01
Maximum Thickness (m)	271.3	312.7	332.2
Variogram Model	Gaussian	Spherical	Linear
Nugget (m^2)	2553	473.4	10 877.86
Sill Nugget (m^2)	5998	1932.0	3372.3
Range (m)	91 116	7540.4	145 326
SSQ	6.533×10^5	4.615×10^5	3.4188×10^8

*thickness of units at DGR1 and DGR2

close to the Bruce DGR site are very significant. From a groundwater flow perspective, the fluid flux in a unit is a product of an energy gradient, the unit permeability and the unit thickness. It is without question that there is the potential for greater variability in the formation or unit permeability than there is in the unit thickness. The possible range in permeability can be an order-of-magnitude or more while the range in the thickness will be a single digit factor.

The semi-variogram data and Gaussian model for the Ordovician shale thickness are plotted in Figure 2.3. The kriged values of mean and variance for the regional-scale model domain are plotted in Figure 2.4 and Figure 2.5 respectively. The black markers on the contour plots indicate the location of the OGSR wells used in the statistical analysis. When the mean shale thickness is analyzed spatially (Figure 2.4), one of the most noticeable trends is that the areas beneath Lake Huron and Georgian Bay both tend toward the mean thickness for the data set. Areas closer to the borehole locations will have a mean thickness closer to the measured value. Outside of the range, the thickness is then approximated with the mean.

The nugget effect in the data is confirmed when the the variances of the units are plotted spatially. For the Ordovician shales (Figure 2.5), areas with low variances can be correlated to the high density of data points, but further away from the data points, a higher variance is estimated. It is important to note for the figure that areas with high variance are found where

the Great Lakes occur. This high variance is evidence of the difficultly of extrapolating beneath Lake Huron and Georgian Bay.

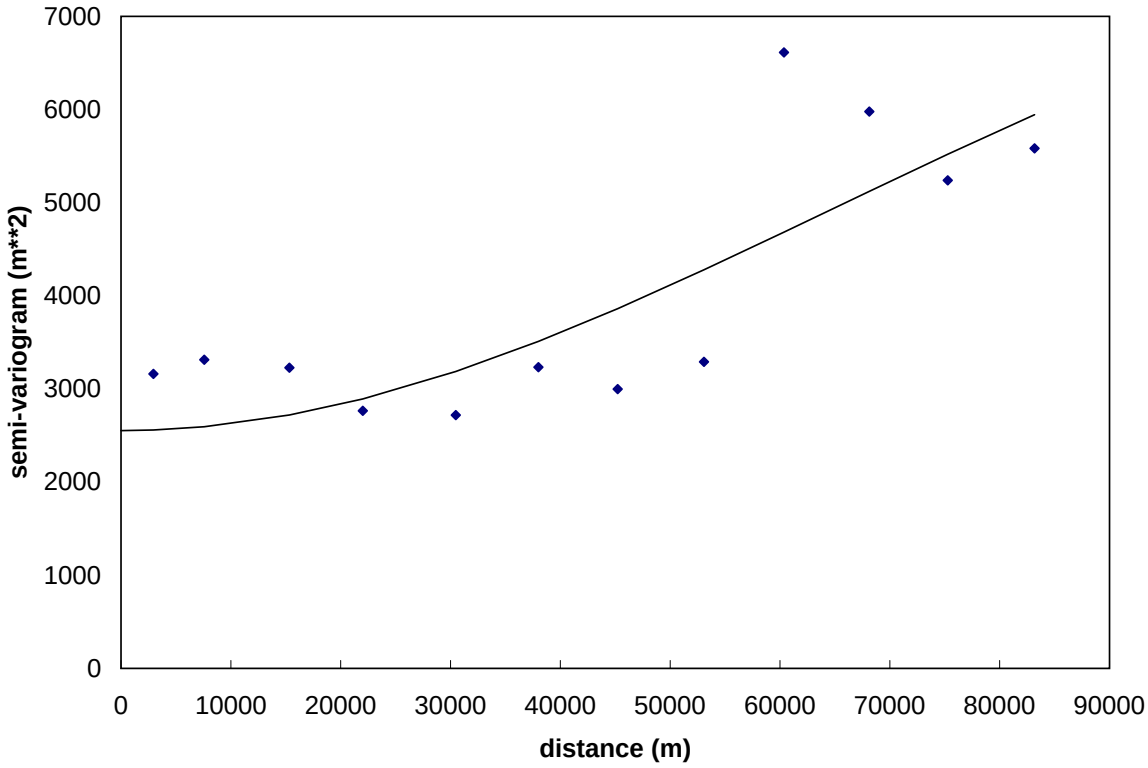

Figure 2.3: Semi-variagram for Ordovician shale thickness.

The semi-variogram data and spherical model for the Ordovician limestone thickness are shown in Figure 2.3. The kriged mean and variance of the limestone thickness are plotted in Figure 2.7 and Figure 2.8 respectively. Because the range for the Ordovician limestone is fairly small compared to that of the shale, the majority of the domain will have estimates that are the mean thickness (refer to Figure 2.7). Figure 2.8 shows the spatial variance of the Ordovician limestone thickness. The smaller range for the uncertainty results in the sill variance being estimated for most of the model domain. The smaller range of 7540 m for the limestone formations, compared to 91 116 m for the shale, is what results in the circular patterns on the figure. Areas within the domain that do not fall within 7.5 km from a data point will have a high variance.

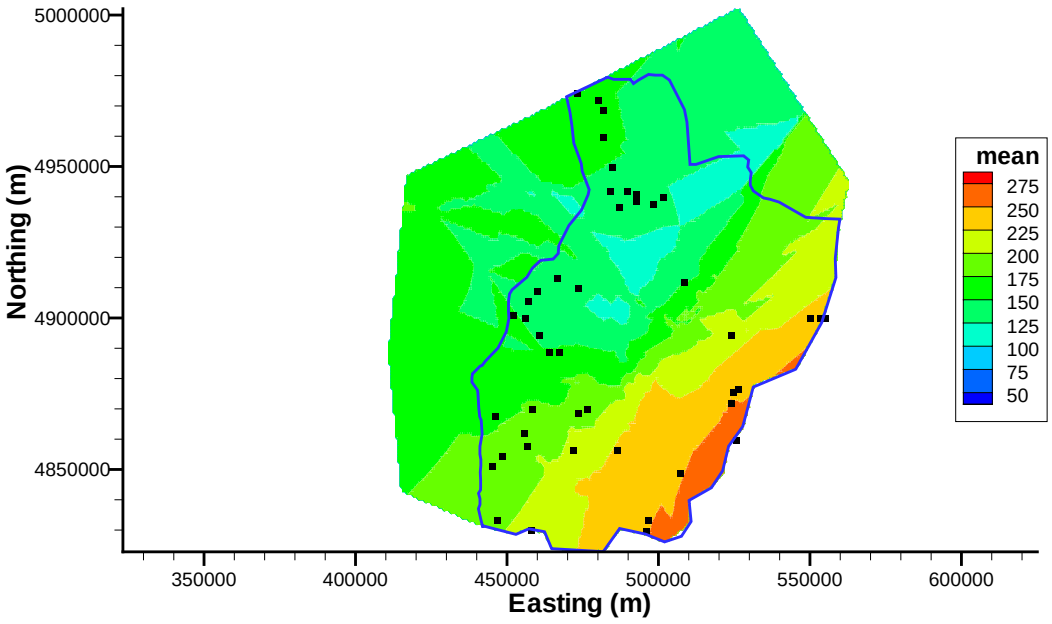

Figure 2.4: Spatial distribution of the mean thickness of the Ordovician shales.

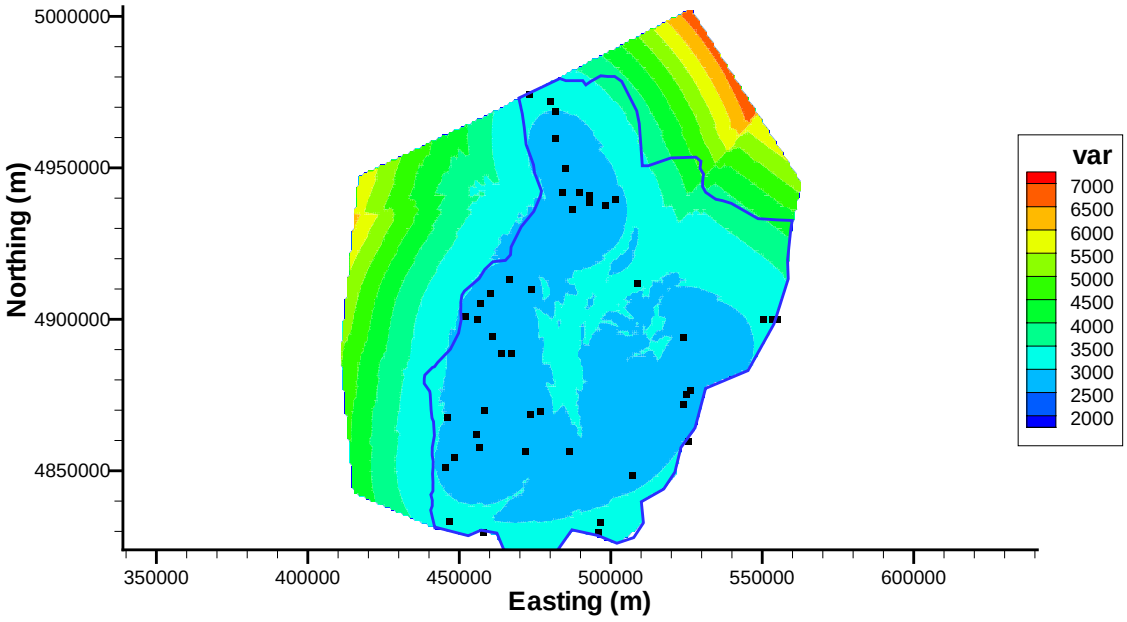

Figure 2.5: Spatial variance of the thickness of the Ordovician shales.

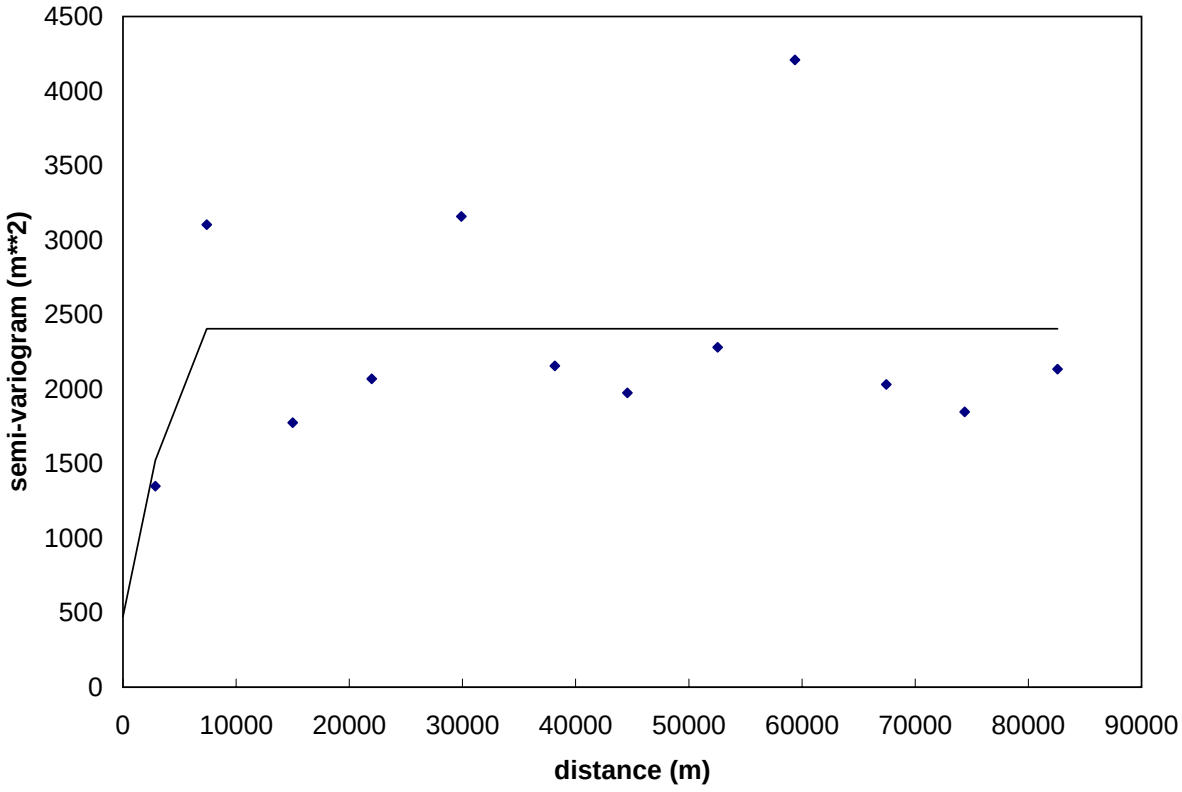

Figure 2.6: Semi-variagram for Ordovician limestone thickness.

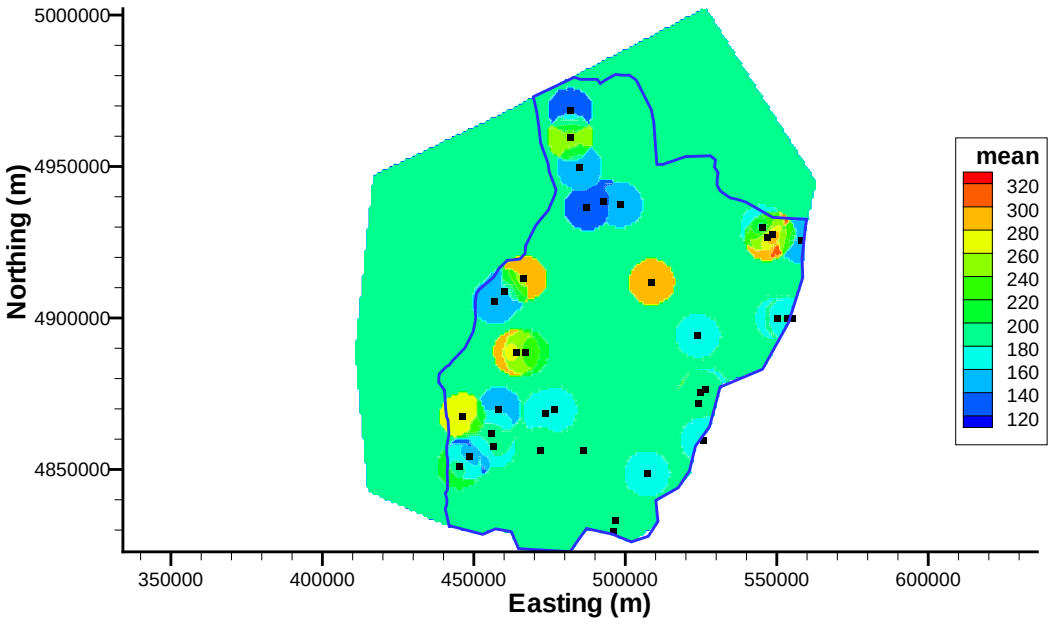

Figure 2.7: Spatial distribution of the mean thickness of the Ordovician limestones.

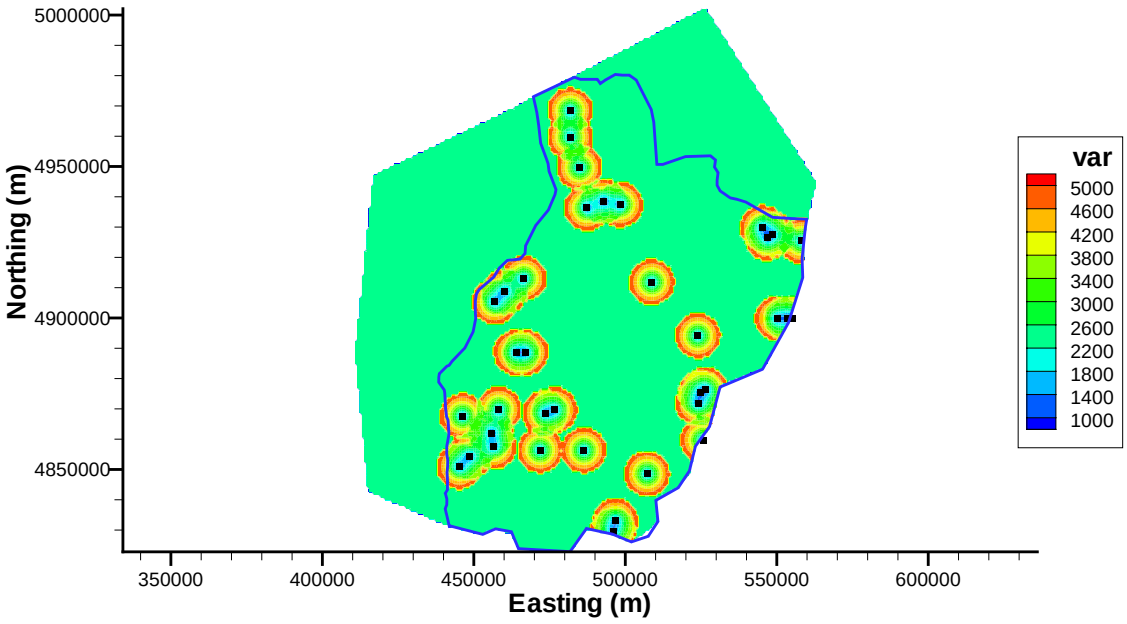

Figure 2.8: Spatial variance of the thickness of the Ordovician limestones.

The semi-variogram data and linear model for the Cobourg thickness are shown in Figure 2.9. The kriged mean and variance of the Cobourg thickness are plotted in Figure 2.10 and Figure 2.11 respectively. Figure 2.11 shows the variance in the thickness of the Cobourg Formation. Since the Cobourg formation is the target for the proposed DGR, it was important to determine how accurately the thickness (Figure 2.10) and its continuity can be predicted. Similar to the variance plots from the Ordovician limestones and shales, the figure of the variance for the Cobourg formation displays the distinct influence of the range effect. Outside of a distance of 145 km, the variance increases dramatically and like the previous figures, the area of high variance corresponds to the areas in the domain beneath Lake Huron and Georgian Bay. However, the very large range strongly supports the conclusion that the Cobourg is continuous and predictable.

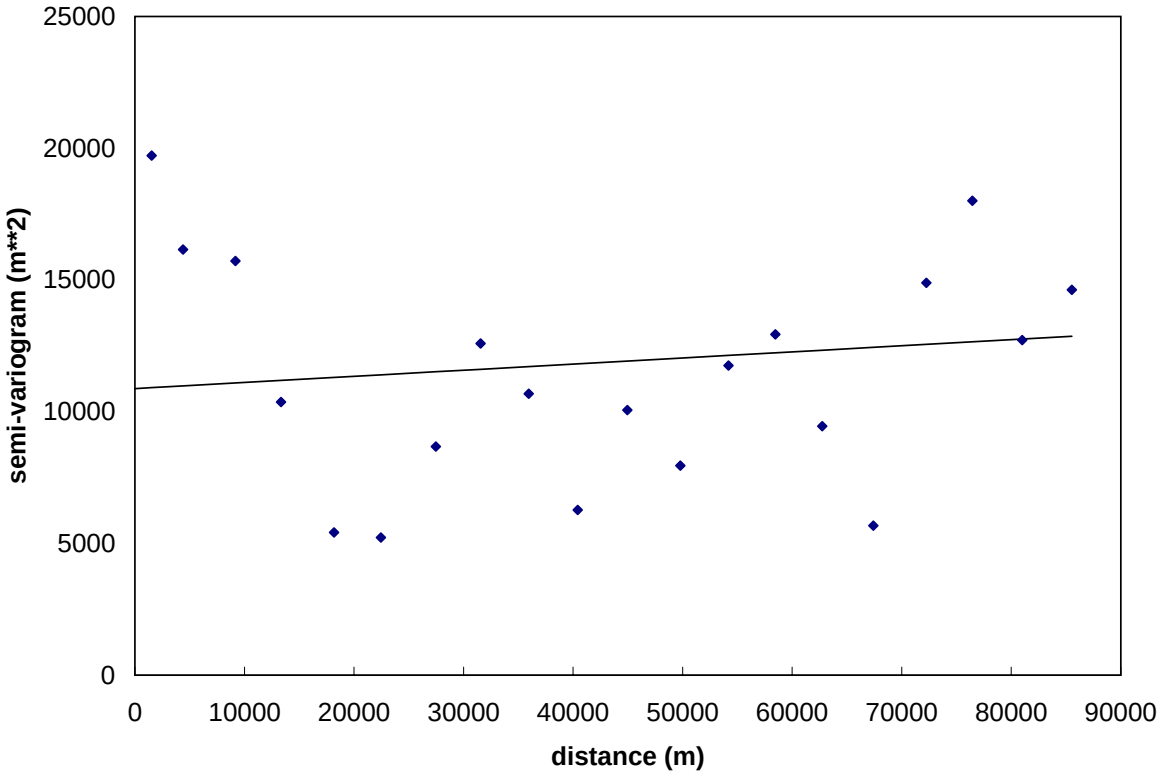

Figure 2.9: Semi-variagram for Cobourg formation thickness.

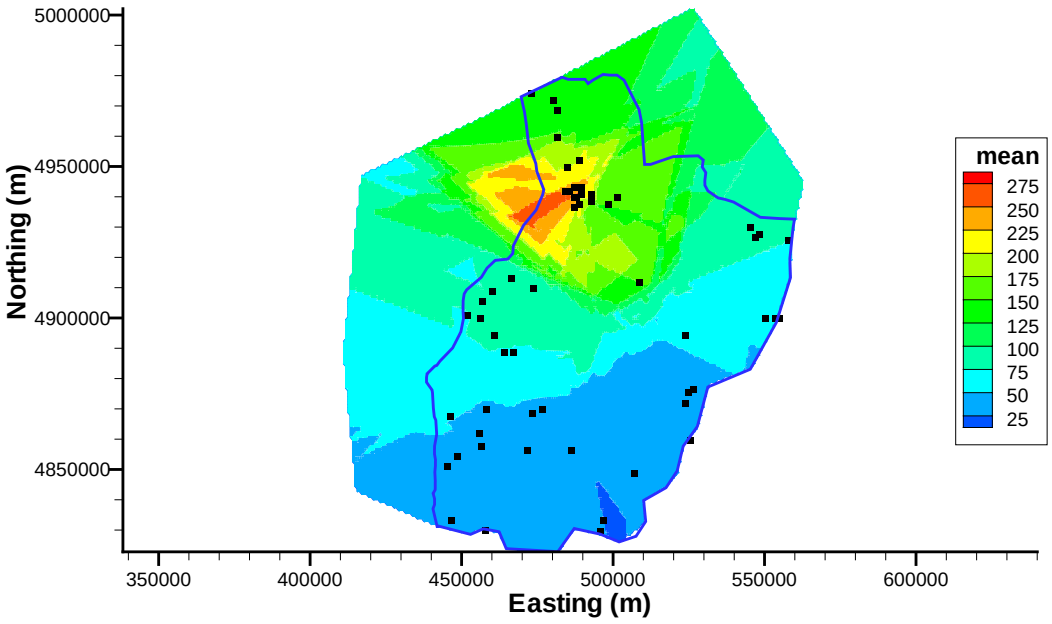

Figure 2.10: Spatial distribution of the mean thickness of the Cobourg formation.

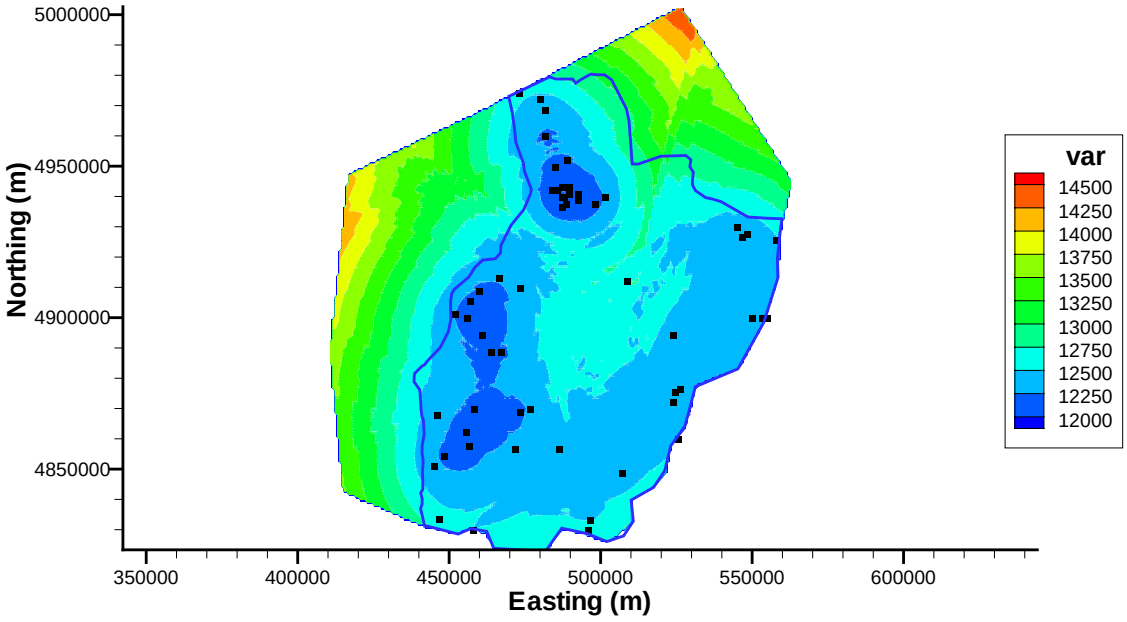

Figure 2.11: Spatial variance of the thickness of the Cobourg formation.

Inspite of the high variability of the data, it should be noted that the presence of the unit is easily predictable given the data. The mean thicknesses of the Ordovician shales and limestones are 183.01 m and 192.71 m respectively. When these average thicknesses and their corresponding standard deviations are taken into account, it can be concluded that despite the high variability in the thicknesses and the uncertainty in accurately predicting the thickiness between known boreholes, the data support the conclusion that the units are continuous across the regional domain with large observed thicknesses occurring in the vicinity of the proposed Bruce DGR.

The borehole data also contained anomalies in the surface elevations used to reference the boreholes. The dataset provided the structural elevations both in terms of meters above sea level and depth below ground surface. Within the dataset, there were occurrences of boreholes whose elevations would be on the order of 10s of meters different from neighbouring boreholes. To compensate for the elevation disparities, a Digital Elevation Model (DEM) of Southern Ontario was used in conjunction with the depth below ground surface data for the geologic interfaces. The use of the DEM ensured that all of the formation contacts would be referenced to a single and known datum. The Digital Elevation Model (DEM) for the conceptual model domain was developed using the 1:250 000 Natural Resources Canada map. The raster data for the DEM has a 3 arc second resolution on an approximately 60 m east-to-west by 100 m north-to-south grid. The integer elevations on the grid range from approximately 176 m to 539 m above mean sea level.

In addition to possible vertical error, there is possibility for error from the spatial location of the coordinates. This can be attributed to wells having incorrect longitude and latitude coordinates. This may possibly explain the instances where boreholes with distinct license names and geological records will have the same x and y coordinates. The error from the spatial location of the well will then become further compounded from the elevation. This will occur because wells in an incorrect location will then be assigned an elevation from the DEM that may be higher or lower than what the actual correct field measurement would have been.

In addition to the borehole data, surficial bedrock geologic data were used to supplement and constrain the data set. The surficial geologic contacts were discretized and subsequently added to the dataset. To discretize the surficial geologic map (Figure 2.12), the contacts between geologic units on the map were rendered into a series of points in GIS. Elevation data were then extracted from the DEM at these points. The addition of the supplemental data was to ensure that during

the spatial interpolation of the borehole data, the geologic units would be forced to intersect the ground surface consistent with surface mapping.

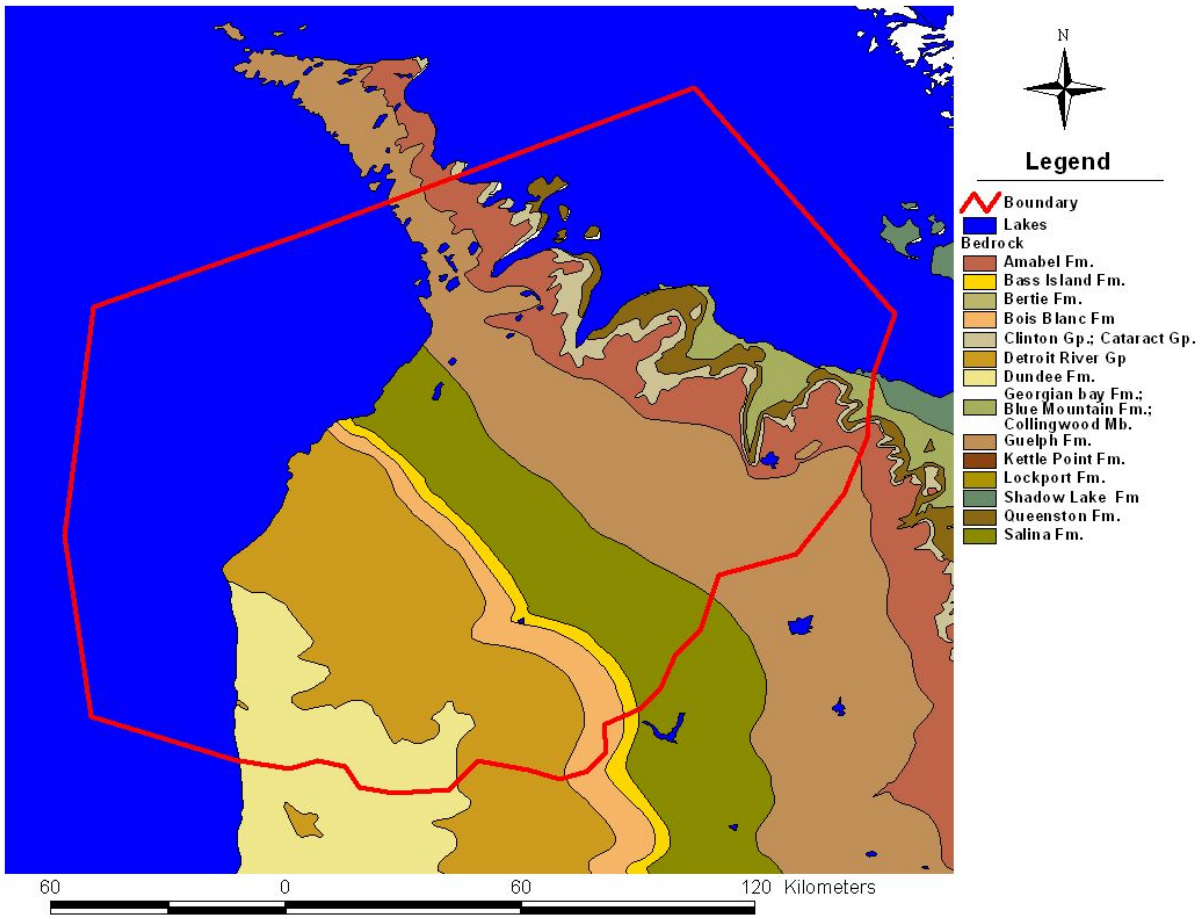

Figure 2.12: Surficial geology for Southern Ontario

In order to create a three-dimensional geologic model of a portion of Southern Ontario, a variety of geostatistical interpolation methods were used. The program Rockworks was selected to perform the geostatistical interpolations. Three different methods were selected. The methods were kriging, inverse distance squared and a first-order polynomial.

For this preliminary phase of the regional analysis, the first-order polynomial method was selected to correlate between boreholes because of the high aptitude it has for extrapolation

and interpolating between scarce points. The first-order polynomial approach fits planar surface through the data points. Although this may cause a reduction in geologic competency of some undulating and generally non-linear geologic features, the first-order polynomial increases the plausibility of fit in areas with few data points. The first order polynomial method is also appropriate to capture the uncertainties, in a first order sense, that are inherent in the borehole dataset used to generate the three-dimensional geologic model. The uncertainty related to extrapolation is recognized here for the regional geologic reconstruction because the extent of the domain extends beyond the shores of Lake Huron and Georgian Bay, where there is a notable absence of borehole data. Other interpolation and extrapolation methods should be investigated in a subsequent phase of the Bruce DGR study.

After the geologic model was created by interpolating between the boreholes, it was necessary to ensure that the volume created corresponds to the known surface elevations and bathymetries. To ensure the topographic and bathymetric control, a script was written using Visual Basic to remove any interpolated volumes that occurred above ground and lake bottom surfaces. Figure 2.13 shows a fence diagram of the geologic layers comprising the model.

2.3 Geochemistry

Regarding the hydrogeochemistry of the Michigan Basin, the groundwater can be typified as being Na-Ca-Cl or Ca-Na-Cl brines. The brines also exhibit levels in total dissolved solids (TDS) that range from approximately $10\,\mathrm{g/L}$ to $400\,\mathrm{g/L}$. The low TDS values are attributed to the shallower geologic formations, such as the Dundee and Lucas formations, where the original saline waters have become diluted. The groundwater in the deeper formations have much higher TDS levels. The higher TDS levels will cause the groundwater to have a comparatively higher density, as Figure 2.14 demonstrates. The high concentrations are also indicative of the absence of recent dilution by freshwater in these units.

2.4 Hydrogeologic Parameters

An important aspect characterizing the regional scale flow system will be the assignment of reasonable permeabilities assigned to various hydrostratigraphic units. Careful selection of perme-

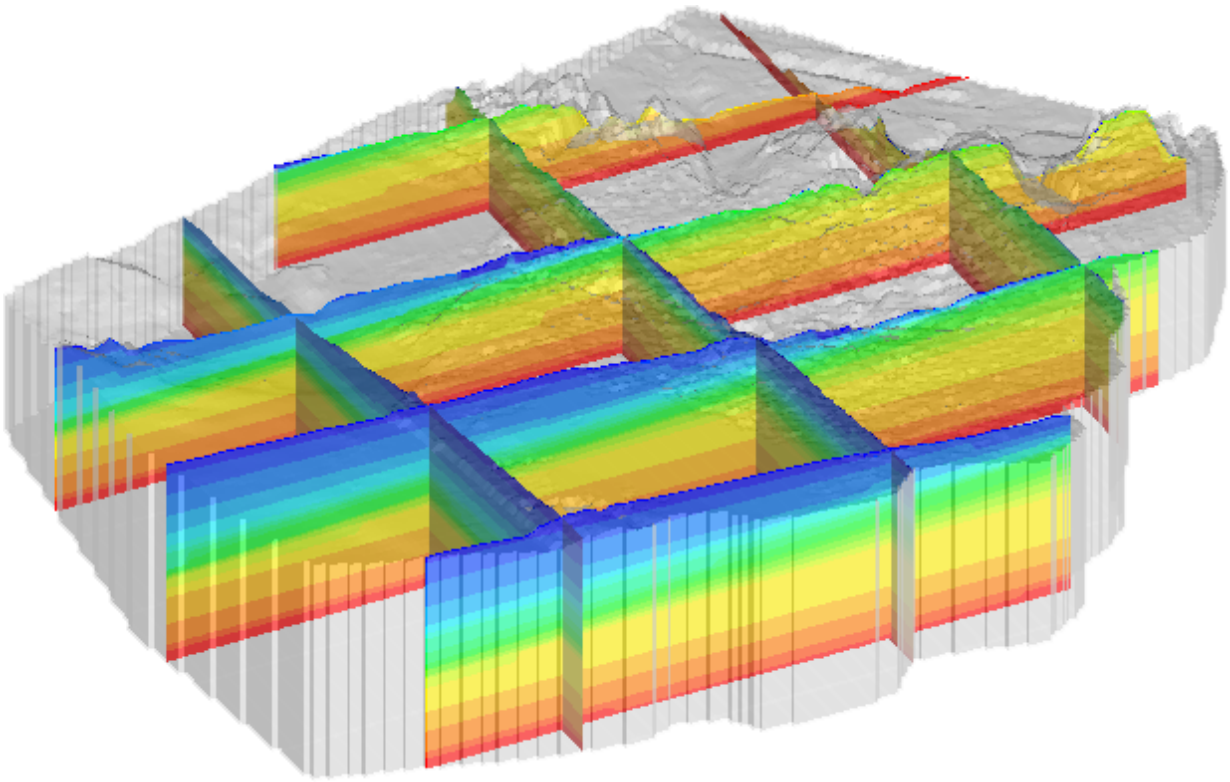

Figure 2.13: Fence diagram from geologic reconstruction

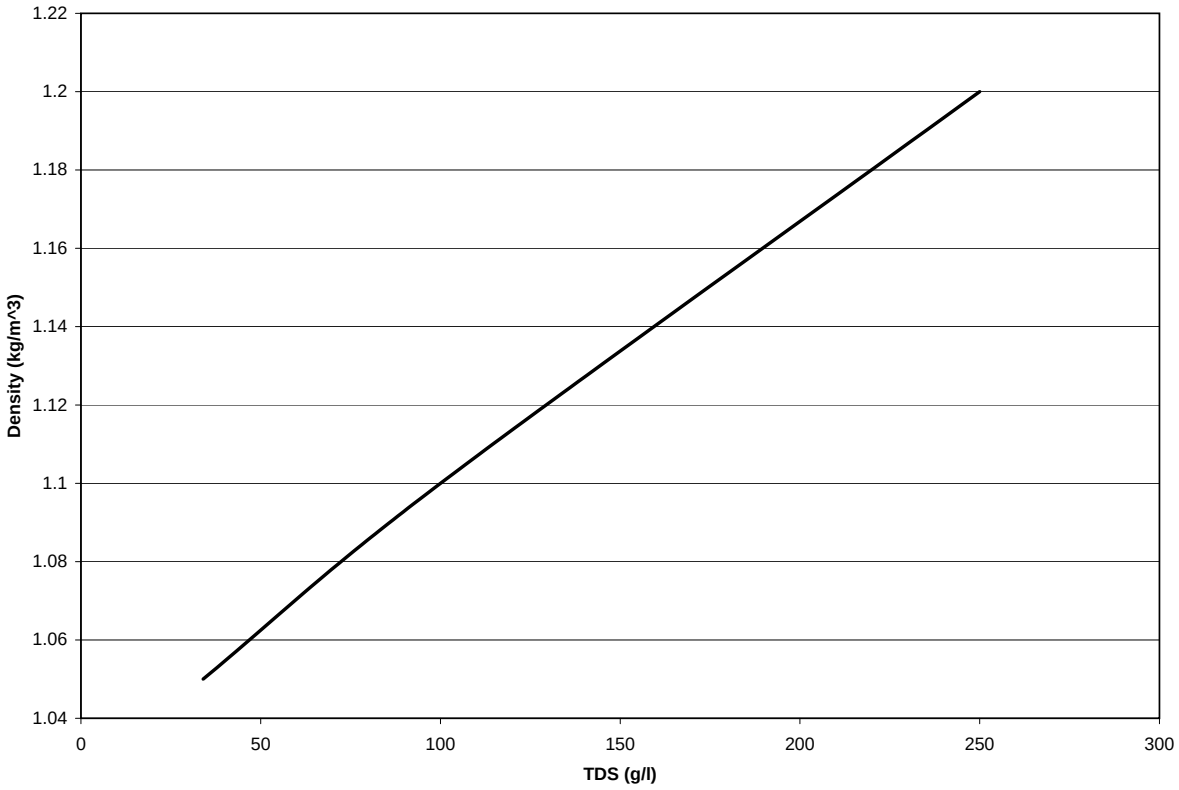

Figure 2.14: Conceptualized relationship between density and concentration.

ability values will help increase the accuracy of the geologic model. The data listed in Table 2.2, Table 2.3, Table 2.4 and Table 2.5 are insitu measurements. It should be noted that in many instances, the minimum hydraulic conductivities reported are at the measurement limit of the hydrogeologic equipment.

In each of the tables, the formations with the lowest measured hydraulic conductivities are the Ordovician shales and limestones, with hydraulic conductivities typically in the range of approximately $1.0 \times 10^{-11}\,\mathrm{m/s}$. The low permeability Ordovician units are bounded above by the Guelph Formation, which is more permeable with hydraulic conductivities typically around $1 \times 10^{-6}\,\mathrm{m/s}$ and the Cambrian Formation, which typically have hydraulic conductivities measured around $1 \times 10^{-11}\,\mathrm{m/s}$. In a field measurement performed on the OPG-2 borehole, a hydraulic conductivity value of $1 \times 10^{-6}\,\mathrm{m/s}$ was measured at the site. Although the hydraulic conductivity for the Cambrian is much higher than the low permeability Ordovician shales and limestones, it is not believed to be a potential pathway for fluid migration because it is discontinuous and bounded above and below by aquitards. Similar to the Cambrian, Guelph Formation, has a much higher permeability than the underlying Ordovician formations, and is also bounded above and below by the low permeability formations. In the case of the Guelph formation, it is bounded by the Salina formation and the Rochester shale. The Guelph Formation is highly continuous.

Table 2.2: Paleozoic hydraulic conductivities from *Raven et al.* [1992]

Formation	Borehole	K min (m/s)	K max (m/s)
Dundee	MDMW-1 Sarnia	4.0×10^{-13}	1.3×10^{-7}
Lucas	MDMW-1 Sarnia	2.5×10^{-9}	3.2×10^{-7}
Amherstberg	MDMW-1 Sarnia	3.2×10^{-11}	7.9×10^{-9}
Guelph	USNI-1 Niagara Falls	1.6×10^{-7}	1.0×10^{-5}
Guelph	NI-1 Niagara Falls	7.9×10^{-9}	6.3×10^{-5}
Goat Island	USNI-1 Niagara Falls	3.2×10^{-08}	1.0×10^{-5}
Goat Island	NI-1 Niagara Falls	3.2×10^{-09}	2.0×10^{-5}
Gasport	USNI-1 Niagara Falls	1.0×10^{-13}	1.0×10^{-13}
Gasport	NI-1 Niagara Falls	2.0×10^{-8}	2.0×10^{-8}
Rochester	USNI-1 Niagara Falls	1.0×10^{-13}	2.5×10^{-7}
Rochester	NI-1 Niagara Falls	1.3×10^{-9}	1.3×10^{-7}
Reynales/Fossil Hill	USNI-1 Niagara Falls	1.0×10^{-12}	2.5×10^{-11}
Reynales/Fossil Hill	USNI-1 Niagara Falls	3.2×10^{-11}	3.2×10^{-11}
Cabot Head	NI-1 Niagara Falls	6.3×10^{-11}	6.3×10^{-11}
Queenston	USNI-1 Niagara Falls	2.5×10^{-13}	2.0×10^{-11}
Queenston	USNI-1 Niagara Falls	4.0×10^{-11}	1.0×10^{-9}
Georgian Bay	OHD-1 Lakeview	1.0×10^{-13}	4.0×10^{-12}
Collingwood	OHD-1 Lakeview	1.0×10^{-12}	1.0×10^{-12}
Cobourg	OHD-1 Lakeview	1.0×10^{-13}	6.3×10^{-12}
Cobourg	UN-2 Darlington	6.3×10^{-14}	1.6×10^{-11}
Sherman Fall	OHD-1 Lakeview	2.0×10^{-14}	1.3×10^{-12}
Sherman Fall	UN-2 Darlington	1.0×10^{-13}	7.0×10^{-9}
Kirkfield	OHD-1 Lakeview	1.0×10^{-13}	4.0×10^{-12}
Kirkfield	UN-2 Darlington	1.0×10^{-13}	4.0×10^{-12}
Gull River	OHD-1 Lakeview	2.5×10^{-14}	2.5×10^{-11}
Gull River	UN-2 Darlington	1.0×10^{-13}	1.0×10^{-12}
Shadow Lake	OHD-1 Lakeview	1.0×10^{-13}	1.0×10^{-09}
Shadow Lake	UND-1 Darlington	1.0×10^{-13}	1.0×10^{-12}

Table 2.3: Paleozoic hydraulic conductivities from *Golder Associates Ltd* [2003]

Formation	Borehole	K min (m/s)	K max (m/s)
Bois Blanc	Bruce	5.0×10^{-11}	9.0×10^{-5}
Cobourg	DDH01/02 Bowmanville	1.3×10^{-12}	4.0×10^{-11}
Sherman Fall	DDH01/02 Bowmanville	5.0×10^{-13}	2.0×10^{-09}
Kirkfield	DDH01/02 Bowmanville	1.0×10^{-11}	6.3×10^{-09}
Gull River	DDH01/02 Bowmanville	2.0×10^{-11}	6.3×10^{-09}
Shadow Lake	DDH01/02 Bowmanville	5.0×10^{-09}	1.0×10^{-08}

Table 2.4: Paleozoic hydraulic conductivities from *Novakowsi and Lapcevic* [1988]

Formation	Borehole	K min (m/s)	K max (m/s)
Guelph	Niagara	1.4×10^{-8}	2.8×10^{-4}
Goat Island	Niagara	7.8×10^{-11}	5.5×10^{-4}
Gasport	Niagara	1.0×10^{-11}	1.7×10^{-06}
Rochester	Niagara	1.0×10^{-11}	1.7×10^{-06}
Reynales/Fossil Hill	Niagara	1.0×10^{-11}	1.7×10^{-06}
Cabot Head	Niagara	1.0×10^{-11}	2.0×10^{-7}
Queenston	Niagara	1.0×10^{-11}	2.4×10^{-10}

Table 2.5: Paleozoic hydraulic conductivities from *Intera Ltd.* [1988]

Formation	Borehole	K min (m/s)	K max (m/s)
Dundee	Sarnia	5.0×10^{-12}	1.0×10^{-9}
Dundee	Ojibway Mine	1.0×10^{-7}	1.0×10^{-6}
Lucas	Sarnia	1.0×10^{-8}	1.0×10^{-7}
Lucas	Goderich Mine	1.0×10^{-7}	1.0×10^{-6}
Lucas	Ojibway Mine	1.0×10^{-7}	1.0×10^{-6}
Amherstberg	Sarnia	1.0×10^{-11}	1.0×10^{-9}
Amherstberg	Goderich Mine	1.0×10^{-7}	1.0×10^{-6}
Amherstberg	Ojibway Mine	1.0×10^{-7}	1.0×10^{-6}
Bois Blanc	Nanticoke Tunnel	1.0×10^{-9}	1.0×10^{-8}
Bass Island	Goderich Mine	1.0×10^{-7}	1.0×10^{-6}
Bass Island	Ojibway Mine	1.0×10^{-7}	1.0×10^{-6}
Cobourg	Darlington Tunnels	1.0×10^{-12}	1.0×10^{-12}
Cobourg	Wesleyville	1.0×10^{-11}	1.0×10^{-08}
Cobourg	Wesleyville	2.0×10^{-10}	4.0×10^{-06}
Sherman Fall	Wesleyville	1.0×10^{-11}	1.0×10^{-08}

Chapter 3

Numerical Model Description and Theory

3.1 FRAC3DVS-OPG

3.1.1 Model Description

The model selected for this study was FRAC3DVS-OPG (cite), which was developed from FRAC3DVS [*Therrien et al.*, 2004]. FRAC3DVS-OPG is a numerical model capable of solving three-dimensional variably-saturated density dependent groundwater flow and solute transport in porous and discretely fractured media. Although the model is capable of handling dual porosity simulations, for the purpose of this regional study, an equivalent porous media approximation was assumed. To solve the density dependent non linear flow equation, a Picard iterative solver is utilized.

3.1.2 Density Dependent Flow and Transport

At greater depths within the Michigan Basin, the pore-fluids begin to become more saline and generally have significantly higher total dissolved solids than shallow groundwater. The increased salinity of the fluid will act as an impediment to flow by reducing the energy gradient and hence the velocities in the deeper formations.

For density dependent flow and transport, the governing equations include Darcy's Law and the continuity equations for flow and transport. The density dependent form of Darcy's Law is

given by:

$$q_i = -\frac{k_{ij}}{\mu}\left(\frac{\partial p}{\partial x_j} + \rho g \eta_j\right) \tag{3.1}$$

where q_i [L T^{-1}] is the flux in the ith direction, k_{ij} L^2 is the permeability tensor, μ is the viscosity [M L^{-1} T^{-1}], p [L] is the pressure, ρ [M L^{-3}] is the density of groundwater and $\eta = 1$ [L]for the vertical(z) direction, while $\eta = 0$ for the horizontal directions (x and y). When (3.1) is rewritten in terms of freshwater equivalent heads (which is defined as follows: $h = p/\rho_0 g + z$), it becomes:

$$q_i = -\frac{k_{ij}}{\mu g}\left(\frac{\partial h}{\partial x_j} + \rho_r \eta_j\right) \tag{3.2}$$

where ρ_r [dimensionless] is the relative density, given by $\rho/\rho - 1$ where ρ_0 is the reference freshwater density. For elastic fluids, the density of a fluid becomes a function of the fluid pressure and solute concentration:

$$\rho = \rho_0 \left[1 + c_w (p - p_0) + \gamma C\right] \tag{3.3}$$

where ρ_0 [M L^{-3}] is the freshwater density at a reference pressure p_0, c_w is the compressibility of water, γ is a constant derived from the maximum density of the fluid, ρ_{max} and is defined as $\gamma = (\rho_{max}/\rho_0 - 1)$ and C is the relative concentration.

Under isothermal conditions, the viscosity μ is a funtion of the concentration of the fluid. For the viscosity, it is assumed that there is a linear relation between the relative concentration so long as the maximum viscosity change is insignificant in isothermal conditions.

$$\mu = \mu_0 \left(1 + \gamma_\mu C\right) \tag{3.4}$$

where μ_0 is the viscosity of freshwater and $\gamma_\mu = (\mu_{max}/\mu_0 - 1)$. When the equations for the elasticity of the fluid and the viscosity are included in the Darcy's equation, it becomes:

$$q_i = -\frac{k_{ij}}{\mu_0 g} \cdot \frac{1}{1 + \gamma_\mu C}\left(\frac{\partial h}{\partial x_j} + \left[c_w (p - p_0) + \gamma C\right] \eta_j\right) \tag{3.5}$$

The groundwater flow equation can then be derived using Equation (3.5) and the continuity of energy principle.

$$\frac{\partial}{\partial t}\left[K^0_{ij} \cdot \frac{1}{1 + \gamma_\mu C}\left(\frac{\partial h}{\partial x_j} + \left[c_w (p - p_0) + \gamma C\right] \eta_j\right)\right] = S_s \frac{\partial h}{\partial t} \tag{3.6}$$

where $K_{ij}^0 = k_{ij}/\mu_0 g$ and S_s is the specific storage term. The solute continuity equation is written in terms of relative concentration as:

$$\frac{\partial}{\partial x_i}\left(\phi D_{ij}\frac{\partial C}{\partial x_j}\right) - \frac{\partial}{\partial x_i}(q_i C) = \theta\frac{\partial C}{\partial t} \tag{3.7}$$

where the Darcy flux q_i is computed by solving Equation (3.6), θ is the porosity and D_{ij} is the hydrodynamic dispersion tensor [*Bear*, 1988]:

$$\phi D_{ij} = (\alpha_l - \alpha_t)\frac{q_i q_j}{|q|} + \alpha_t |q|\delta_{ij} + \phi\tau D_{free}\delta_{ij} \tag{3.8}$$

where α_l and α_t are the longitudinal and transverse dispersivities respectively, $|q|$ is the magnitude of the Darcy flux, τ is the tortuosity, D_{free} is the free solution diffusion coefficient and δ_{ij} is the Kronecker delta. The effective diffusion coefficient is obtained by τD_{free}.

It should be noted that the equations for density dependent flow and transport are nonlinear; to solve the flow (3.6), the relative densities, which are dependent upon the transport (3.7), which itself requires Darcy fluxes from Equation (3.6), are required.

For more detail on the implementation of density dependent flow in FRAC3DVS-OPG, refer to *Therrien et al.* [2004]

3.2 System Performance Measures

As part of the safety case assessment of the DGR, the host formation of the repository is required to have sufficiently low hydraulic conductivities and hydraulic gradients, as well as favourable retardation properties. These parameters have the potential for a large range of natural variability and uncertainty. In trying to robustly characterize the groundwater flow and transport regimes in the deeper basinal formations, it is prudent to determine and quantify what impact, if any, the variability of these parameters will have upon the model results. It is by demonstrating and determining the sensitivity of the model to perturbations in model parameters that a more rigorous understanding of the groundwater system at depth, as well as the impact of the model on these characterizations, can be achieved.

3.2.1 State Variables

In order to gauge the performance of the groundwater system being characterized in the model, it is prudent to perform some form of sensitivity or uncertainty analysis. These analyses are done to determine the influence a change in parameter will have on the model. For these scenarios, a state variable will be chosen as the performance indicator. The influence of parametric perturbations is then determined by measuring any changes to the state variable as a function of a change in parameter:

$$S_{ij} = \frac{\partial P_i}{\partial \alpha_j} \tag{3.9}$$

where S_{ij} is the sensitivity coefficient, $P_i(p)$ is the state variable, which itself is dependent upon α_j, an independent parameter. The sensitivity coefficient S_{ij} can be interpreted as the change in P_i given a change in α_j. A negative sensitivity coefficient implies that a positive change in α_j will yield a decrease in P_i. The sensitivity coefficient as expressed by Equation (3.9) are local derivatives. A normalized sensitivity coefficient can be determined by modifying equation (3.9) such that:

$$S_{ij} = \frac{\partial P_i}{\partial \alpha_j} \cdot \frac{\bar{\alpha}}{\bar{P}} \tag{3.10}$$

where $\bar{\alpha}$ is the mean value of the state variable and $\bar{P}$, which represents the mean value for the perturbed parameter. The normalized sensitivity coefficient S_{ij} are dimensionless and indicate the percent change in P_i for a percent change in α_j. The normalized sensitivity coefficient for different parameters α_j can be directly compared so as to reveal the system performance to which P_i is most sensitive.

Possible variables that may be used in these instances as state variables are heads, concentrations, groundwater velocity directions and magnitudes or travel time and lifetime expectancy.

3.2.2 Lifetime Expectancy as a Performance Indicator

Groundwater age can be defined as being a relative quantity with respect to a starting location with an assumed age of zero [*Cornaton and Perrochet*, 2006]. For a given spatial position within a domain, the age (denoted as a variable A) of a particle at that position can be determined by the time elapsed since the water particle entered the system from a boundary condition. The boundary conditions would have an assumed age of zero. Conversely, the lifetime expectancy (denoted

as a varibale E) of a particle at the same spatial position can be estimated by determining the time required for a particle from that position to reach a potential outflow point. This definition of lifetime expectancy results in outflow points within the model having a mean lifetime expectancy of zero. The variables for both age and lifetime expectancy are random variables and as such their behaviour can be characterized by that of a probability density function describing the distribution of water particles with respect to time.

For the travel time probability, the amount of time required for a particle to travel from a starting point x_i to a position x is characterized by $g_t(t,x|t_0,x_i)$. In the case of the location probability, the density characterizing the probability of finding a particle at a point x at a time t after the release from a starting point x_i is $g_x(x,t|x_i,t_0)$. Furthermore, if the inlet to a system is correspondent with an inflow source (Γ_-), the traveltime will correspond with the groundwater age. Conversely, if the inlet to a system is correspondent with an outflow source (Γ_+), the traveltime will correspond with the lifetime expectancy. It is through a solution to the Advection Dispersion Equation (ADE) that the age and lifetime expectancy probability density functions (PDF) can be obtained. These PDFs are determined through applications of specialized boundary conditions.

3.2.3 Forward Model

When ADE is solved for the case of a unit tracer applied to an inlet (Γ_-), the age PDF for a position x within a domain Ω can be determined. This calculation will result in the probabilistic age distribution. The age PDF is determined by solving the following boundary value problem for a pre-solution of a velocity field:

$$\frac{\partial \theta g}{\partial t} = - \bigtriangledown \cdot \mathbf{q} g + \bigtriangledown \cdot \theta \mathbf{D} \bigtriangledown g + q_I \delta(t) - q_O g \quad \text{in } \Omega \tag{3.11a}$$

$$g(x,0) = g(x,\infty) = 0 \quad \text{in } \Omega \tag{3.11b}$$

$$\mathbf{J}(x,t) \cdot \mathbf{n} = (\mathbf{q} \cdot \mathbf{n} \delta(t)) \quad \text{on } \Gamma_- \tag{3.11c}$$

$$\mathbf{J}(x,t) \cdot \mathbf{n} = 0 \quad \text{on } \Gamma_0 \tag{3.11d}$$

where $g(\mathbf{x},t) = g_A(\mathbf{x},t)$ represents the transported age PDF [T^{-1}], $\mathbf{q}$ represents the groundwater flux vector [LT^{-1}], q_I and q_O are the fluid source and sink terms [T^{-1}], $\mathbf{J}(x,t)$ represents the total age mass flux vector [LT^{-1}]. $\mathbf{D}$ is the macro-dispersion tensor [L^2T^{-1}], $\mathbf{x} = (x,y,z)$ is the vector of

cartesian coordinates [L], t represents time [T], $\theta = \theta(x)$ is the either the porosity or the mobile water-content [dimensionless], **n** represents a normal outward unit vector and finally, $\delta(t)$ is the time-Dirac delta funtion [T^{-1}]. The purpose of the time-Dirac delta funtion is to ensure a pure impulse on Γ_-. The total mass age flux vector, $\mathbf{J}(x,t)$, is then defined as being:

$$\mathbf{J}(x,t) = \mathbf{q}g(x,t) - \mathbf{D} \bigtriangledown g(x,t) \tag{3.12}$$

which is the sum of the advective and dispersive fluxes.

3.2.4 Backwards Model

The life expectancy probability density function is solved by using the backwards form of the ADE which acts to reverse time and space, thereby allowing the life expectancy to be determined.

$$\frac{\partial \theta g}{\partial t} = \bigtriangledown \cdot \mathbf{q}g + \bigtriangledown \cdot \theta \mathbf{D} \bigtriangledown g - q_I g \quad \text{in } \Omega \tag{3.13a}$$

$$g(x,0) = g(x,\infty) = 0 \quad \text{in } \Omega \tag{3.13b}$$

$$\mathbf{J}(x,t) \cdot \mathbf{n} = -(\mathbf{q} \cdot \mathbf{n}\delta(t)) \quad \text{on } \Gamma_+ \tag{3.13c}$$

$$-\mathbf{D} \bigtriangledown g(x,t) \cdot \mathbf{n} = 0 \quad \text{on } \Gamma_0 \tag{3.13d}$$

where $g(\mathbf{x},t) = g_E(\mathbf{x},t)$ represents the transported life expectancy PDF [T^{-1}] and the total life expectancy mass flux vector is:

$$\mathbf{J}(x,t) = -\mathbf{q}g(x,t) - \mathbf{D} \bigtriangledown g(x,t) \tag{3.14}$$

3.2.5 Age and Lifetime Statistics

From a given age and/or lifetime expectancy probability density function, the mean and standard deviations can be calculated. The case of the mean age or mean life expectancy can be determined by taking the first moment of the PDF solution $g_t(t,x)$:

$$\mu(x) = \int_0^{+\infty} t g_t(t,x) dt \tag{3.15}$$

The standard deviation for the age and lifetime distributions can be determined using:

$$\sigma(x) = \sqrt{\int_0^{+\infty} t^2 g_t(t,x) dt - \mu^2} \tag{3.16}$$

3.2.6 Direct Solutions for Mean Age and Life Expectancy

It is possible to derive direct solutions for mean age and mean lifetime expectancy by taking the first moments of equations (3.11b) and (3.13). The equation for the mean age is the following:

$$-\bigtriangledown\cdot\mathbf{q}\langle A\rangle+\bigtriangledown\cdot\theta\mathbf{D}\bigtriangledown\langle A\rangle-q_O\langle A\rangle+\theta=0\quad\text{in }\Omega \tag{3.17}$$

where $\langle A\rangle$ represents mean age. The equation requires the following boundary conditions:

$$\langle A\rangle(x)=0\quad\text{on }\Gamma_- \tag{3.18a}$$

$$\mathbf{J}(x)\cdot\mathbf{n}=0\quad\text{on }\Gamma_0 \tag{3.18b}$$

Using the same method, the equation for mean life expectancy can be obtained as follows:

$$\bigtriangledown\cdot\mathbf{q}\langle E\rangle+\bigtriangledown\cdot\theta\mathbf{D}\bigtriangledown\langle E\rangle-q_I\langle E\rangle+\theta=0\quad\text{in }\Omega \tag{3.19}$$

$$\langle E\rangle(x)=0\quad\text{on }\Gamma_- \tag{3.20a}$$

$$-\mathbf{D}\bigtriangledown\langle E\rangle(x)\cdot\mathbf{n}=0\quad\text{on }\Gamma_0 \tag{3.20b}$$

Using these formulations, mean ages and mean lifetime expectancies will be continuously calculated during groundwater flow. This results because $\theta=\theta(x)$ will act as a source term in equations (3.17) and (3.19) and implies that the groundwater will be aging an average of one unit per unit time.

Chapter 4

Regional-Scale Groundwater Flow Model

4.1 Model Domain

The regional scale domain, shown in Figure 4.1, occupies an aerial extent of approximately 18 000 km^2. It has vertical elevations that range from -1000 m at the lowest point in the Precambrian to 539 m at the highest point on the Niagara Escarpment. The figures shown in this thesis have vertical exaggerations between 40 and 60 times. The domain was discretized into slices with 27 728 nodes each which were then used to create quadrilateral elements. These quadrilateral elements have sides of 750 m in the East-West direction by 900 m in the North-South direction. Each of the 37 units from the geologic reconstruction was assigned a model layer so that the numerical model would closely resemble that of the geologic model. This resulted in 37 layers in the numerical model. In the occurrence of a pinching or otherwise discontinuous geologic layer, the layer in the numerical model was assigned a minimum thickness of 0.5 m and this layer was then assigned the parameters of the layer beneath. Although there is a large amount of congruency in the hydraulic and material properties of the 37 layers and the number of layers in the numerical model could be reduced by grouping lithofacies, the 37 unique lithofacies were included so that future analyses with more robust salinity data might be used.

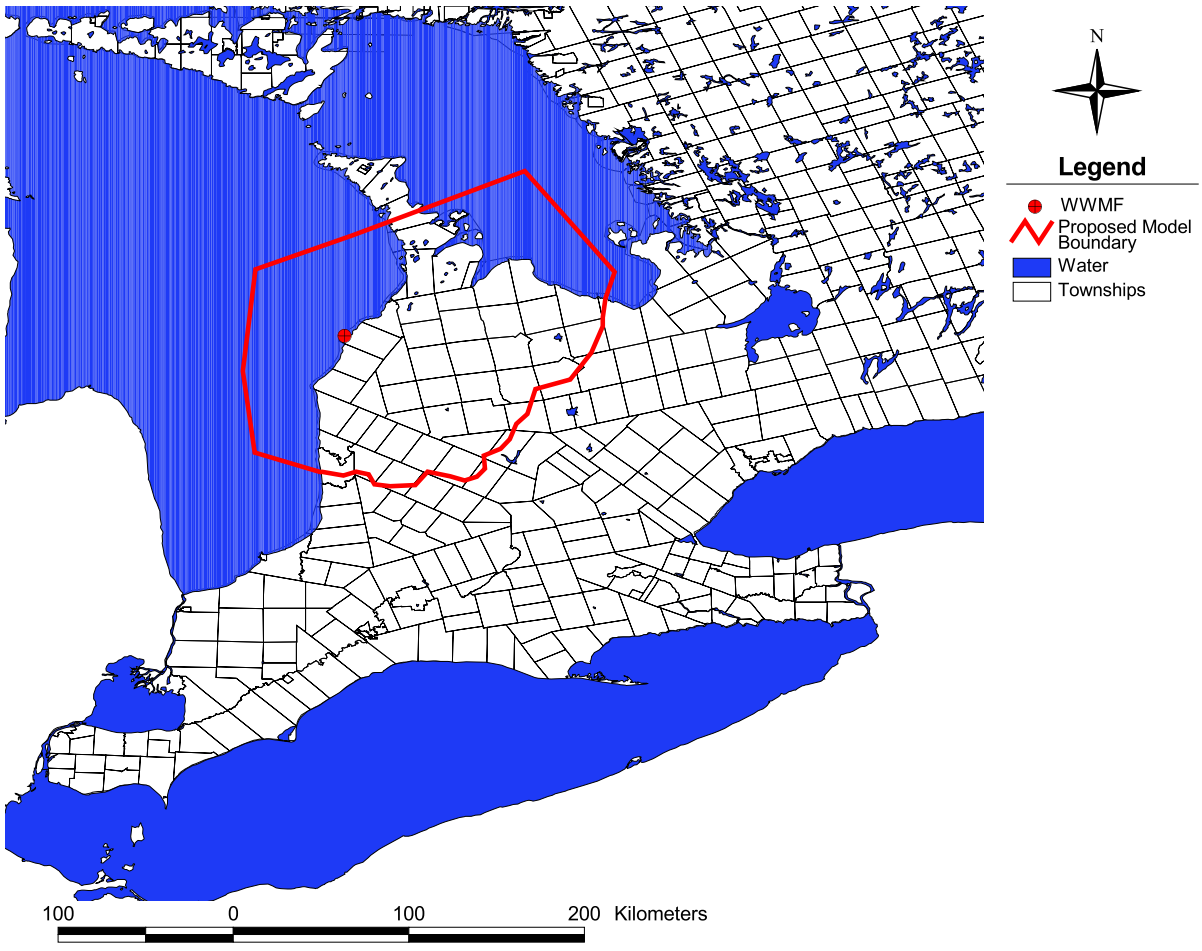

Figure 4.1: Regional model boundary

4.2 Boundary and Initial Conditions: Base Case

4.2.1 Flow

The boundary conditions of the model were Neumann no-flow boundary conditions for the sides and bottom, and type-one or Dirichlet for the surface of the model. The elevation of the nodes at the top of the model domain are defined by either the DEM or the lake bathymetry. For surface nodes with an elevation greater than 176 m, the assigned prescribed head was set as the elevation minus 3 m but not less than the 176 m Lake Huron water elevation. Areas within the domain that are occupied by either Lake Huron or Georgian Bay have a prescribed head matching the lake elevation, 176 m. The imposed surface boundary condition permits recharge and discharge to occur as determined by the surface topography and the hydraulic conductivity of the top model layer. The assigned head represents a water table occurring 3 m below ground surface. Because of the resolution of the DEM, stream channels are conceptualized to have a depth to water that is 3 m less than defined by the DEM. The impact of varying the depth to the water table can be investigated in a sensitivity analysis. Alternate conceptualizations of the upper boundary that were investigated in this thesis included using prescribed heads for grid blocks that coincided with major rivers and creeks, and recharge elsewhere. The impact of alternate elevations of the water table below ground surface was also investigated.

One important issue that pertains to the boundary conditions is the impact of the Niagara Escarpment. When the low hydraulic conductivities for the deeper geological formations, such as the Ordovician shales and limestones, are maintained continuously to the surface where the formation outcrops, the high head signature from the elevation at the escarpment is transmitted vertically down the stratigraphic column (Figure 4.2). The explanation for this is, in part, the relatively coarse spatial discretization and steep slopes in the vicinity of the escarpment. When a conservatively estimated weathered zone is assumed to exist for the near surface materials, which assumes a conductivity that is comparable to open fractures, the transmission of the high head signature does not occur (Figure 4.3). For the analysis shown in the figure, the weathered rock zone was assumed to occur to a depth of 15 meters below ground surface and to have a hydraulic conductivity of 1×10^{-4} m/sec. The inclusion of the weathered rock zone was adopted for all analyses in this thesis.

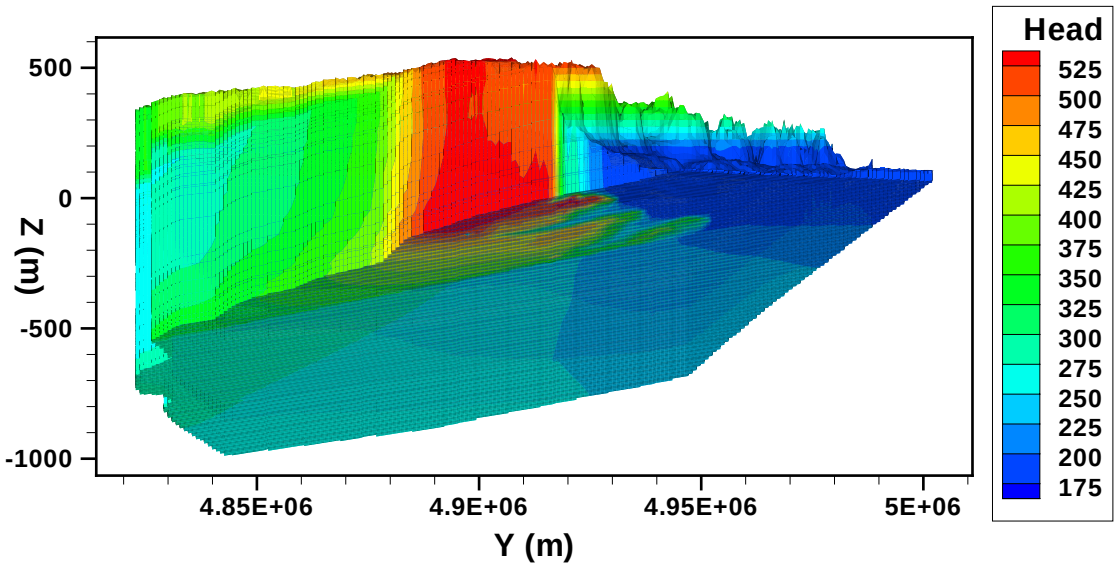

Figure 4.2: Head Profile at Niagara Escarpment.

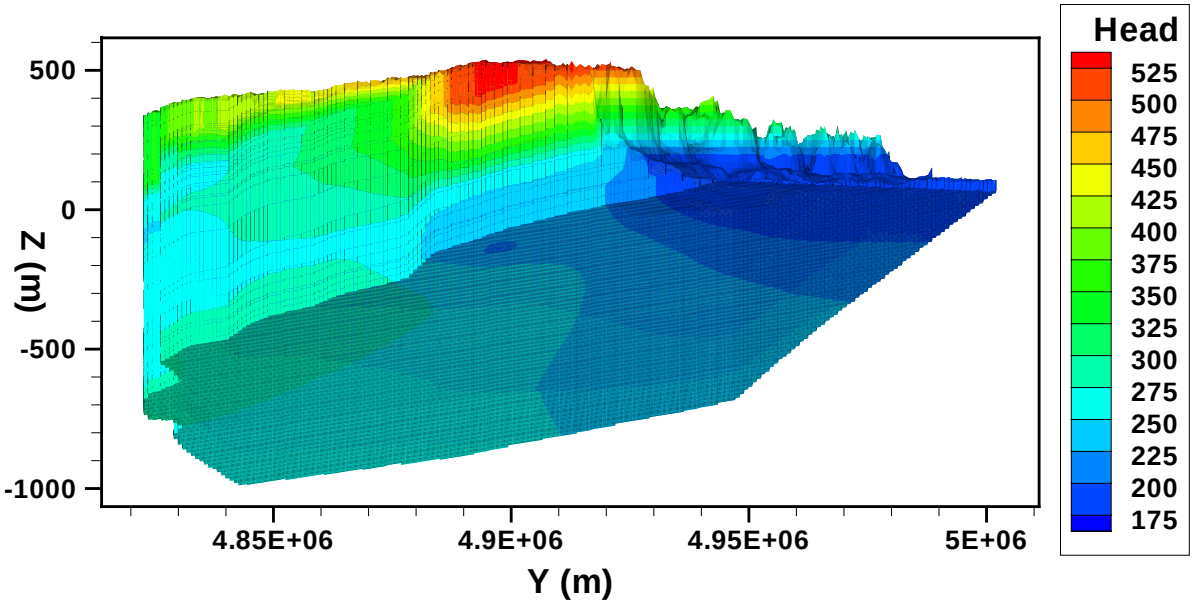

Figure 4.3: Head Profile at Niagara Escarpment with weathered zone.

4.3 Parameters: Base Case

The initial base-case data set for the numerical model consists of 37 model layers, with each layer corresponding to a unit in the stratigraphic section. Table 4.1 shows the layers and their associated hydraulic conductivities determined in part from data compiled by *Golder Associates Ltd* [2003]. The bottom layer is set to be the Precambrian. Table 4.2 shows further model parameters.

4.3.1 Total Dissolved Solids

Salinity plays an important role with regard to the fluid flow within the computational domain. As mentioned previously, an increase in the concentration of total dissolved solids (TDS) will result in an increase in the density of the water. The increase in density of the deeper fluids will then act as an inhibiter of active flow at depth. The explanation for this is that the potential energy gradient increases for positive elevation changes and positive changes in density. Within recharge areas, the density will increase along the flow path while the elevation decreases. It is therefore important to understand the impact that the salinity profile will have on the flow system behaviour.

The total dissolved solids distribution in the model can be assigned using different conceptual models. One way to characterize the brine distribution is to use an initial prescribed salinity distribution and allow the density-dependent flow to equilibrate to a new state from the initial prescribed profile. In using this method to characterize the salinity, the total mass of dissolved solids and its distribution in the model domain is assumed to be known and will be a maximum initially as there are no sources to generate dissolved solids (it is further assumed that there are no dissolved solids in the water recharging the domain.) With this approach, as time progresses, the dissolved solids will gradually reduce as the groundwater flushes through the system. An alternate conceptualization to represent the presence of the total dissolved solids is to assume a source that generates the fluid composition.

The sensitivity of the groundwater flow to the conceptual model for the total dissolved solids concentration distribution is discussed in the following paragraphs. For the case with a defined initial total dissolved solids concentration distribution, the concentration boundary conditions were: the surface of the model was set as a type 3 boundary condition, except areas beneath

Table 4.1: Base-case parameters modified from *Golder Associates Ltd* [2003]

Unit	K (m/s)	Porosity
Drift	1.00×10^{-7}	0.10
Dundee	1.00×10^{-7}	0.10
Lucas	1.00×10^{-7}	0.10
Amherstburg	1.00×10^{-7}	0.10
Bois Blanc	1.00×10^{-7}	0.10
Bass Island	1.00×10^{-7}	0.10
G-Unit	1.00×10^{-7}	0.08
F-Unit	1.00×10^{-10}	0.03
E-Unit	1.00×10^{-7}	0.08
D-Unit	1.00×10^{-10}	0.03
C-Unit	1.00×10^{-10}	0.03
B-Unit	1.00×10^{-13}	0.08
B-Salt	1.00×10^{-13}	0.08
B-Anhydrite	1.00×10^{-13}	0.08
A2-Carbonate	1.00×10^{-7}	0.08
A2-Salt	1.00×10^{-13}	0.08
A2-Anhydrite	1.00×10^{-13}	0.08
A1-Carbonate	1.00×10^{-13}	0.08
A1-Evaporite	1.00×10^{-13}	0.08
Guelph	1.00×10^{-7}	0.08
Goat Island	1.00×10^{-7}	0.08
Gasport	1.00×10^{-7}	0.08
Rochester	1.00×10^{-7}	0.08
Reynales	1.00×10^{-7}	0.08
Cabot Head	1.00×10^{-10}	0.03
Manitoulin	1.00×10^{-8}	0.03
Queenston	1.00×10^{-12}	0.11
Georgian Bay	1.00×10^{-12}	0.11
Collingwood	1.00×10^{-12}	0.11
Cobourg	7.00×10^{-13}	0.02
Sherman Falls	3.00×10^{-12}	0.02
Kirkfield	3.00×10^{-12}	0.02
Coboconk	4.00×10^{-12}	0.02
Gull River	4.00×10^{-12}	0.02
Shadow Lake	8.00×10^{-12}	0.01
Cambrian	1.00×10^{-6}	0.01
Precambrian	8.00×10^{-12}	0.01

Table 4.2: Model parameters

Parameter	Value
Storage Coefficient	0.001
Tortuosity	0.1
Diffusion Coefficient	0.0378432
Transverse Dispersivity/Longitudinal Dispersivity	0.1
Vertical Transverse Dispersivity/Longitudinal Dispersivity	0.01

Lake Huron and Georgian Bay, which had a prescribed relative concentration of zero. Zero-flux Neumann boundary conditions were used for the sides and bottom of the domain. The salinities used for the initial concentration conditions for each of the geologic units are documented in Table 4.3 The assigned initial-total-dissolved-solids concentration for the regional-scale model domain is plotted in Figure 4.4 and Figure 4.5. The highest total dissolved solids concentrations are assigned to the Ordovician shale units, while the shallow active groundwater flow zone of the Devonian units have low dissolved solids concentrations. The initial condition for the transient, fully-coupled density-dependent flow equation was the steady-state density-independent head distribution.

The initial condition for total-dissolved-solids specified concentrations that were constant for a given lithology and independent of the depth of the unit below ground surface. Unfortunately, data is not available for either the actual distribution in the shallow units or the spatial distribution, particularly, in the deeper units. In the absence of data, a plausible TDS distribution was generated using the physically-based regional model. For the coupled density-dependent flow and transport system, fresh water can recharge at the surface, reducing the TDS concentration in the shallow zone. However, the time to flush the dissolved solids from a unit is a function of the permeability of the unit and the energy of the displacing fluid as compared to the energy of the fluid being displaced. Fluids with lower total dissolved solids, such as recharging water, will have a lower energy as compared to higher total dissolved solids water with the same elevation and pressure. Therefore, for low-permeability units with a relatively high total dissolved solids concentration, the time to flush the unit or displace the fluids in it can be very long. Complete flushing may only occur as a result of diffusion because energy gradients may not be sufficient

Table 4.3: Base-case salinity concentrations modified from *Golder Associates Ltd* [2003].

Unit	TDS (mg/l)	Relative Concentration
Drift	45	2.00×10^{-4}
Dundee	2500	1.11×10^{-2}
Lucas	2500	1.11×10^{-2}
Amherstburg	2500	1.11×10^{-2}
Bois Blanc	2500	1.11×10^{-2}
Bass Island	2500	1.11×10^{-2}
G-Unit	200000	8.88×10^{-1}
F-Unit	200000	8.88×10^{-1}
E-Unit	200000	8.88×10^{-1}
D-Unit	200000	8.88×10^{-1}
C-Unit	200000	8.88×10^{-1}
B-Unit	200000	8.88×10^{-1}
B-Salt	200000	8.88×10^{-1}
B-Anhydrite	200000	8.88×10^{-1}
A2-Carbonate	200000	8.88×10^{-1}
A2-Salt	200000	8.88×10^{-1}
A2-Anhydrite	200000	8.88×10^{-1}
A1-Carbonate	200000	8.88×10^{-1}
A1-Evaporite	200000	8.88×10^{-1}
Guelph	200000	8.88×10^{-1}
Goat Island	200000	8.88×10^{-1}
Gasport	200000	8.88×10^{-1}
Rochester	200000	8.88×10^{-1}
Reynales	200000	8.88×10^{-1}
Cabot Head	200000	8.88×10^{-1}
Manitoulin	200000	8.88×10^{-1}
Queenston	225000	1.00
Georgian Bay	225000	1.00
Collingwood	225000	1.00
Cobourg	112500	5.00×10^{-1}
Sherman Falls	112500	5.00×10^{-1}
Kirkfield	112500	5.00×10^{-1}
Coboconk	112500	5.00×10^{-1}
Gull River	112500	5.00×10^{-1}
Shadow Lake	112500	5.00×10^{-1}
Cambrian	112500	5.00×10^{-1}
Precambrian	112500	5.00×10^{-1}

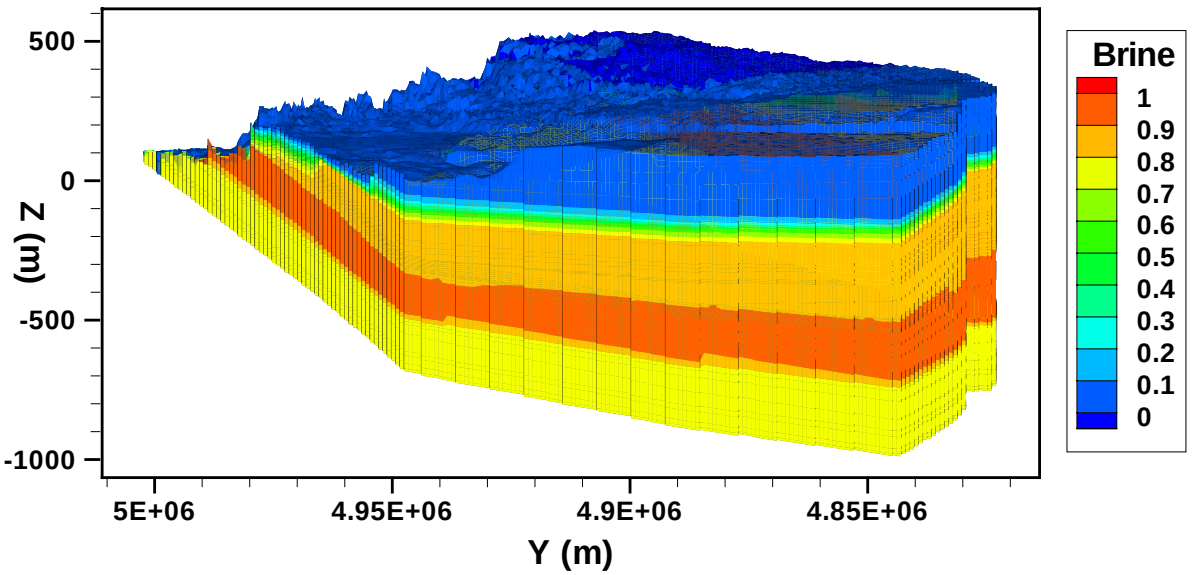

Figure 4.4: Salinity profile at 0 years using prescribed initial concentrations (front).

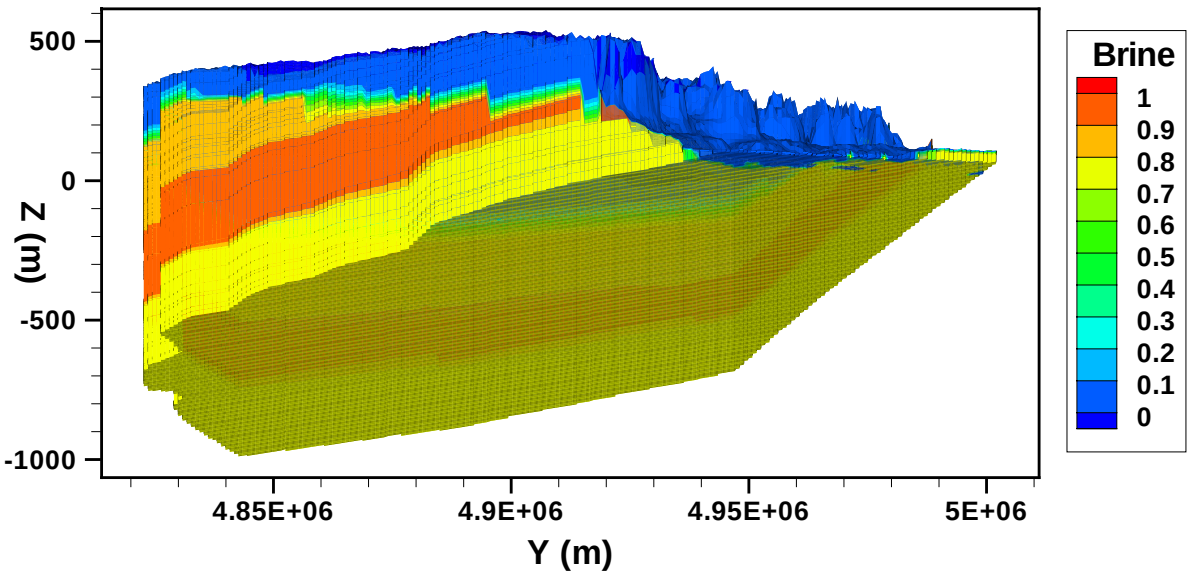

Figure 4.5: Salinity profile at 0 years using prescribed initial concentrations (back).

for advective displacement to occur.

The computational burden for the simulation and analysis of density-dependent flow is significant. The computer time is a function of factors including the number of degrees-of-freedom, the length of time steps for the necessary transient analysis, the spatial discretization and the size of grid blocks, and the assigned tolerance level for convergence at a time step. Of these, the length of time steps is most critical. In FRAC3DVS-OPG, the length of a time step is controlled, in part, by the cell Peclet number for the grid blocks with higher velocities. Within the regional domain, the shallow Devonian units have significantly higher velocities than the deeper Ordovician units. To control numerical dispersion and potential instability problems in the higher velocity shallow units, small time steps are required. In numerical experiments, it was found that time steps on the order of days were required in order to obtain results with satisfactory convergence. Thus, there is a balance between the accuracy of a solution, the length of time required for the system to reach a pseudo-equilibrium between energy, fluid flux and total dissolved solids distributions, and computer time. In this thesis, a suitable balance was established by assuming that pseudo-equilibrium would be obtained 1,000,000 years after the imposed initial conditions. The impact of this assumption and cut-off time can be investigated in a sensitivity analysis. It is important to recognize that the state of the system is assumed to be invariant over the time duration of the analysis. Changes in state may be more significant than the temporal changes in the velocity and total dissolved solids distribution for a scenario.

After 1 000 000 years, the model, having been allowed to reach pseudo-equlibrium, produces salinity profiles as shown in Figure 4.6 and Figure 4.7. In the north-eastern end of the domain, the brine is unable to accumulate because of a combination of the absence of the source term and the effect of recharge near Georgian Bay where the Ordovician formations outcrop. This is contrasted by the southern end of the domain which, because of the absence of a suitable velocity to transport the brine from the system, maintains a high salinity concentration. The location of the proposed DGR repository is located within this area. This results in a stagnation of the groundwater due to the effect the density will have on reducing the velocity.

One of the major differences between the different conceptualizations for the salinity profile is the computational time required. For large-scale problems such as the one investigated in this thesis, computational time can be an important criterion. Although there is a large degree of similarity between the case using a prescribed initial condition and the case using a first-order

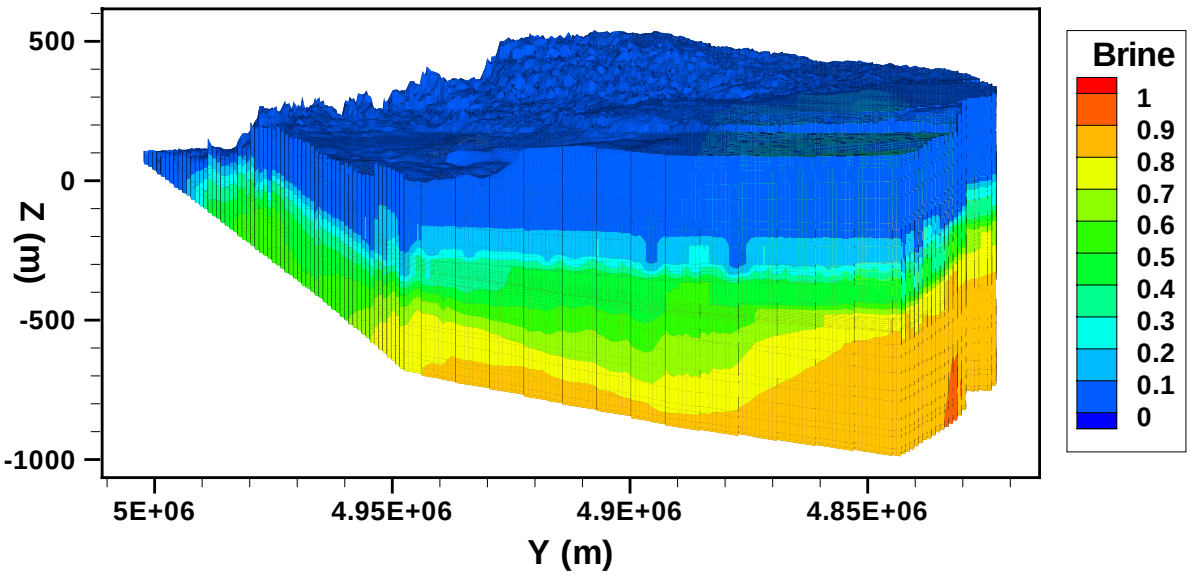

Figure 4.6: Salinity profile after 1 000 000 years using prescribed initial concentrations (front).

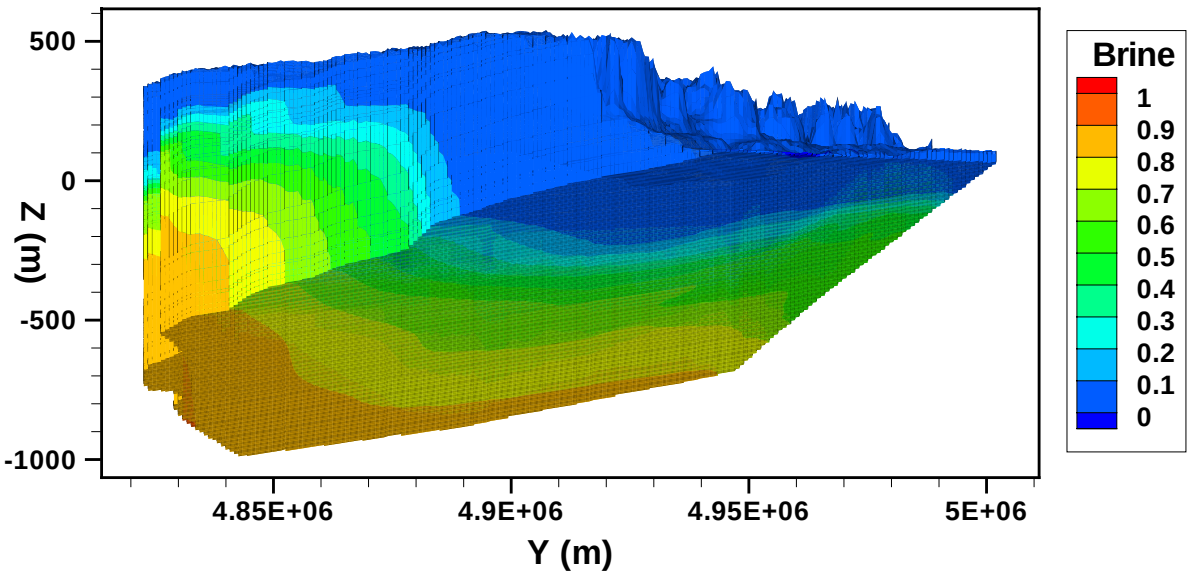

Figure 4.7: Salinity profile after 1 000 000 years using prescribed initial concentrations (back).

source term in the Silurian salt units, the computational time can be effectively halved by using the prescribed initial concentrations. The total dissolved solids distribution for the case with a Silurian source term is presented in the following section.

4.3.2 Alternate Total Dissolved Solids Concentration Distributions

An alternate way to characterize the brine distribution in the model is to use a first-order source term in the Silurian salt units to generate the brine. This method will result in the continual creation of salinty with time, until a maximum relative concentration of 1 is reached. The surface of the model was set as a type 3 boundary condition, except areas beneath Lake Huron and Georgian Bay, which had a prescribed relative concentration of 0. As shown in (Figure 4.8) and (Figure 4.9), the domain is initially free of salinity.

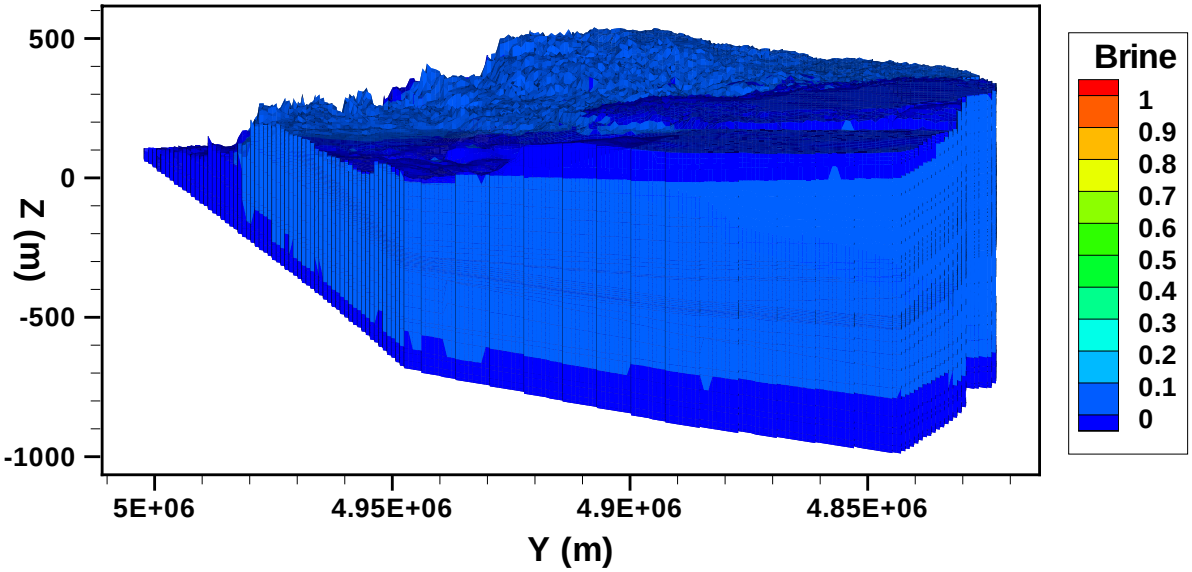

Figure 4.8: Initial salinity profile at 0 years using source term (front).

After sufficient time has passed, the model will reach a pseudo-steady-state brine distribu-

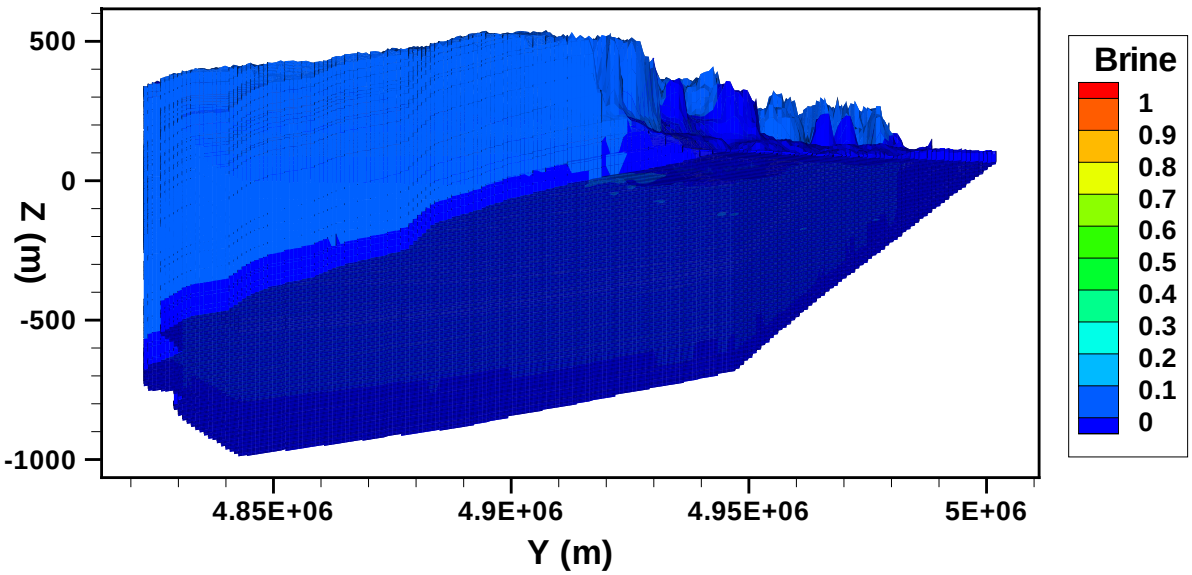

Figure 4.9: Initial salinity profile at 0 years using source term (back).

tion. Figure 4.10 and Figure 4.11 show the brine distribution after 1 000 000 years. The first-order source term should create a salinity profile that is very similar to the profile created by using prescribed initial concentrations. The northeastern part of the domain, specifically at the Niagara Escarpment and beneath Georgian Bay has low concentrations. These low concentrations can be attributed to the freshwater that recharges at the outcrop for the deeper units near Georgian Bay. In regions remote from the escarpment, where there is markedly less impact from Georgian Bay and recharge, the brine accumulates. As was the case based on the prescribed initial concentrations, the formations found at the target horizon of the DGR again have high salinity levels, which will act to reduce groundwater flow rates.

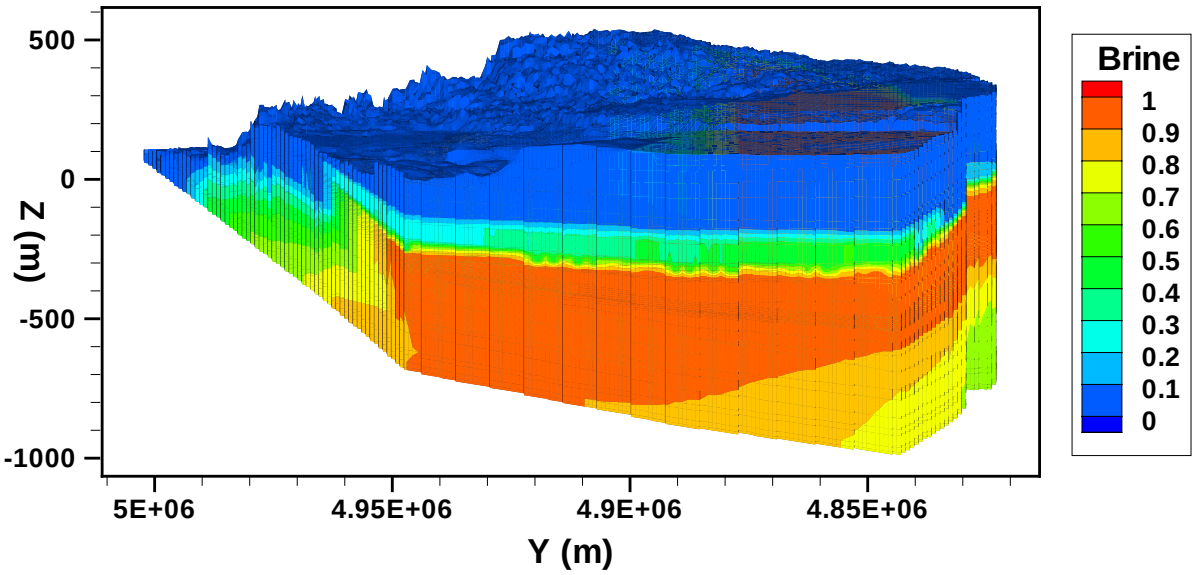

Figure 4.10: Salinity profile after 1 000 000 years using source term (front).

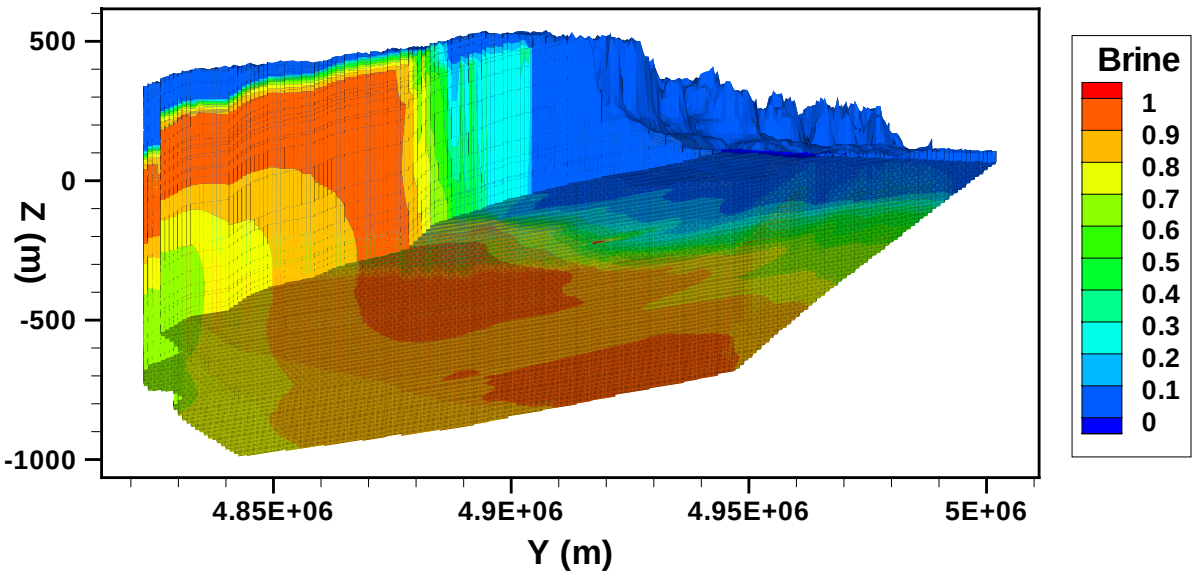

Figure 4.11: Salinity profile after 1 000 000 years using source term (back).

4.4 Alternate Scenarios for Regional Scale System

4.4.1 Alternate Geologic Models

The geologic model conceptualization will play an important role in the way that the groundwater system in the lower flow regime is characterized. The presence and continuity of the impervious salina formation, as well as the tight shales overlying the Cobourg limestone segregates the lower and upper flow regimes. For example, as previously mentioned, the presence of an upper weathering zone at the Niagara Escarpment will play an important role in the ability of the model to transmit pressure from the surface of the model to depth. Without the weathered zone, the lower flow regime has a much higher pressure that must then be propagated through the lower domain (Figure 4.2). It is through the inclusion of the weathered upper region at the escarpment into the geologic model that the pressure is dissipated (Figure 4.3).

Chapter 5

Regional-Scale Groundwater Flow and Brine Migration Analyses

5.1 Analysis of the Base-Case for the Regional Scale Domain

The equivalent freshwater head distribution for the base-case simulation after 1 000 000 years is shown in Figure 5.1 and it clearly demonstrates the segregation of the upper and lower groundwater zones. The upper flow regime is the area which has heads between 200 m and 500 m. It is dominated by flow that mimics topography, similar to that described in the theory by *Toth* [1963]. Beneath the upper groundwater zone, the heads are not controlled to the same extent by the elevation of the surface. The main control for the gradient at depth is the elevation at the Niagara Escarpment, where the geologic formations outcrop, and the density-dependent energy gradients begin to dominate. The head signature will be transmitted from the outcrop area and will be dissipated, depending on the energy gradient, across the domain.

In addition to the elevation component of the gravitational gradient imposed by the Niagara Escarpment, the density of the brines in the deep groundwater zone will act to reduce the energy gradients. The salinity profile for the base-case (Figure 5.2) consists of a relatively fresh groundwater zone, which corresponds with the upper groundwater zone and an area with much higher relative concentrations, which corresponds with the deep groundwater zone. The upper groundwater zone will remain devoid of salinity because the continual higher flow of groundwater through the zone will dilute any salinity, preventing the accumulation of elevated con-

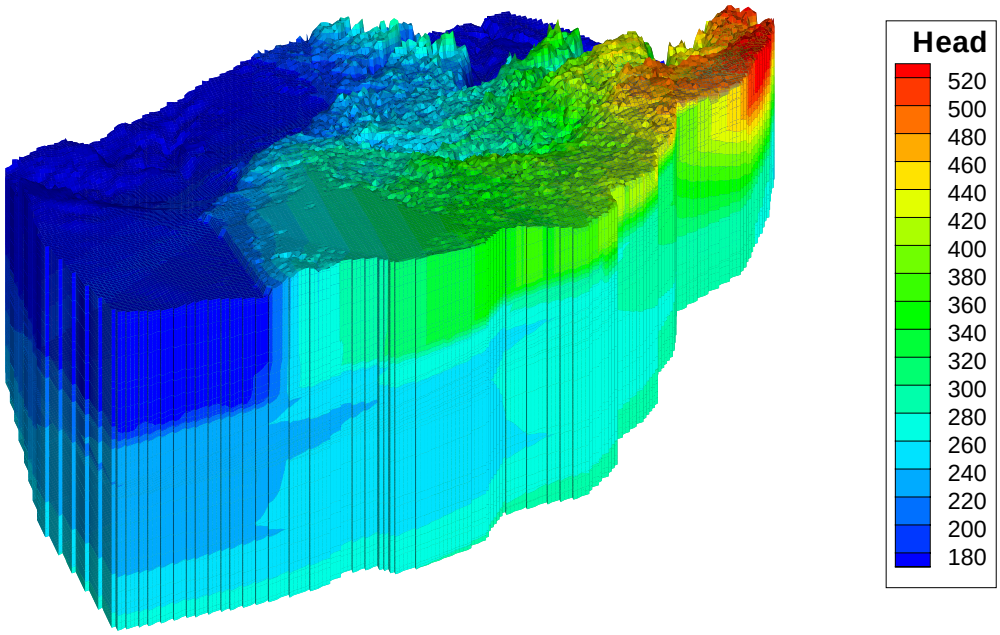

Figure 5.1: Base case head (m) distribution.

centrations. The brine concentrations in the area surrounding the Niagara Escarpment will also experience some flushing as well; however, the higher density groundwater found in the deeper zone that has a higher energy than water with low total dissolved solids will prevent any significant penetration of freshwater into the deep groundwater zone.

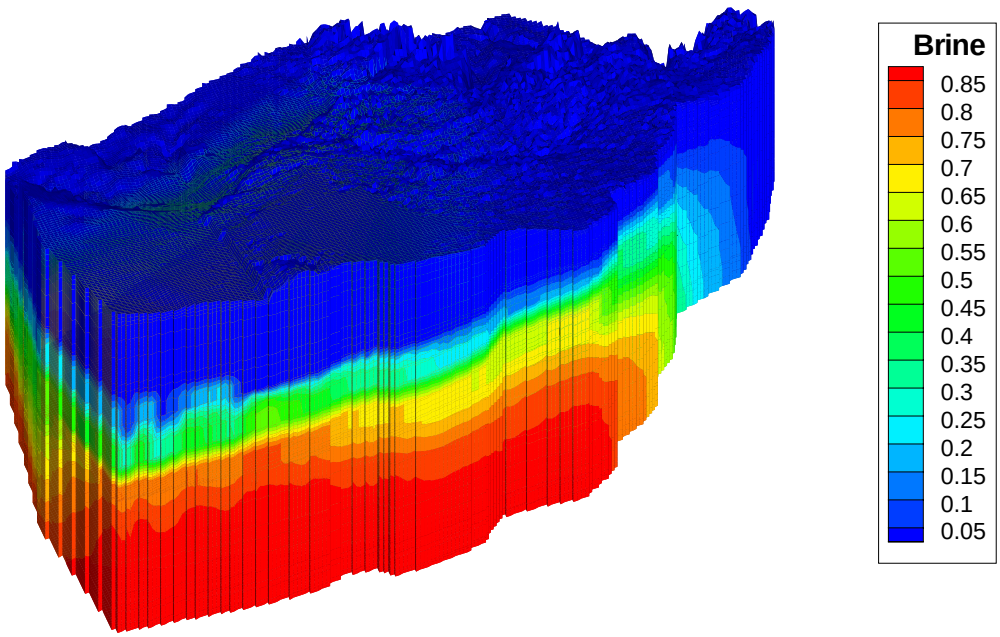

Figure 5.2: Base case relative concentration distribution.

The base-case groundwater velocities(Figure 5.3) demonstrate a similar trend to that which is present in the head distribution (Figure 5.1). The upper groundwater zone, which is highly dependent on topography, has much higher groundwater velocities compared to the deep groundwater zone. The deep groundwater zone typically has average linear groundwater velocities of approximately $0.001\,\mathrm{m/year}$ or less and is diffusion dominated. In the low-permeability Ordovician shale and limestone units these minimal velocities are predominantly either upward or downward with the direction being influenced by surface topography and the thickness of the

overlying Silurian and Devonian units. In the eastern part of the domain, the velocities are generally downward while there is a trend for upward flow at the western part of the regional flow domain.

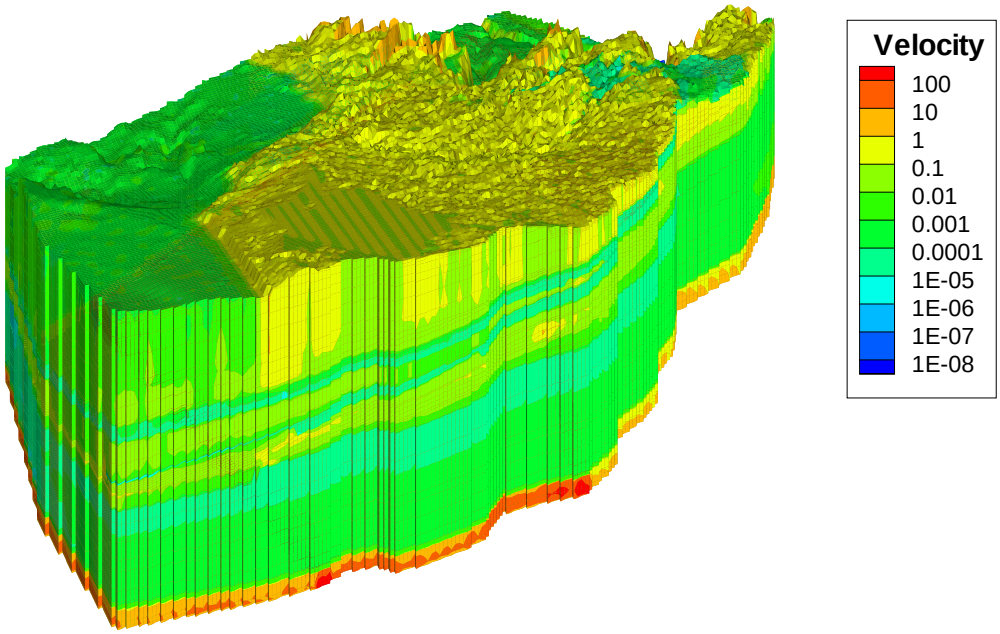

Figure 5.3: Base case velocity (m/a)distribution.

Figure 5.4 displays the base-case velocity distribution in cross-sections, in order to obtain a clearer picture of the velocity field in the formation proposed for the DGR. The velocity in the Cobourg formation near the Bruce DGR site is calculated to be between 1×10^{-5} m/year and 1×10^{-6} m/year.

In the Cambrian formation, the higher groundwater velocities can be attributed to the formation's higher permeability and the assigned porosity. The constant head across the deep groundwater zone, imparted at the Niagara Escarpment, will result in the higher groundwater velocity in the Cambrian compared to the velocities in the overlying lower permeability Ordovician lime-

stone and shale units. The higher groundwater velocities in the Cambrian formation does not have a significant impact on the flow in the Cobourg Formation because of the very low permeability of the Sherman Fall, Kirkfield, Coboconk and Gull River Ordovician limestone units, that act as an aquitard and lay between the Cobourg and the Cambrian formation.

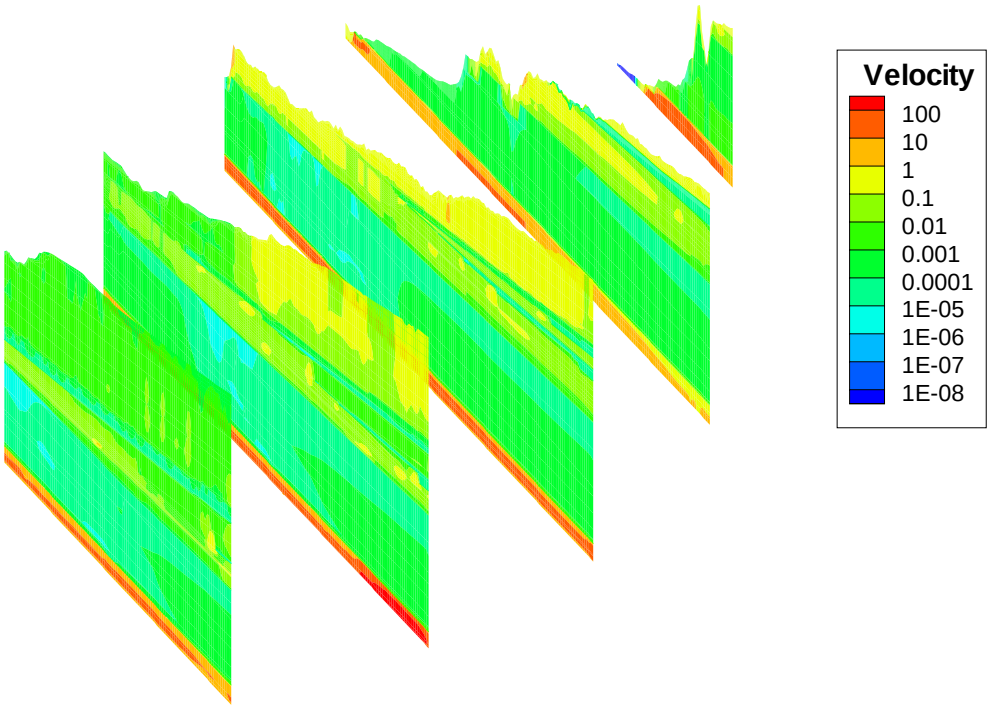

Figure 5.4: Fence diagram of base case velocities (m/a).

Figure 5.5 shows the Peclet numbers calculated for the base-case simulation. The Peclet number is a ratio of the advection to diffusion for a system and as such, it is a useful indicator of the relative importance of advection versus diffusion as transport mechanisms. For the analyses presented in this study, a scale length of unity has been used in calculating the Peclet numbers. The distributions in the figures can thus be readily scaled using, for example, a scale length that reflects longitudinal dispersivity, or a scale length that reflects a pore size. Peclet numbers greater than 1 will correspond to zones with higher groundwater velocities, whereas Peclet numbers less

than 1 will correspond to diffusion-dominant regions. As previously indicated in the discussion on the groundwater velocities (Figure 5.3 and Figure 5.4), the area surrounding the proposed DGR is diffusion dominant with Peclet numbers less than 0.01 with this reflecting the highly diffusion dominated environment.

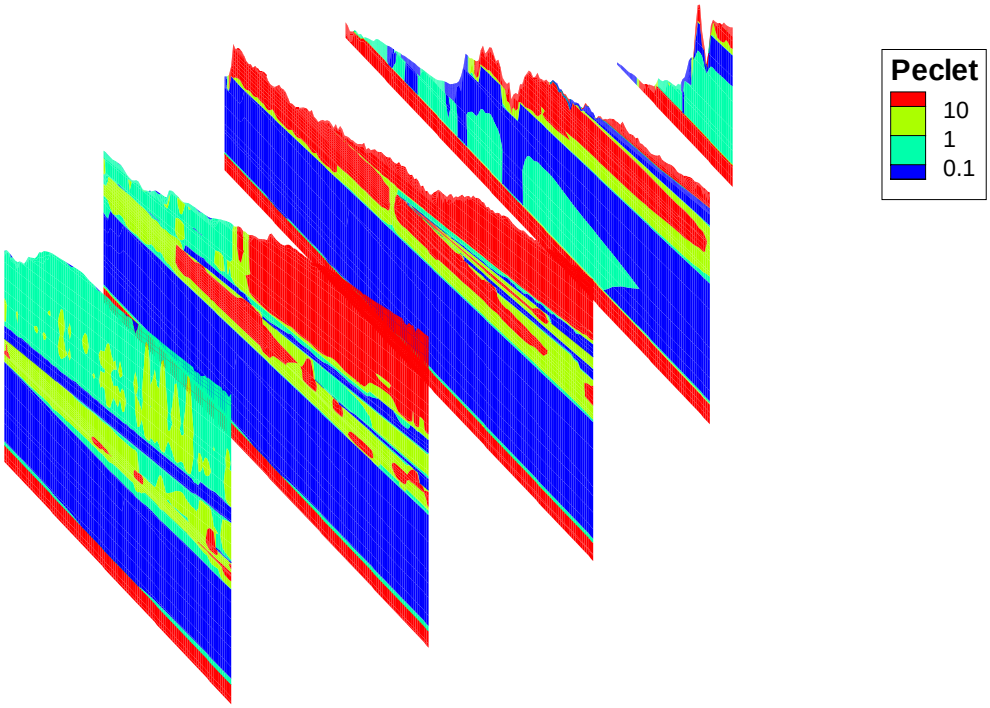

Figure 5.5: Fence diagram of peclet numbers.

The performance measure selected for the evaluation of the groundwater system and calculation of the sensitivity coefficients is the mean life expectancy (Figure 5.6). The general trend for the mean life expectancy is similar to that found in the head and velocity distributions. The upper groundwater zone has significantly shorter life expectancies compared to the deep groundwater zone. The groundwater area surrounding the proposed DGR (shown in a fence diagram, Figure 5.7) is calculated to have a mean life expectancy of approximately 1 500 000 years or greater.

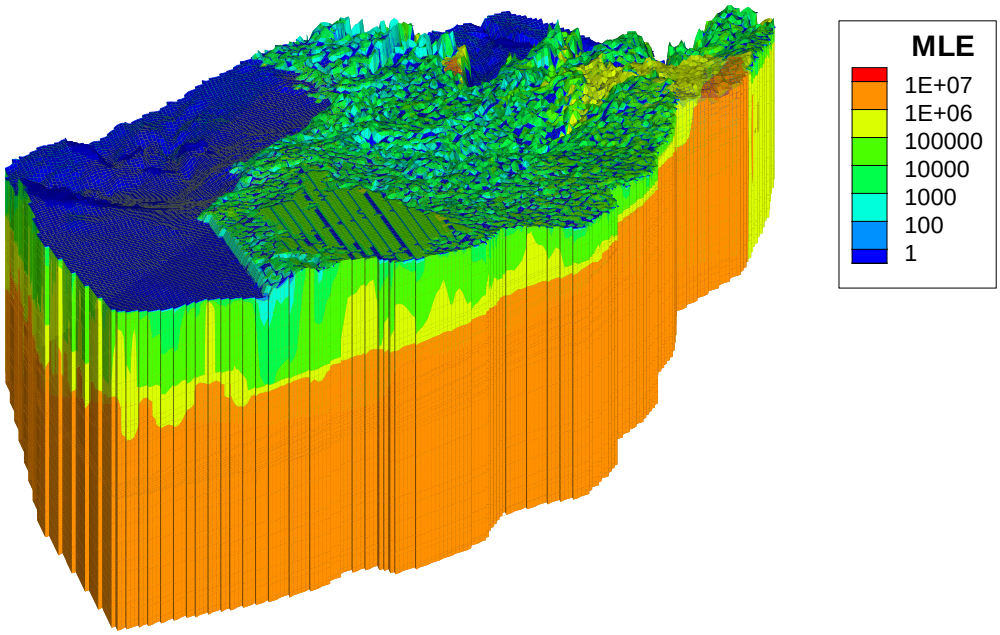

Figure 5.6: Base case mean life expectancies (years).

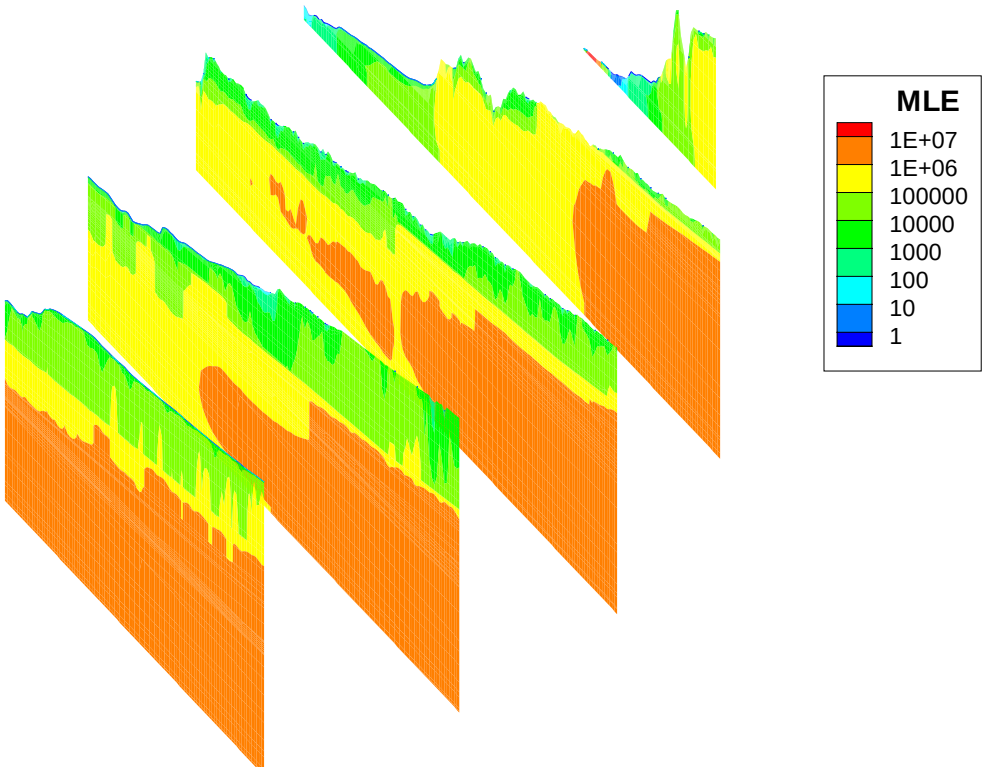

Figure 5.7: Fence diagram of base case mean life expectancies (years).

5.2 Sensitivity Analysis: Alternative Regional Scale Simulations

This investigation has developed a conceptual model of regional groundwater flow in the Bruce Megablock of the Michigan Basin and its effect on flow and transport in the vicinity of the proposed Bruce DGR. Of particular importance in the analysis are the characteristics of the Cobourg Ordovician limestone that is the host unit for the proposed repository. The characteristics relevant to this study include estimated energy gradients, estimated groundwater velocity and calculated pressures at the repository horizon as well as Mean Life Expectancy (MLE). The MLE is an estimate of the average time that a water particle will take to migrate from a point of interest, in this case the repository, to an exit point or biosphere discharge point for the system. The robustness of the estimate of the MLE can be assessed in a sensitivity analysis. This analysis can investigate the sensitivity of the estimate of the MLE to changes in the system parameters. These parameters include the spatial distribution of permeabilities and porosities, the transport parameters including dispersivity, effective diffusion coefficient, and the boundary conditions and initial conditions used to describe the salinity distribution. The sensitivity analysis can also include an investigation of the sensitivity of MLE to the geologic conceptual model and the extent of the regional spatial domain. A complete and thorough analysis of all factors that influence the DGR MLE is beyond the scope of this study, but can be completed as part of subsequent regional-scale investigations. Therefore, this thesis will only investigate the sensitivity of the DGR MLE to the permeability of the low-permeability Ordovician limestone and shale units and the transport parameter dispersivity. The rationale for this subset of parameters is that the primary geologic barrier for the DGR is the Ordovician. Further, the scale of the regional model and the developed discretization is not appropriate for the evaluation of the importance of diffusion processes. This can be be more readily accomplished in a site scale analysis that has multiple model layers for the units such as the Cobourg limestone. Finally, in this thesis, the sensitivity analysis is investigated by calculating the normalized sensitivity coefficients that express the percent change in the MLE that will result from a 1% change in the parameter of interest. These sensitivity coefficients are local derivatives. The range of validity of these derivatives will be investigated in subsequent analyses. The sensitivity coefficients can also depend on the the size of the perturbation of the parameter of interest. While it is common to perturb parameters by several percent in a sensitivity

analysis, because of the very large range in the permeabilities for the 37 geologic units found in this study, parameters were perturbed by a factor of two. This perturbation of the permeabilities by a factor of two was done in order to minimize the effect, if any, of computer round-off errors.

The following sections investigate the sensitivity of the MLE at all grid blocks in the spatial domain to the permeability for the Ordovician units. The sensitivity of MLE to the dispersivity is also developed.

5.2.1 Queenston Shale

Because the Queenston Shale will play an important part in segregating the different groundwater domains, as well as preventing any potential contaminant releases from reaching the surface, it is important to determine how sensitive the model and the estimate of MLE is to the permeability assigned to the unit. In order to quantify the sensitivity of the MLE to the Queenston Shale, its permeability was increased by a factor of two. A fully transient, density-dependent analysis was then undertaken, with the parameters and boundary conditions being identical to the base-case, with the exception of the permeability of the Queenston Shale. Pseudo-equilibrium was assumed to be reached in 1 000 000 years. As expected in a sensitivity analysis that estimates local derivatives, the equivalent fresh water head distribution appears to be very similar to that of the base-case provided in Figure 5.8.

The brine distribution (Figure 5.9) also appears to have few, if any visual differences between the base-case analysis and results obtained with simulation for the perturbed Queenston permeability.

Similar to the base-case velocity distribution, the distribution of velocities (Figure 5.10) for the perturbed Queenston permeability simulation have the pattern of two groundwater zones. The upper groundwater zone is impacted by topography and will have relatively higher velocities than the deep groundwater zone. A fence diagram of the velocities for the perturbed Queenston permeability simulation (Figure 5.11) demonstrate that perturbing the permeability by a factor of two does not result in a significant change in the velocities found in the area of the potential DGR.

A fence diagram of the Peclet numbers for the perturbed Queenston permeability simulation is presented in Figure 5.12. The horizon of the proposed Bruce DGR site is diffusion dominated.

Figure 5.13 displays the mean life expectancies for the perturbed Queenston permeability

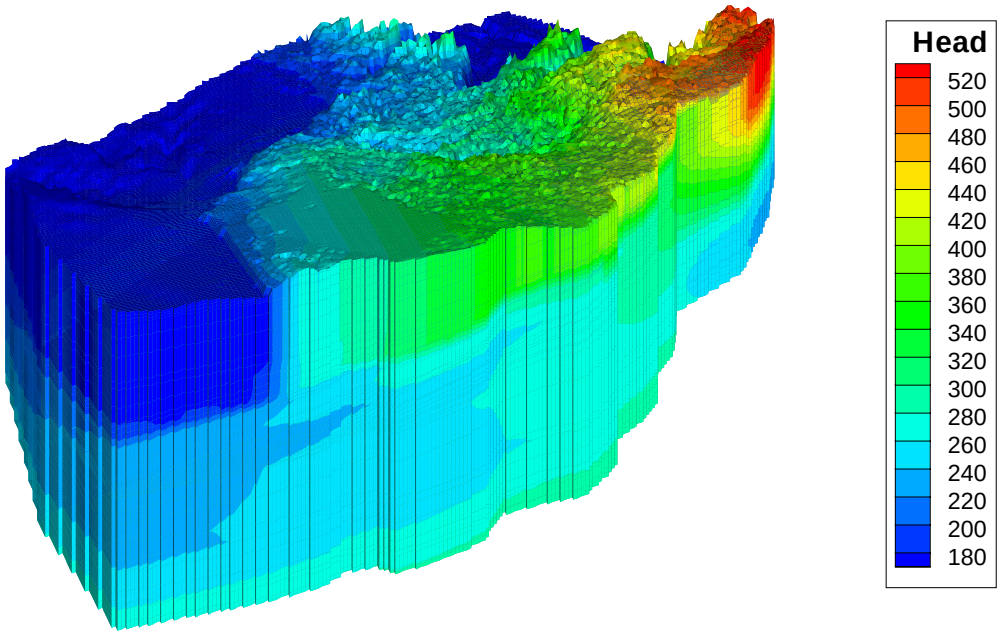

Figure 5.8: Head (m) distribution for Queenston Shale sensitivity analysis.

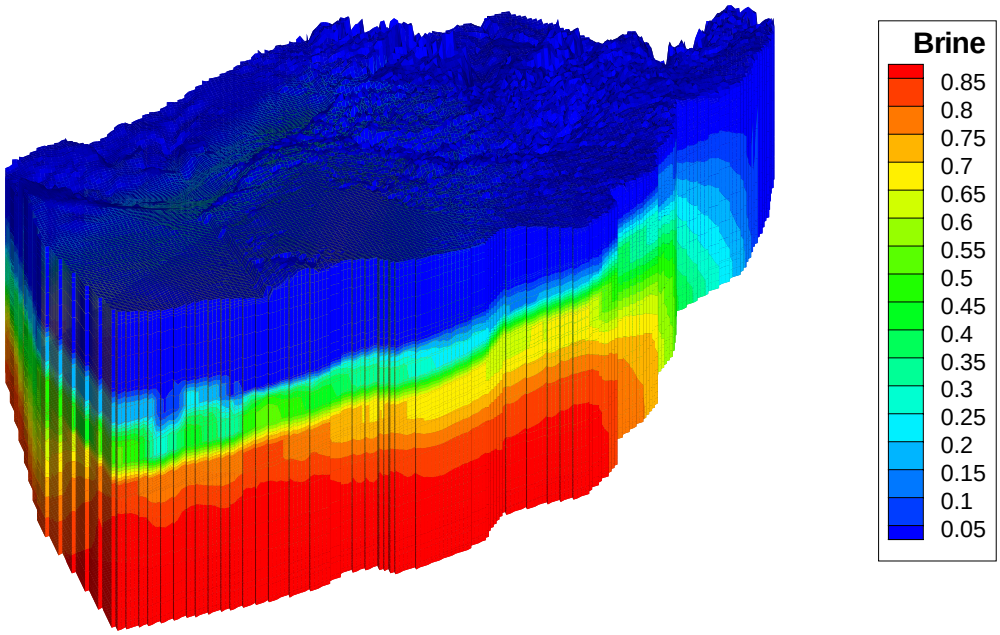

Figure 5.9: Relative concentration distribution for Queenston Shale sensitivity analysis.

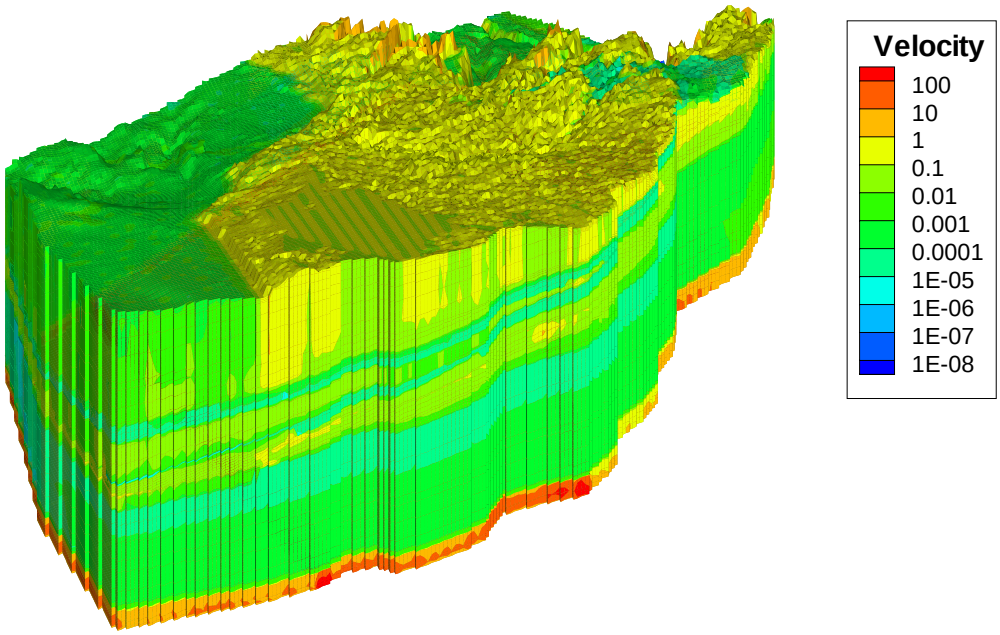

Figure 5.10: Velocity (m/a)distribution for Queenston Shale sensitivity analysis.

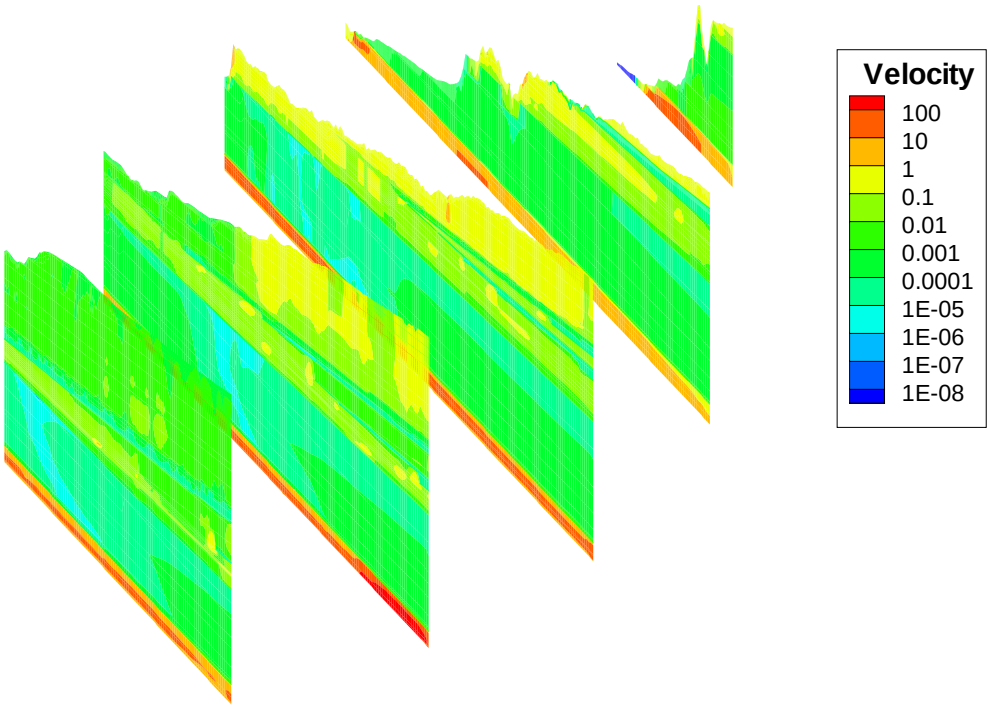

Figure 5.11: Fence diagram showing velocity (m/a)distribution for Queenston Shale sensitivity analysis.

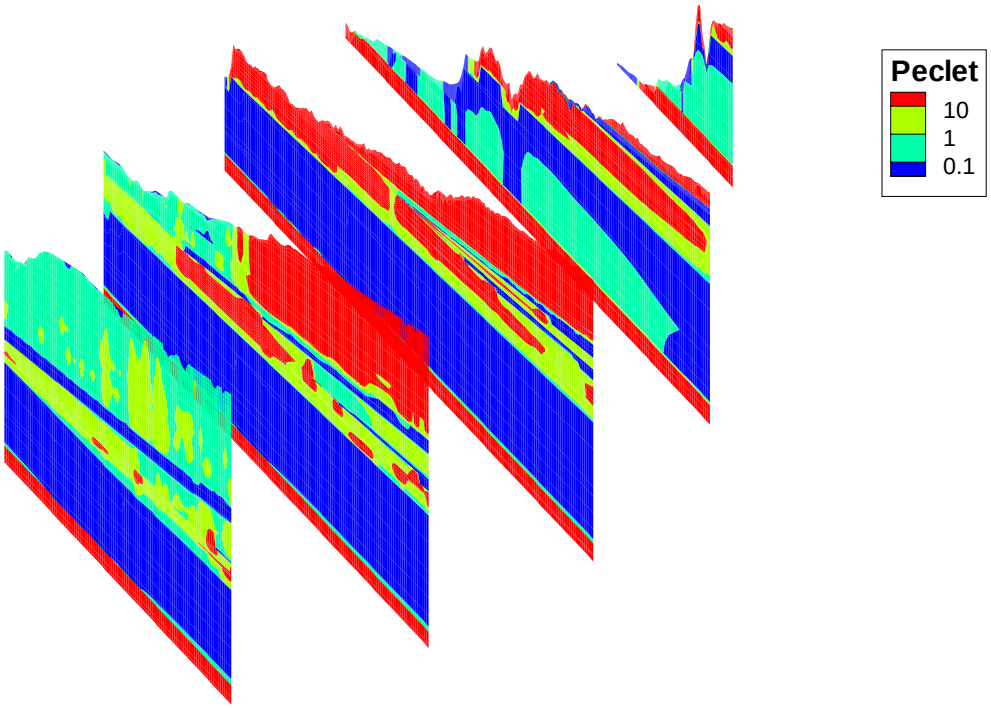

Figure 5.12: Fence diagram of Peclet numbers for Queenston Shale sensitivity analysis.

simulation. The mean life expectancy distribution demonstrates the pattern that results from segregation of the groundwater regimes. The upper groundwater zone will have much younger ages than the older, lower groundwater zone. At the horizon of the proposed Bruce DGR site (Figure 5.14), the groundwater will typically have groundwater ages greater than 1 500 000 years.

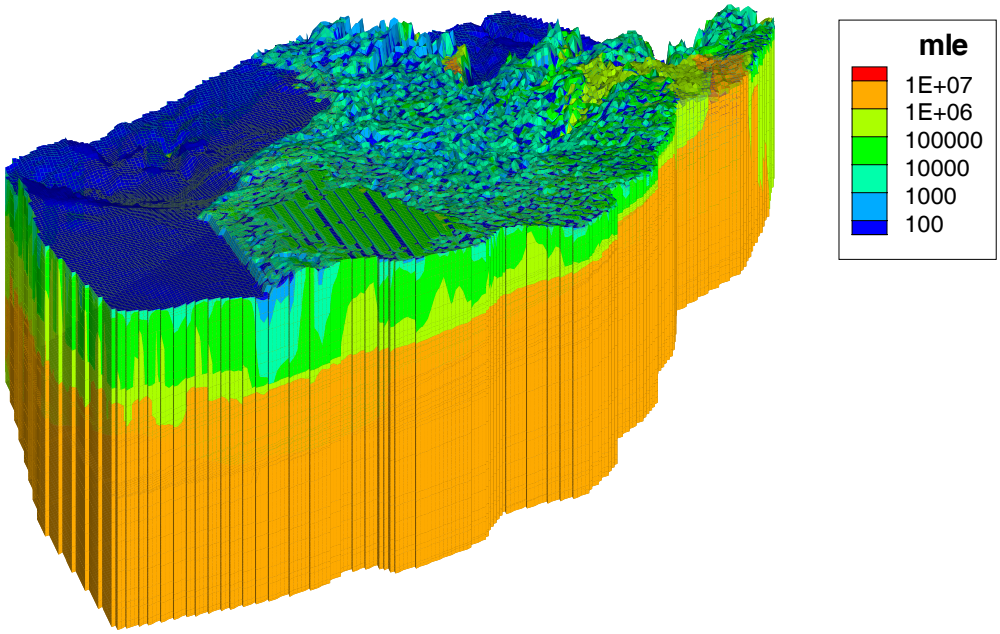

Figure 5.13: Mean life expectancies for Queenston Shale sensitivity analysis (years).

The mean life expectancies for the perturbed Queenston permeability simulation were then used, in conjunction with the mean life expectancies from the base-case analysis, to calculate normalized sensitivity coefficients. The sensitivity coefficients calculated give the sensitivity of the model estimated MLE to a change in the permeability of the Queenston shale. Figure 5.15 shows the distribution of the normalized sensitivity coefficients within the domain. The sensitivity coefficients represent the relative change in the MLE at a given location or point in the system. Thus an increase in the MLE from, for example, 10 years to 15 years will have the same normal-

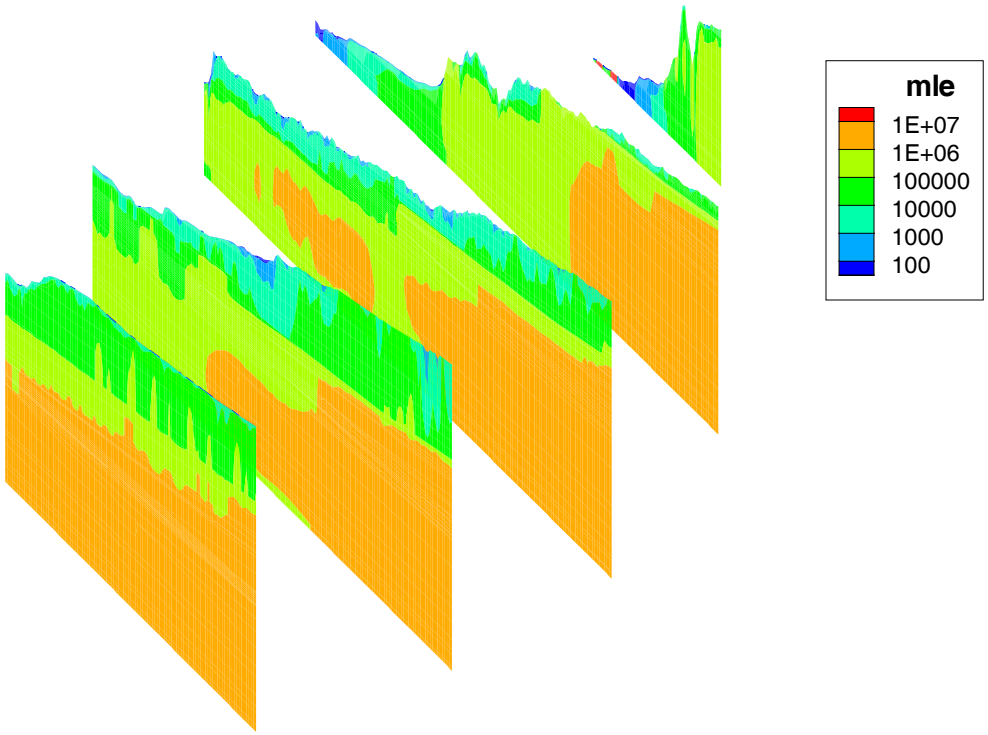

Figure 5.14: Fence diagram of mean life expectancies for Queenston Shale sensitivity analysis (years).

ized sensitivity coefficient as that for a point where the MLE increases from 1 000 000 years to 1 500 000 years. Along the boundary of the domain at points of groundwater discharge, the MLE is insensitive to the change in permeability of Queenston.

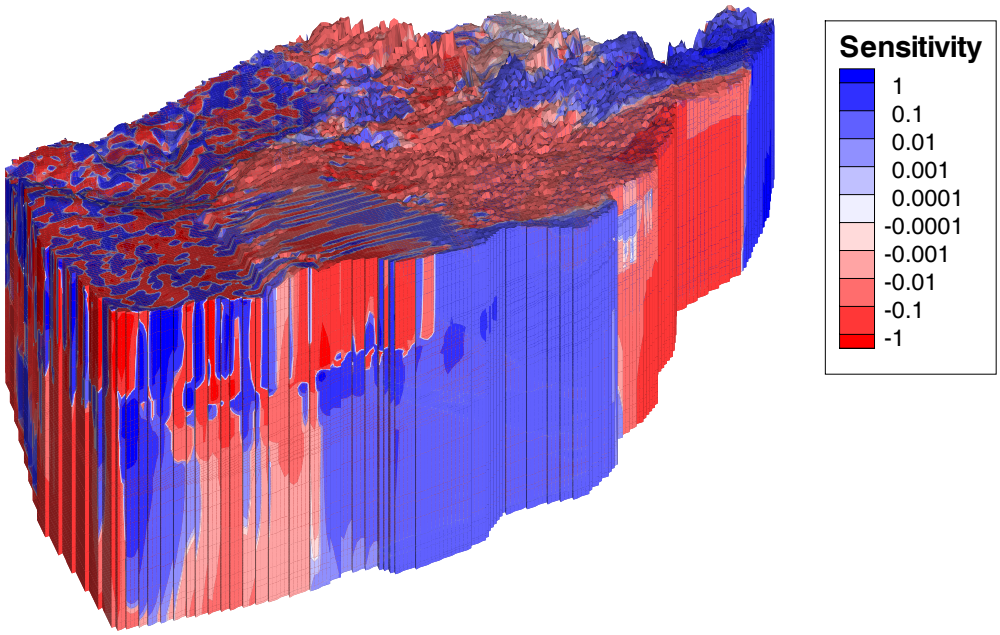

Figure 5.15: Sensitvity coefficients for Queenston Shale permeability.

At the proposed location for the Bruce DRG in the Cobourg (Figure 5.16), the model estimated MLE has a normalized sensitivity of 0.29, which reflects the sensitivity of the proposed horizon to a change in the permeability of the Queenston shale. When the velocity direction vectors are plotted on a cross-section of the sensitivities (Figure 5.17), the areas with the highest sensitivity coefficient can be seen to occur where the predominantly vertically upward or downward velocity vectors change direction. The sensitivity of the MLE is thus related to shifts in the divides in the deep flow system and the resulting change in the flow paths to a biosphere point. The sensitivity coefficients are positive in areas where an increase (decrease) in the Queenston

permeability results in a corresponding increase (decrease) in the MLE. Conversely, negative sensitivity coefficients are predicted where increases (decreases) in the permeability results in a corresponding decrease (increase) in the MLE. It is important to emphasize that the model estimated velocity vectors in the Ordovician units throughout the regional domain are predominantly vertical and that the magnitude of the velocity is very small.

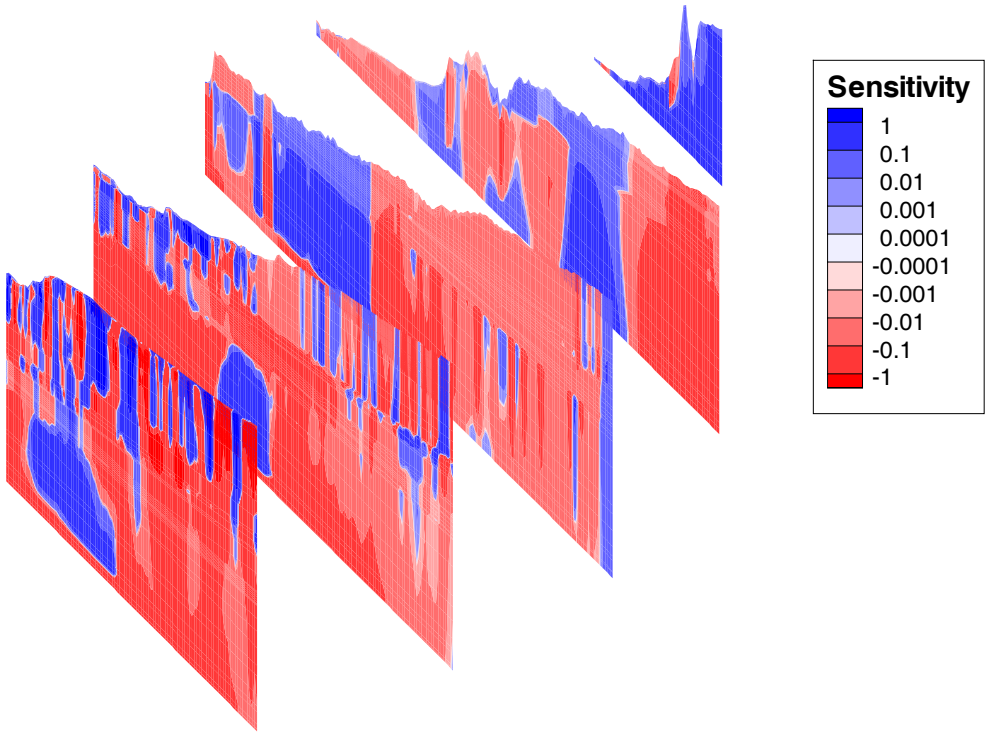

Figure 5.16: Fence diagram of sensitvity coefficients for Queenston Shale permeability.

5.2.2 Georgian Bay Formation

Similar to the Queenston, the Georgian Bay Formation will also play a critical role in the prevention of vertically upward migration from the Cobourg Formation, as well as contribute to the groundwater zone segregation. It is therefore important to determine how sensitive the model

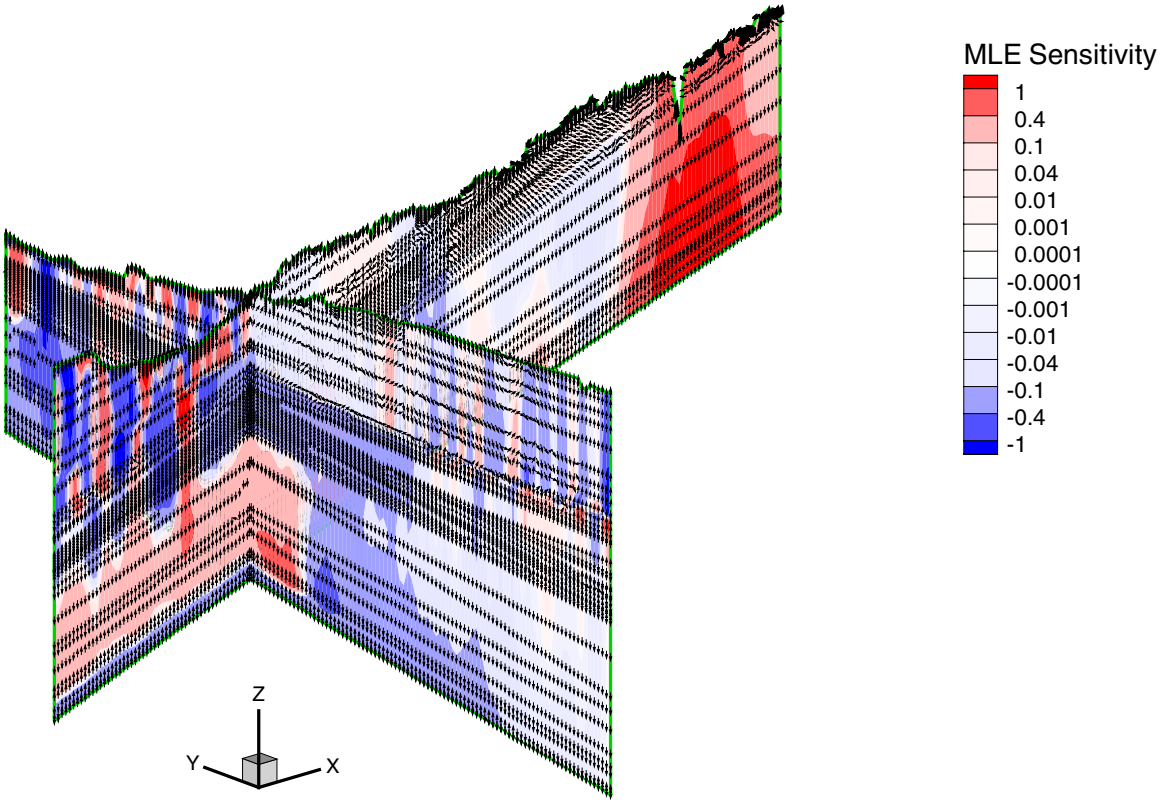

Figure 5.17: Cross-section of sensitivity coefficients for Queenston Shale permeability with velocity vectors.

MLE will be to the permeability assigned to the Georgian Bay Formation. Figure 5.18 displays the equivalent fresh water head distribution for the Georgian Bay permeability analysis. The head distribution for this case demonstrates the groundwater zone segregation seen in the base-case simulations, where the upper groundwater zone, found above the Silurian Salina formation, will be highly influenced by topography. The deep groundwater zone, found beneath the Salina formation, will not be influenced by topographic effects and will have much lower energy gradients.

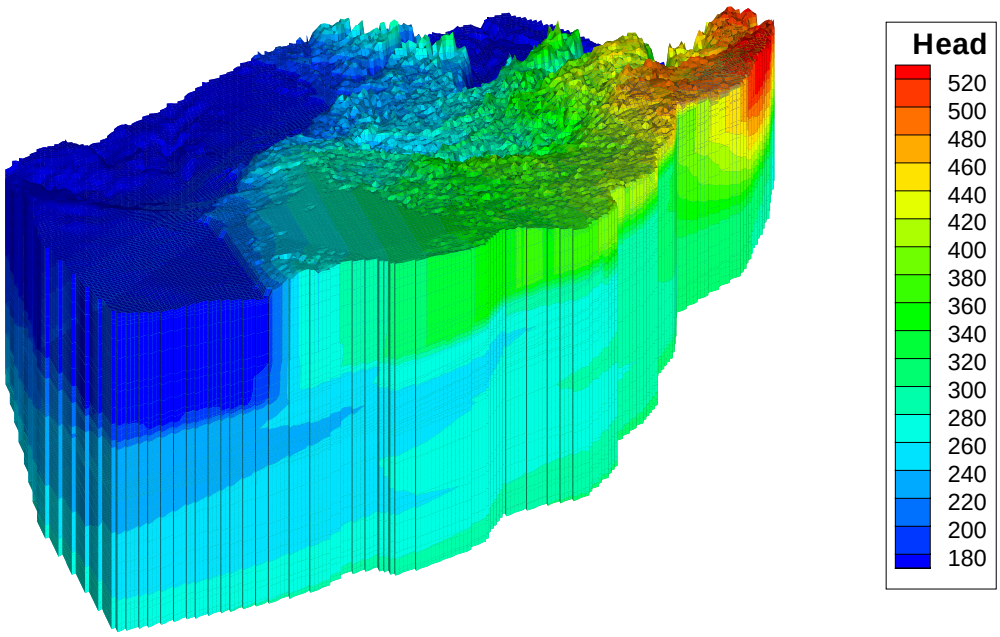

Figure 5.18: Head (m) distribution for Georgian Bay sensitivity analysis.

The brine distribution (Figure 5.19) will not experience much significant change between the Georgian Bay permeability sensitivity simulation and base-case simulations.

The deep groundwater zone, as in the base-case, will have very low groundwater velocities (Figure 5.20). The upper groundwater zone will still be influenced by topography. Even by

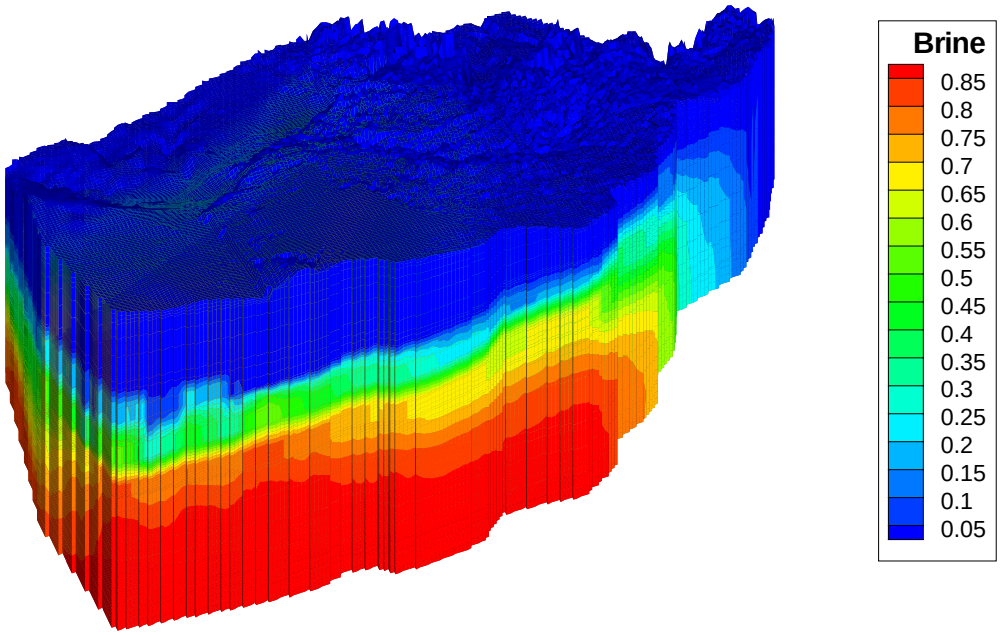

Figure 5.19: Relative concentration distribution for Georgian Bay sensitivity analysis.

doubling the permeability of the Georgian Bay shales, the velocities in the deep groundwater zone are still markedly low.

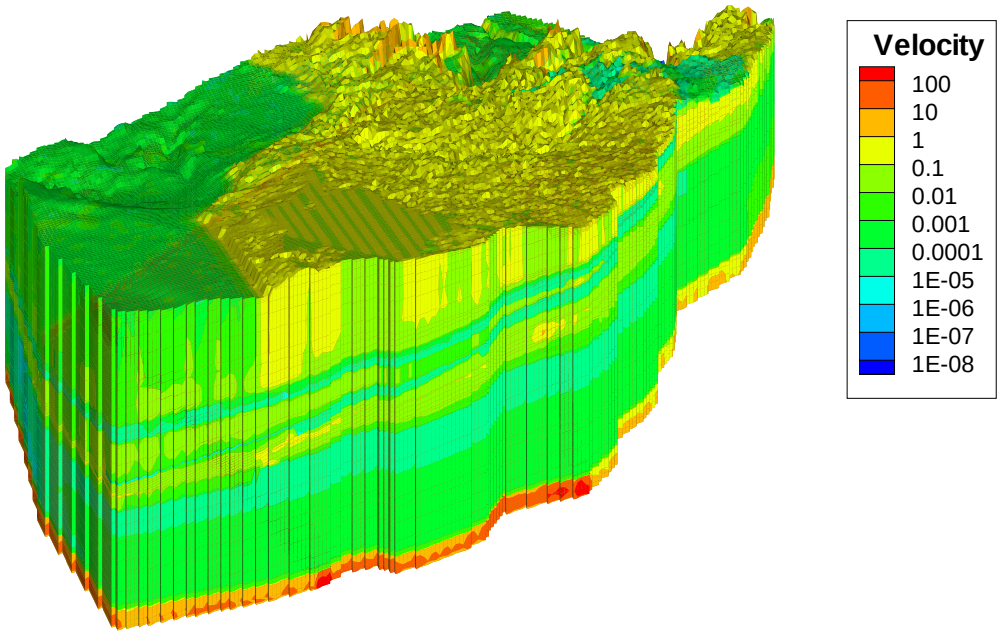

Figure 5.20: Velocity (m/a)distribution for Georgian Bay sensitivity analysis.

The proposed horizon for the Bruce DGR in the Cobourg, seen in Figure 5.21, will have groundwater velocities between 1.0×10^{-4} m/year and 1.0×10^{-5} m/year.

The Peclet numbers, good indicators of either advective or diffusional flow, are displayed in Figure 5.22. The Peclet number for the horizon of the proposed Bruce DGR site is well within the range of diffusional dominance, with a Peclet number of 0.01 or less.

The mean life expectancies for the Georgian Bay permeability sensitivity analysis also demonstrates the pattern of groundwater zone segregation (Figure 5.23). The mean life expectancies for the deep groundwater zone are calculated to be very old, whereas the upper groundwater zone, which has much higher groundwater velocities, will have younger ages.

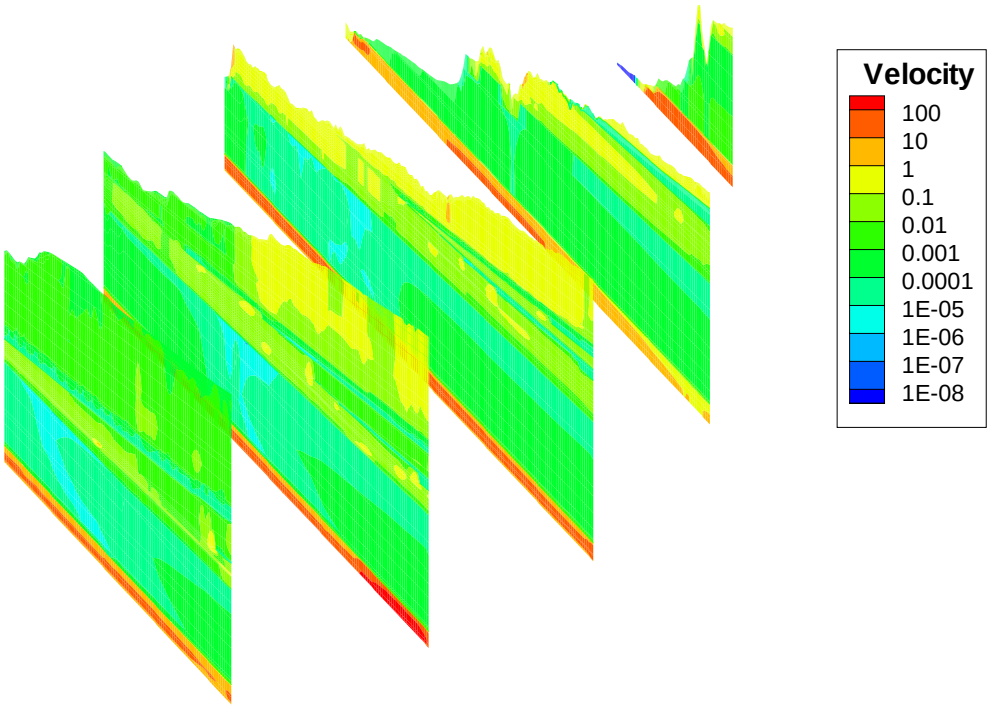

Figure 5.21: Fence diagram showing velocity (m/a)distribution for Georgian Bay sensitivity analysis.

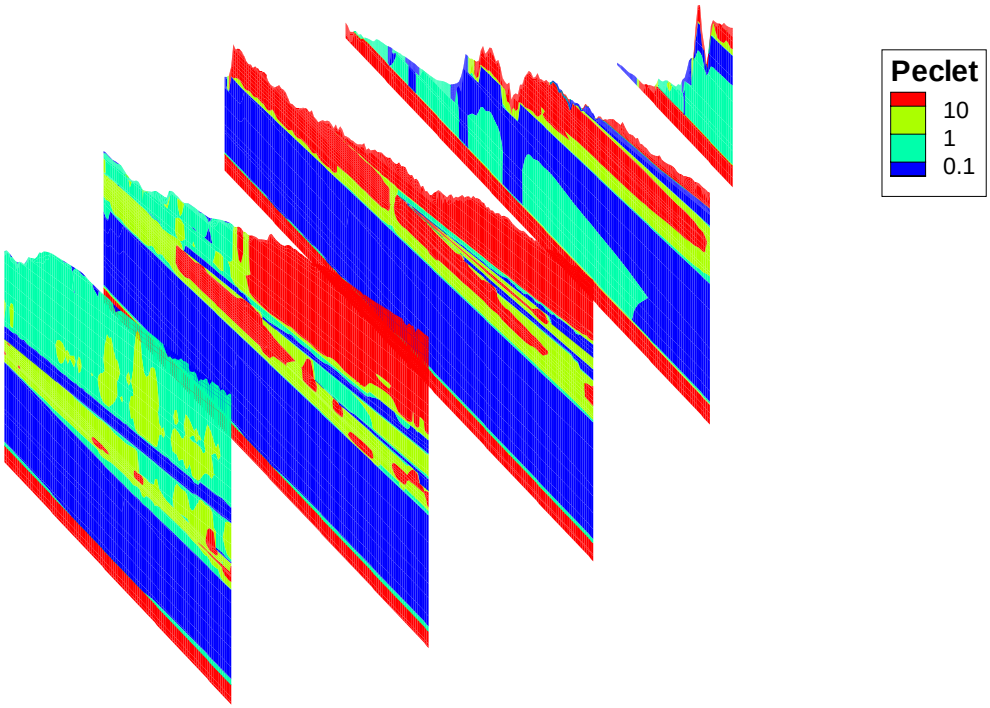

Figure 5.22: Fence diagram of Peclet numbers for Georgian Bay sensitivity analysis.

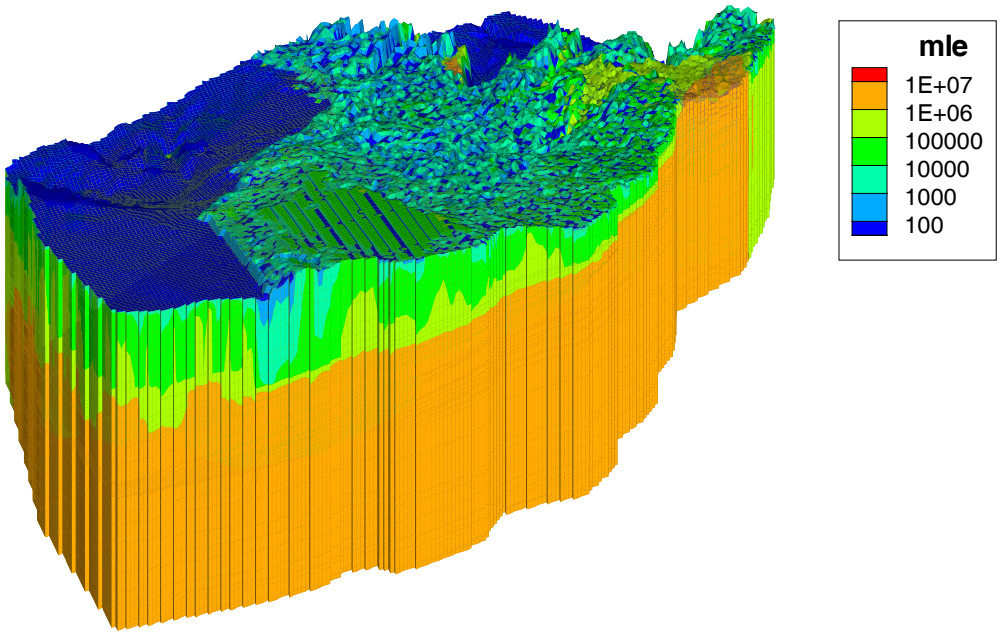

Figure 5.23: Mean life expectancies for Georgian Bay sensitivity analysis (years).

At the horizon of the proposed Bruce DGR, the life expectancy for groundwater is computed to be greater than 1.5×10^6 years (Figure 5.24).

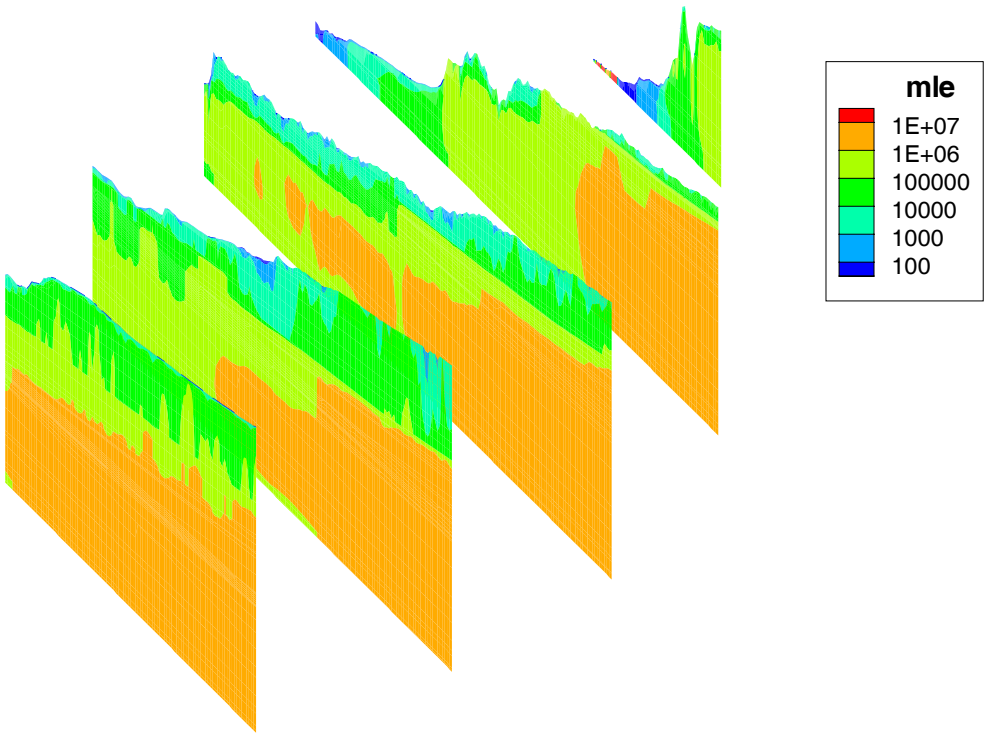

Figure 5.24: Fence diagram of mean life expectancies for Georgian Bay sensitivity analysis (years).

The mean life expectancies for the Georgian Bay permeability sensitivity simulation were used to calculate the sensitivity of the model MLE to a change in permeability of the Georgian Bay shales. The sensitivity was normalized in order to facilitate comparison. Figure 5.25 displays the calculated sensitivity coefficients. The pattern of the sensitivity coefficients is similar to that of the Queenston Shale analysis. Higher sensitivities are associated with shifts in groundwater divides and the resulting change in flow paths. The sensitivity coefficients are low at points of groundwater discharge.

At the horizon of the proposed Bruce DGR, seen in Figure 5.26, the model is relatively

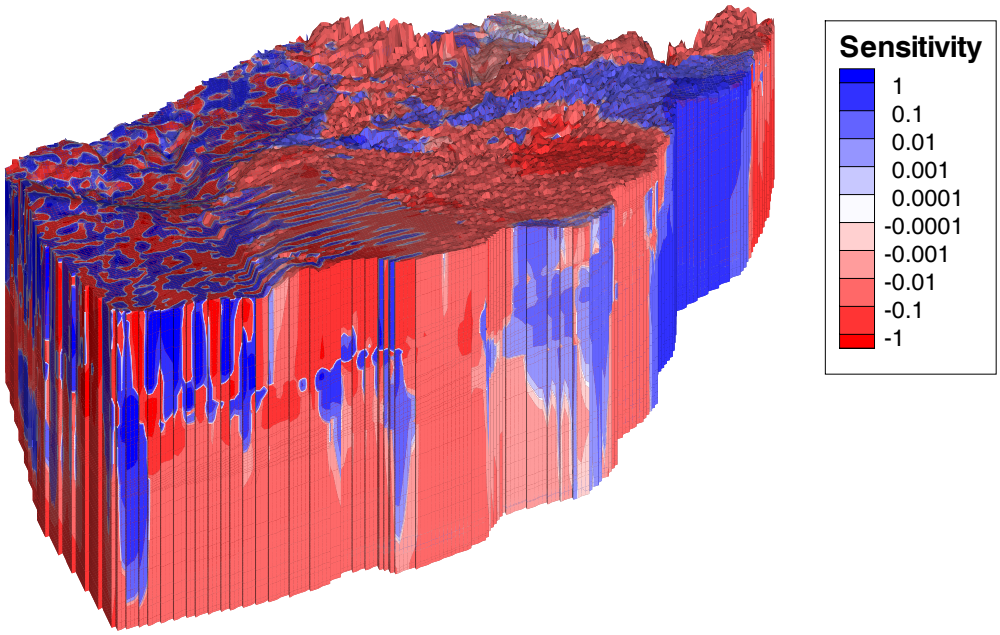

Figure 5.25: Sensitvity coefficients for Georgian Bay permeability.

insensitive to the change in permeability of the Georgian Bay shale.

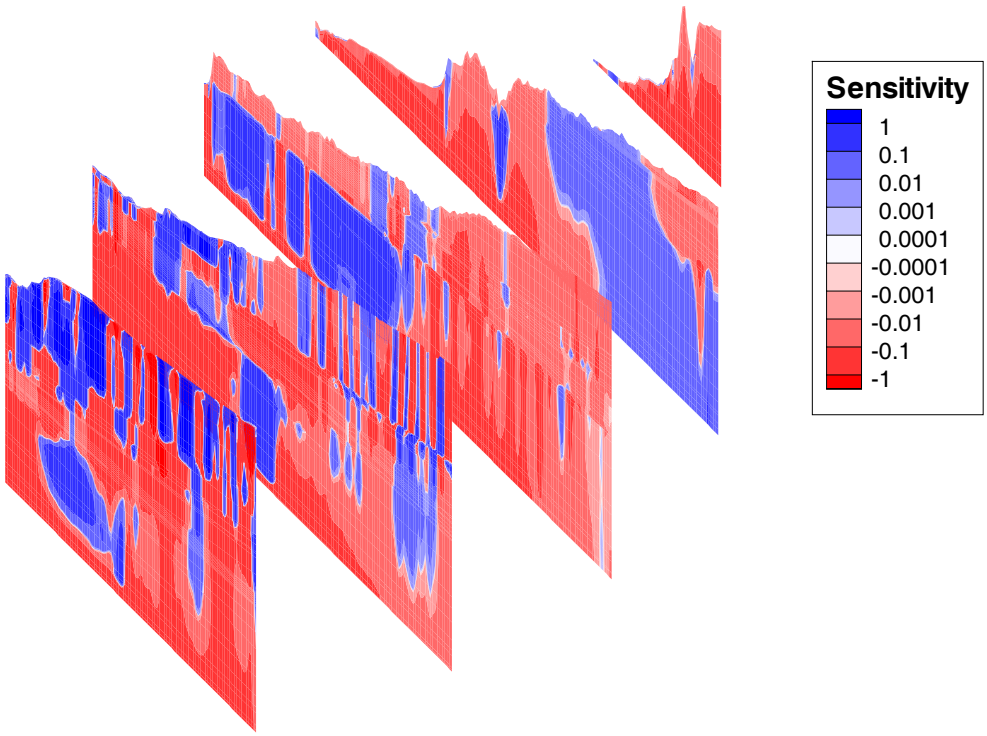

Figure 5.26: Fence diagram of sensitvity coefficients for Georgian Bay permeability.

5.2.3 Collingwood Formation

Because the Collingwood Formation lies directly above the Cobourg Formation, it is important to determine any impact on uncertainty in the permeability of the Collingwood Formation will have on the model estimated MLE. This is important because the Collingwood Formation, along with the other lower Ordovician shales will comprise one of the barriers preventing contaminant migration to the surface. In order to determine the sensitivity coefficient, the permeability of the Collingwood limestone was increased by a factor of two.

Figure 5.27 displays the equivalent freshwater head distribution for the Collingwood perme-

ability sensitivity analysis. Despite the change in the permeability of the Collingwood Formation, the head distribution still has the distinct pattern of the groundwater zone segregation.

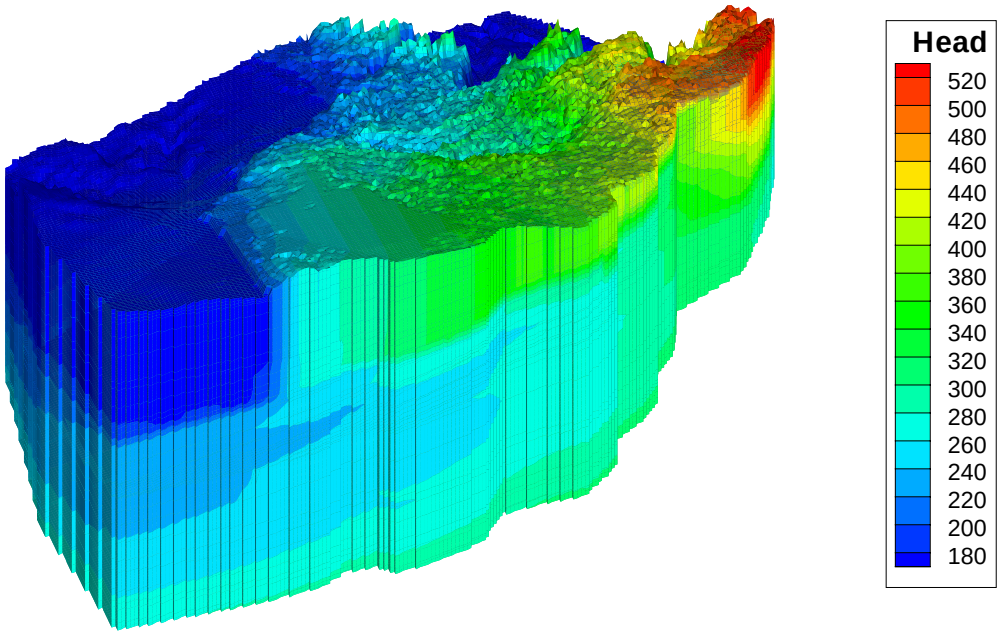

Figure 5.27: Head (m) distribution for Collingwood sensitivity analysis.

The brine distribution (Figure 5.28) does not exhibit any significant change between the Collingwood permeability sensitivity simulation and the base-case simulation.

Figure 5.29 displays the groundwater velocity distribution for the Collingwood permeability sensitivity simulation. The estimated groundwater velocity still displays the pattern of groundwater zone segregation, with the upper groundwater zone having higher velocities, whereas the deep groundwater zone has much, much lower groundwater velocities.

At the horizon of the proposed Bruce DGR, the groundwater velocities (Figure 5.30) remain very low, between 1.0×10^{-4} m/year and 1.0×10^{-5} m/year.

The Peclet number for the horizon of the proposed DGR (Figure 5.31), because of the very

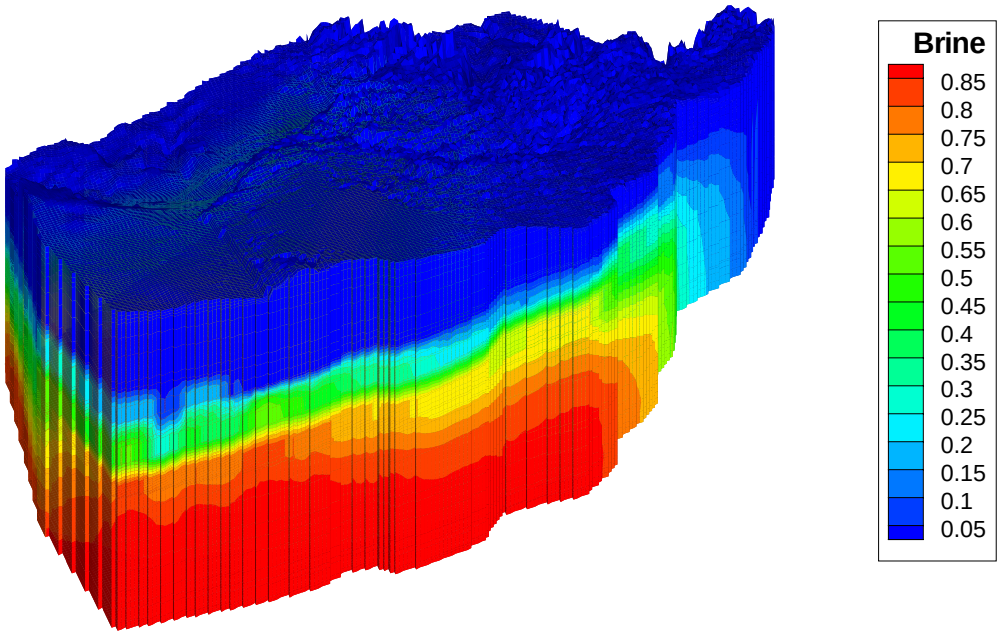

Figure 5.28: Relative concentration distribution for Collingwood sensitivity analysis.

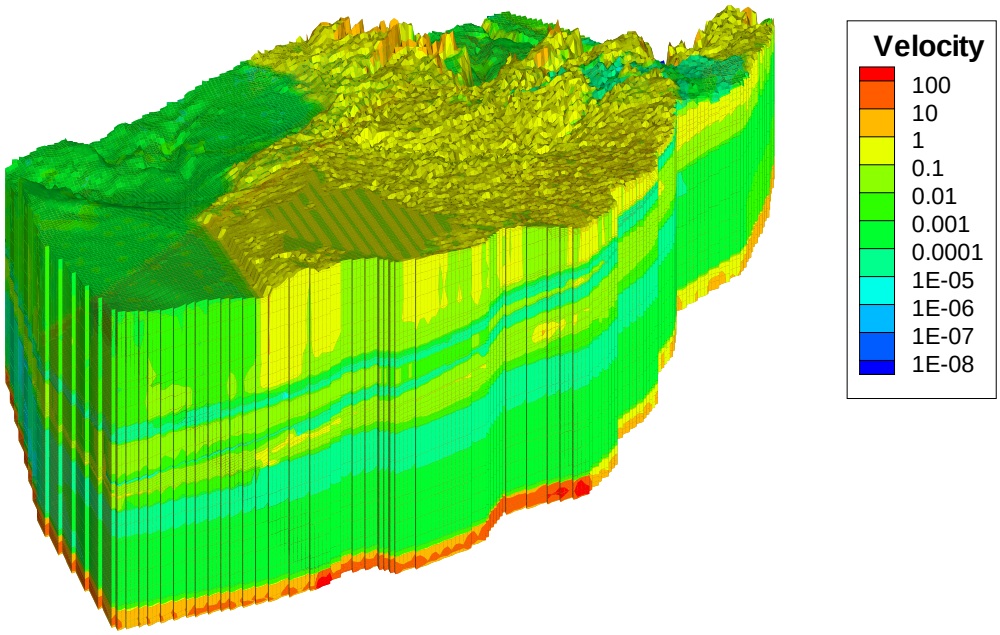

Figure 5.29: Velocity (m/a) distribution for Collingwood sensitivity analysis.

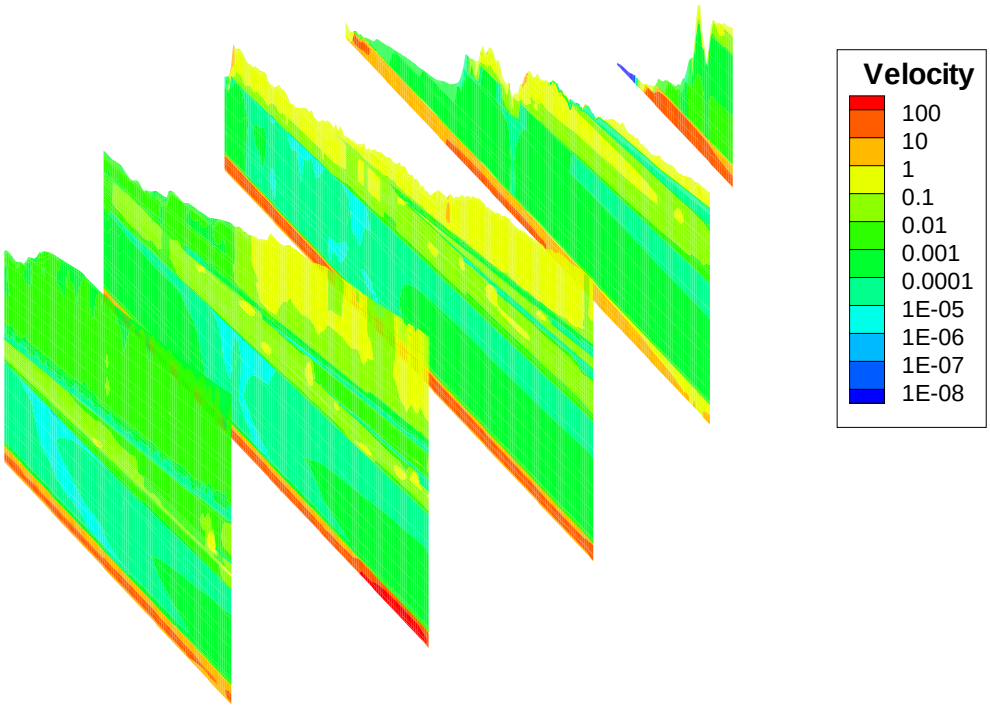

Figure 5.30: Fence diagram showing velocity (m/a) distribution for Collingwood sensitivity analysis.

low groundwater velocities, is still calculated to be dominated by diffusional transport.

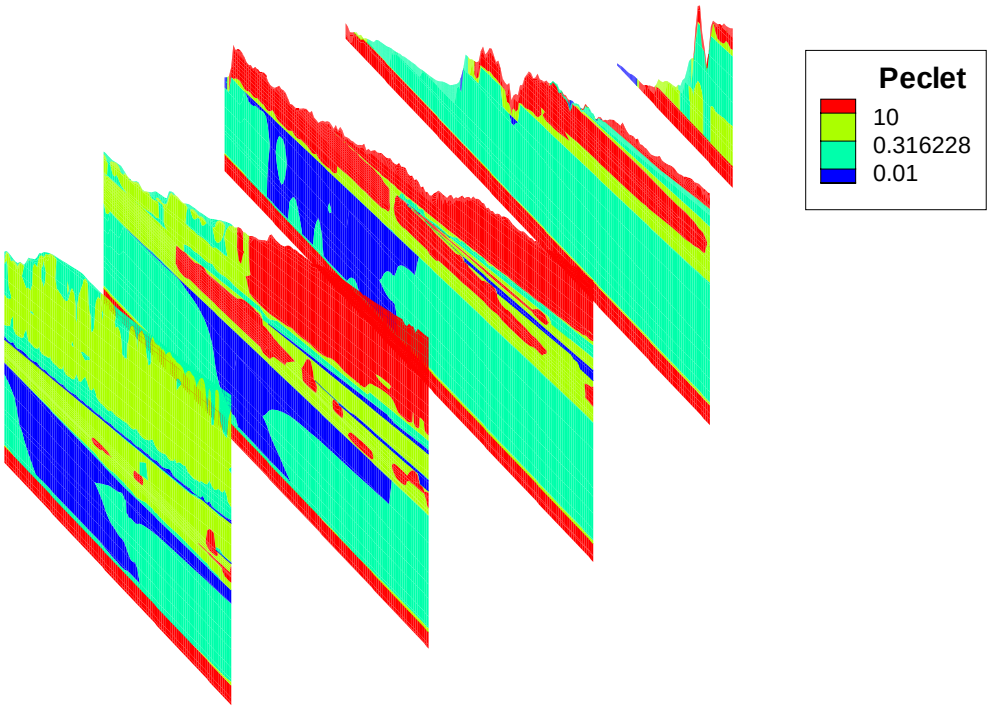

Figure 5.31: Fence diagram of Peclet numbers for Collingwood sensitivity analysis.

The mean life expectancies for the Collingwood permeability sensitivity simulation can be found in Figure 5.32. The pattern of groundwater zone segregation, seen in the head and velocity distributions, will also be present in the the mean life expectancy distribution. The upper groundwater zone have much younger ages than the older, lower groundwater zone. At the horizon of the proposed Bruce DGR site (Figure 5.33).

The mean life expectancies for the Collingwood permeability sensitivity simulation were used to calculate sensitivity coefficients. These coefficients quantify the sensitivity of the regional model MLE distribution to a change in the permeability of the Collingwood Formation. Figure 5.34 displays the sensitivity coefficients. Because the Collingwood Formation is a much thinner unit than the Georgian Bay and the Queenston, the model estimated MLE is much less

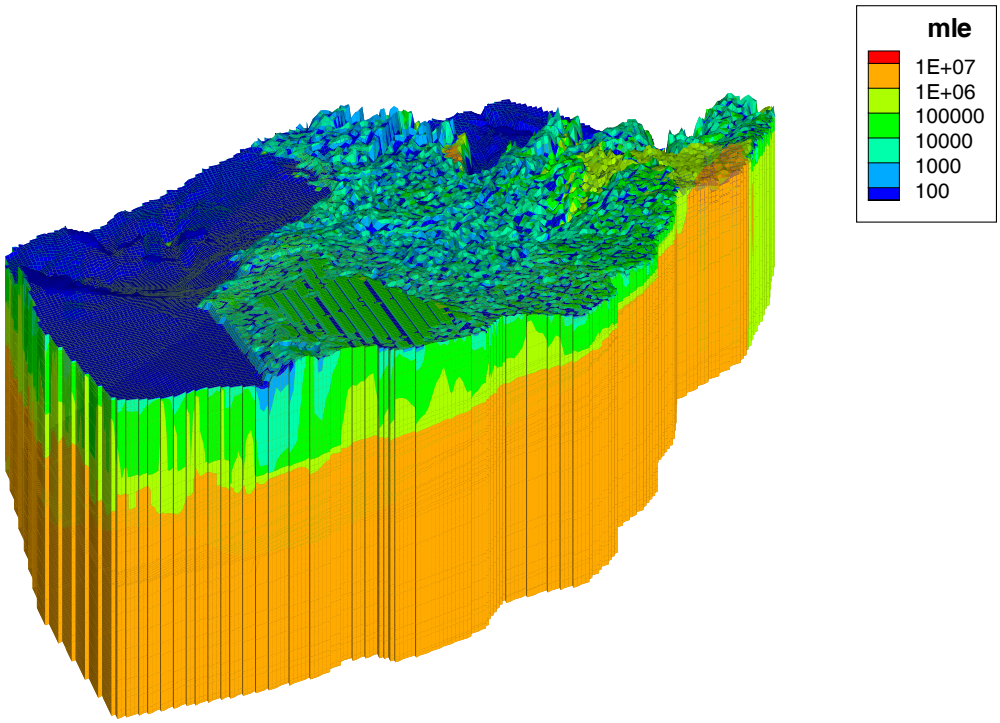

Figure 5.32: Mean life expectancies for Collingwood sensitivity analysis (years).

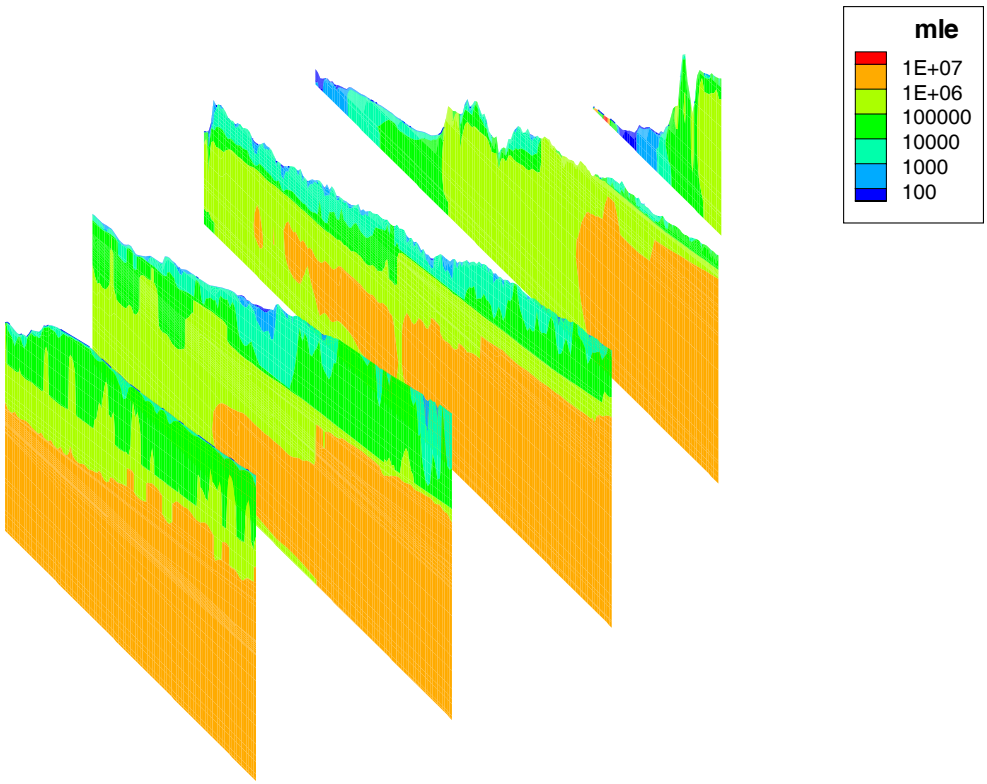

Figure 5.33: Fence diagram of mean life expectancies for Collingwood sensitivity analysis (years).

sensitive, with sensitivity coefficients approaching zero. In the area of the proposed DGR (Figure 5.35), the model MLE is insensitive to changes in the Collingwood permeability.

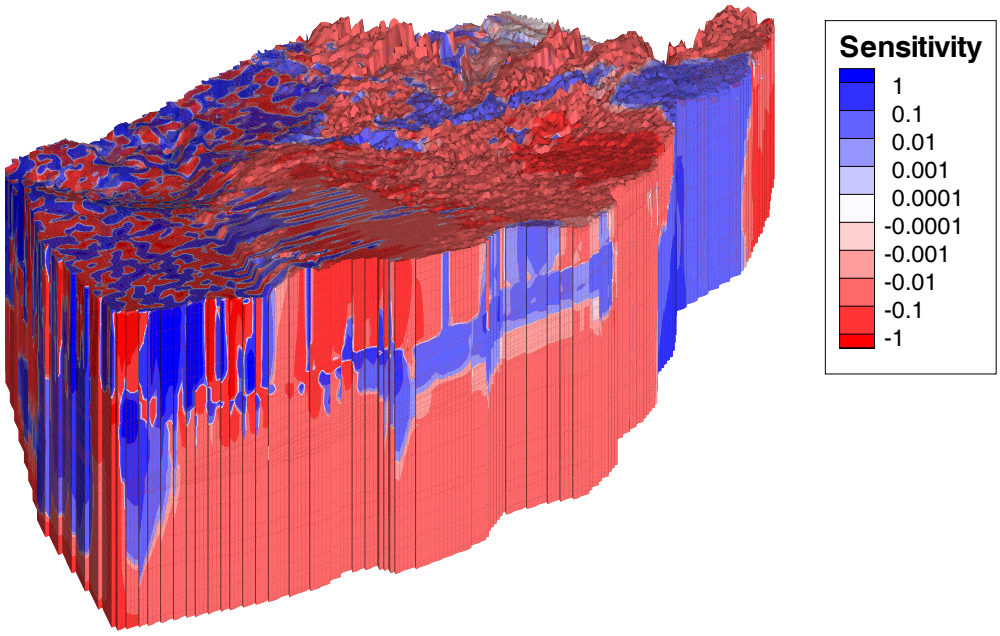

Figure 5.34: Sensitvity coefficients for Collingwood permeability.

5.2.4 Cobourg Formation

The final sensitivity analysis that was performed concerns the permeability of the Cobourg limestone. This unit is of crucial importance to the safety of the system since it is the target horizon and as such, any sensitivity the model estimated MLE may have to the permeability of the Cobourg limestone should be assessed. In order to determine the sensitivity of the model MLE, the permeability of the Cobourg limestone will be increased by a factor of two.

The equivalent freshwater head distribution for this scenario, found in Figure 5.36, demon-

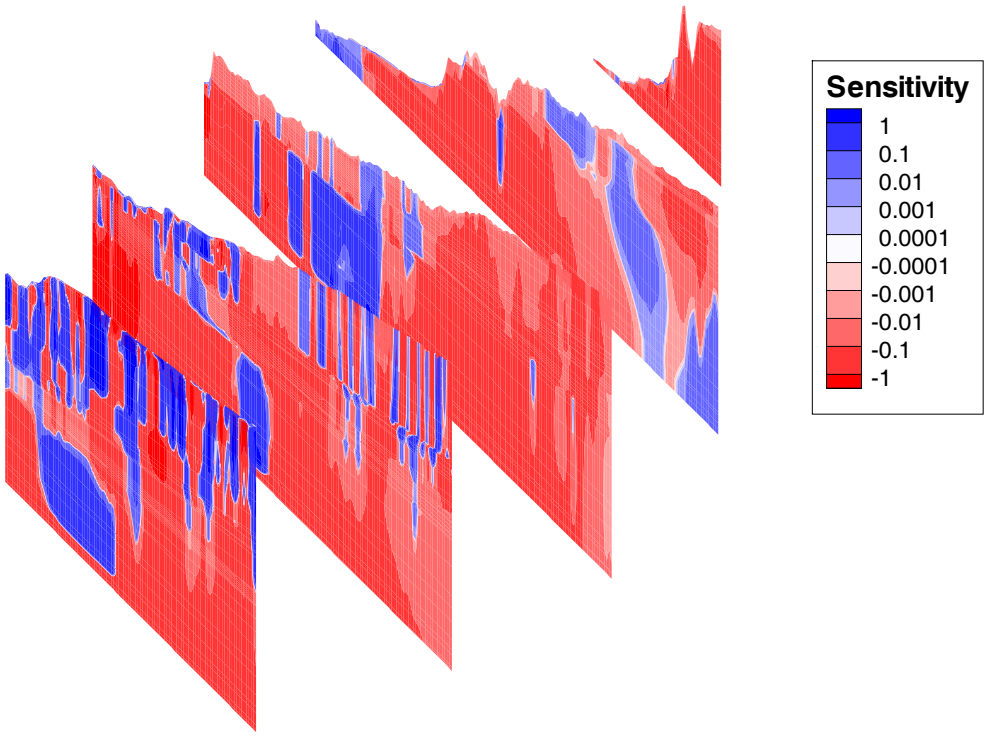

Figure 5.35: Fence diagram of sensitvity coefficients for Collingwood permeability.

strates the typical pattern of the groundwater zone segregation, with the heads of the upper zone influenced by the elevation of the surface and with the deep groundwater zone having much lower, almost negligible gradients.

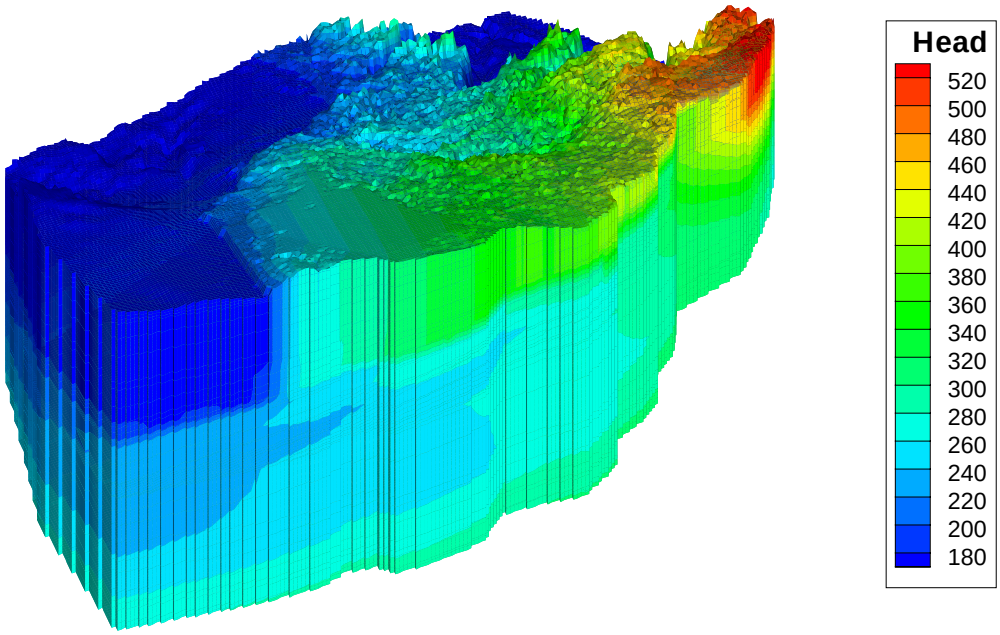

Figure 5.36: Head (m) distribution for Cobourg sensitivity analysis.

The brine distribution (Figure 5.37) also does not exhibit any significant change between the Cobourg permeability sensitivity simulation and base-case simulation.

Similar to the head distribution, the distribution of the velocities (Figure 5.38) also exhibit the signature of groundwater zone segregation. The upper groundwater zone has much higher groundwater velocities when compared with the velocities of the deep groundwater zone. The deep groundwater zone (seen in cross-section in Figure 5.39) has computed velocities between 1.0×10^{-4} m/year and 1.0×10^{-5} m/year.

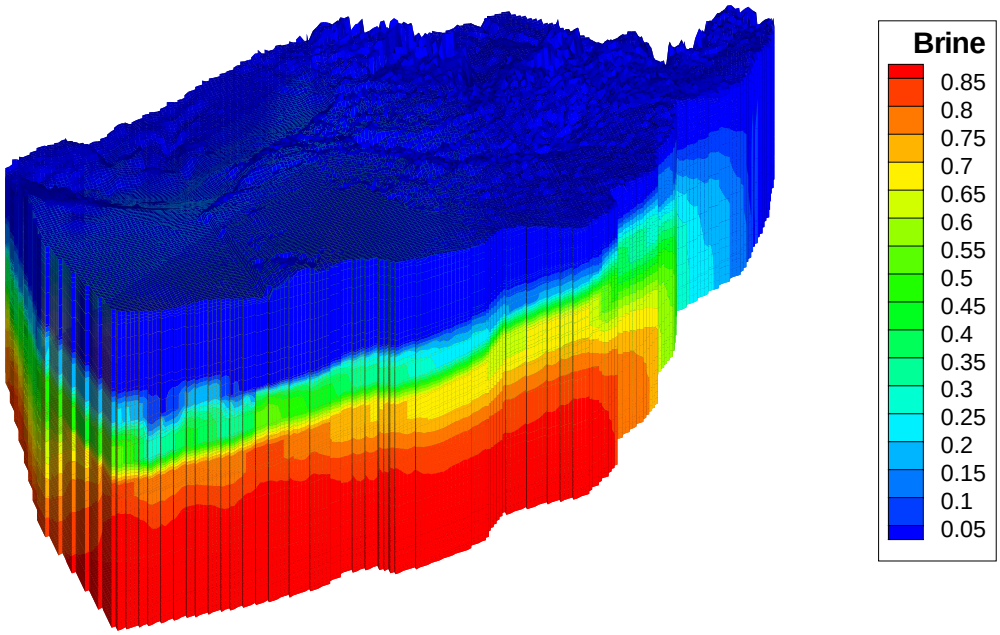

Figure 5.37: Relative concentration distribution for Cobourg sensitivity analysis.

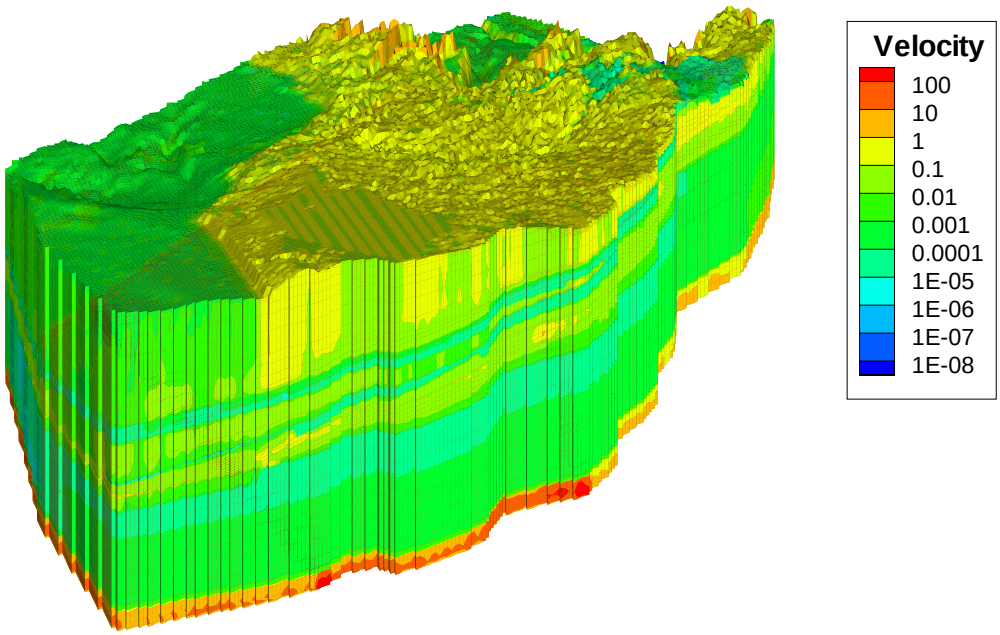

Figure 5.38: Velocity (m/a)distribution for Cobourg sensitivity analysis.

The Peclet numbers for the area surrounding the proposed location of the Bruce DGR (Figure 5.40) confirm that transport in the area should be diffusion dominant.

Figure 5.41 shows the mean life expectancy distribution for the Cobourg permeability sensitivity analysis. The mean life expectancy also demonstrates the segregation of the domain into upper and lower groundwater zones. The upper groundwater zone should exhibit much younger ages, whereas the deep groundwater zone, with very low gradients and with diffusion-dominant conditions should have much older ages.

At the horizon of the proposed Bruce DGR site (Figure 5.42), the groundwater is calculated to typically have ages in the range of 1×10^5 years and 1×10^6 years or greater.

The mean life expectancies for the sensitivity scenario involving the Cobourg permeability were used to determine the sensitivity coefficients. These coefficients can be used to quantify

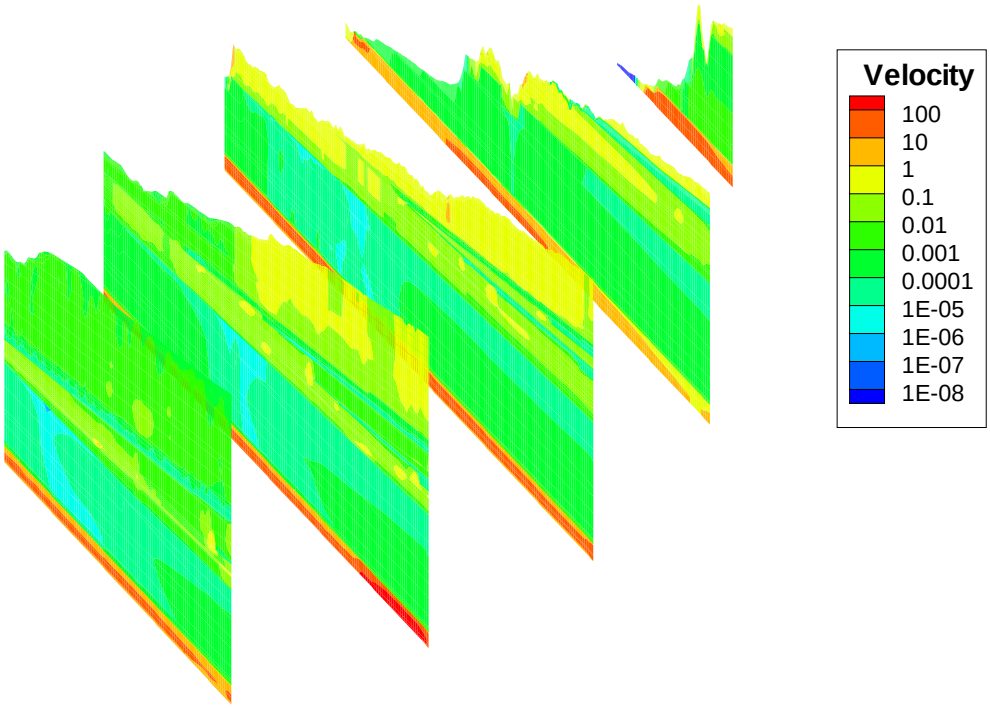

Figure 5.39: Fence diagram showing velocity (m/a)distribution for Cobourg sensitivity analysis.

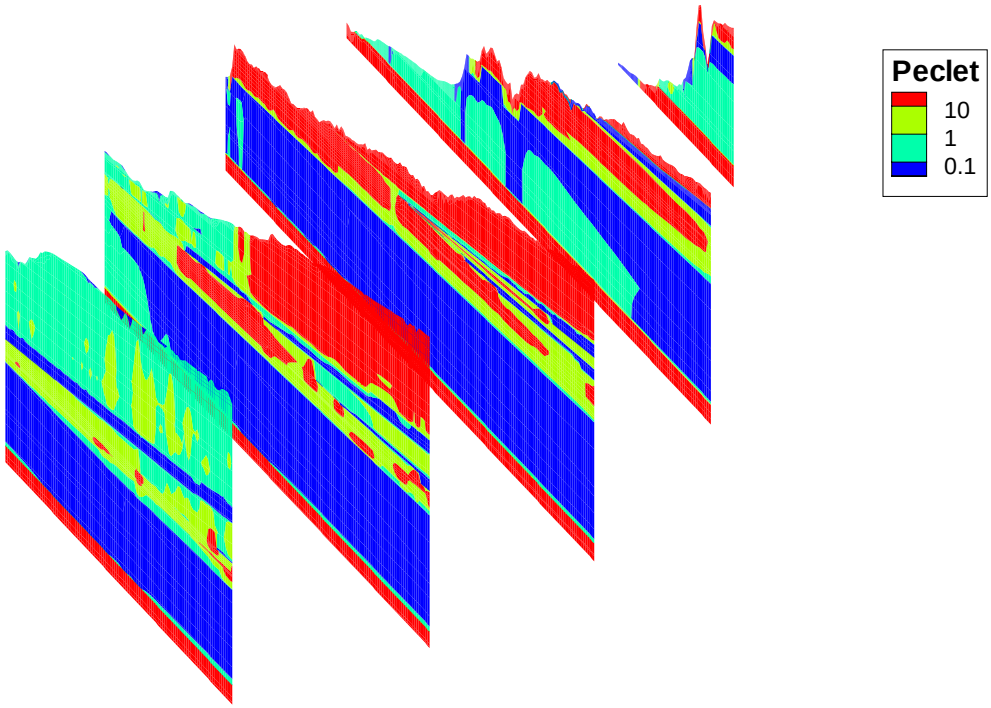

Figure 5.40: Fence diagram of Peclet numbers for Cobourg sensitivity analysis.

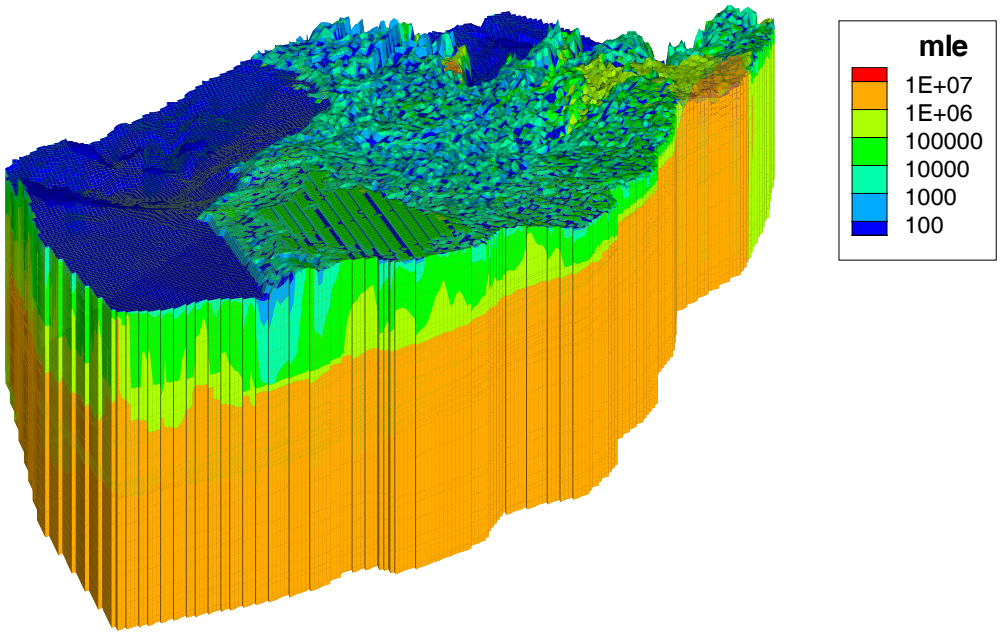

Figure 5.41: Mean life expectancies for Cobourg sensitivity analysis (years).

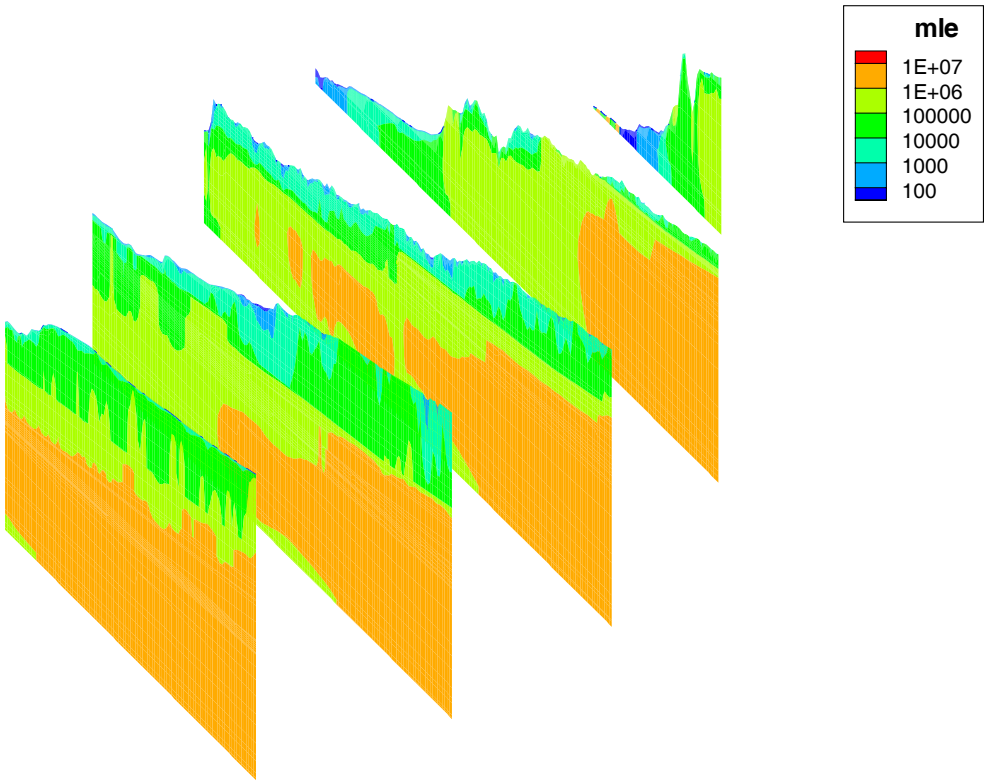

Figure 5.42: Fence diagram of mean life expectancies for Cobourg sensitivity analysis(years).

the sensitivity of the regional model to a change in the permeability of the Cobourg Formation. Figure 5.43 displays the sensitivity coefficients calculated in this analysis. The upper groundwater zone is estimated to be much more sensitive to a change in the permeability of the Cobourg Formation, whereas the deep groundwater zone will be more or less insensitive. This insensitivity may be attributed to the highly dense water at depth. Although the permeability of the Cobourg was doubled, this change produced little to no additional gradient to induce significant flow. The lack of a gradient in the deep groundwater zone is confirmed by the computed velocity distribution and the Peclet numbers.

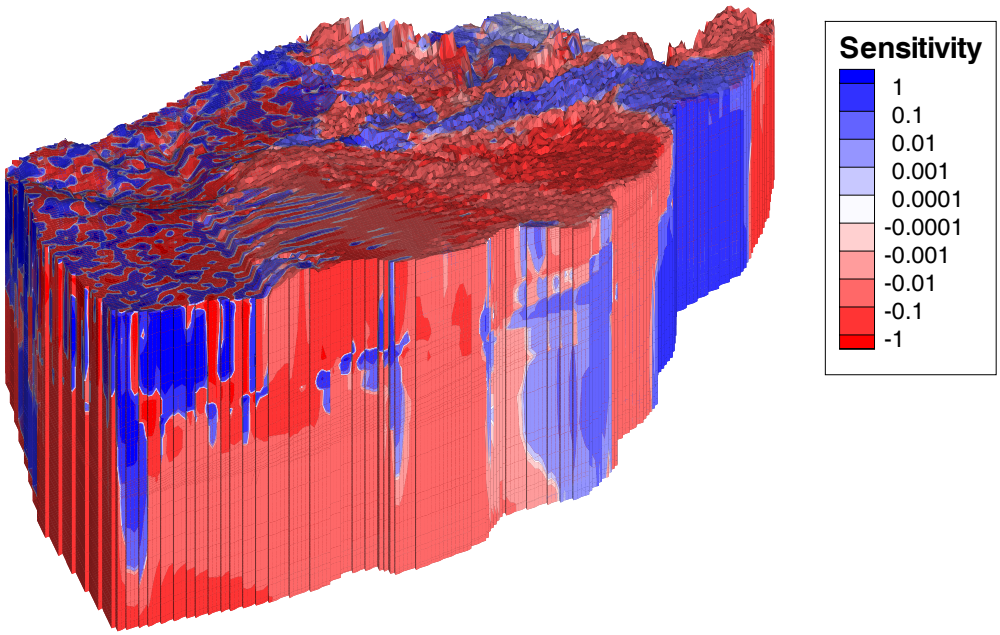

Figure 5.43: Sensitvity coefficients for Cobourg permeability.

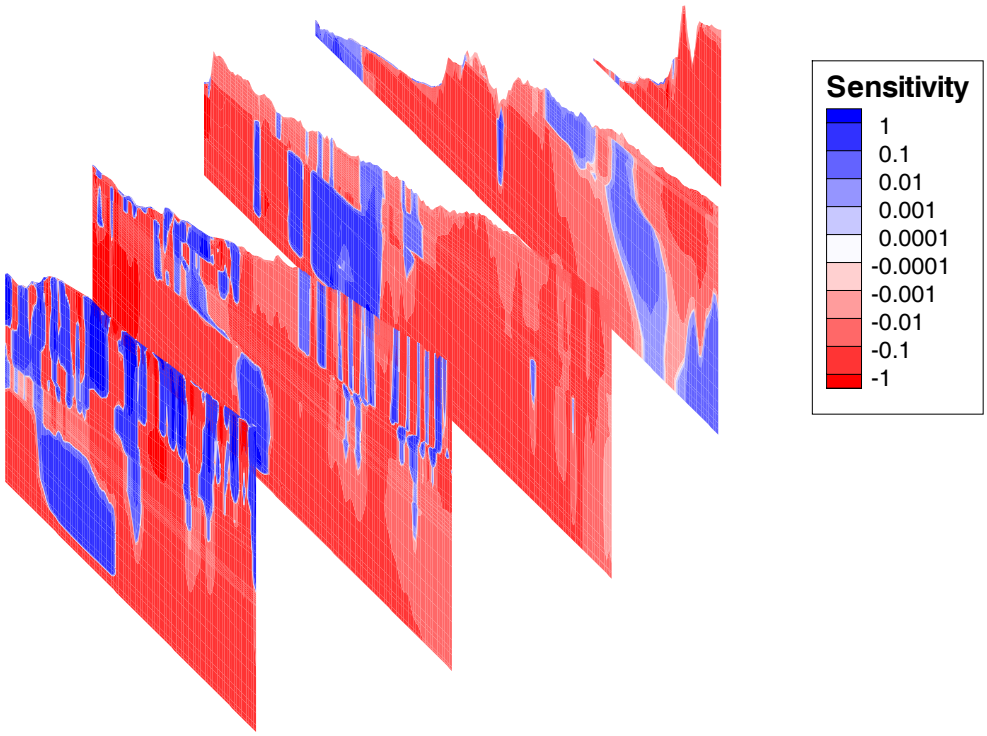

Figure 5.44: Fence diagram of sensitvity coefficients for Cobourg permeability.

5.2.5 Analysis of the Impact of Salinity

The total dissolved solids distribution in the Silurian and deeper units of the Michigan Basin play a significant role in reducing the energy gradients and related velocities within those units. The analyses presented earlier in this section have investigated the sensitivity of the model estimated MLE to perturbations in the permeability of selected units and have included the impact of fluid density in the simulations. An additional analysis was undertaken to determine the effect of the inclusion of fluid density on estimates of mean life expectancy. This analysis also focused on an assessment of the permeability of the Cobourg limestone and the impact that it has on estimates of mean life expectency in the absence of the influence of varying fluid density. A steady-state density-independent flow analysis was used for the simulations. The parameters and boundary conditions are the same as the base-case analysis. To estimate the sensitivity of the model estimated MLE, the permeability of the Cobourg Formation was increased by a factor of two from that use in the base-case analysis. The lack of fluid density in the deeper units had a large impact on the development of the flow system. This results in the higher sensitivity coefficients compared to that estimated for the analysis that included density. The inclusion of fluid density reduces the energy gradients and increases the estimated MLE compared to the case without density. Figure 5.45 depicts the sensitivity coefficients for this analysis. Because the density effect is not present to impede the migration of the groundwater, the groundwater is able to travel at a faster rate compared to simulations with density. The model MLE for the base-case density-independent scenario was 1.3×10^6 years, while the model MLE for the base-case density-dependent scenario was 1.59×10^6 years.

5.2.6 Summary of Sensitivity Analysis

Table 5.1 summarizes the mean life expectancies and the calculated sensitivity coefficients from the sensitivity analysis. The values shown are taken in the Cobourg Formation at the repository depth. It is important to note that for all of the simulations, the mean life expectancy of a water particle at the repository is at least one million years. The lowest calculated mean life expectancy, from the simulation without density, was still greater than 1 million years.

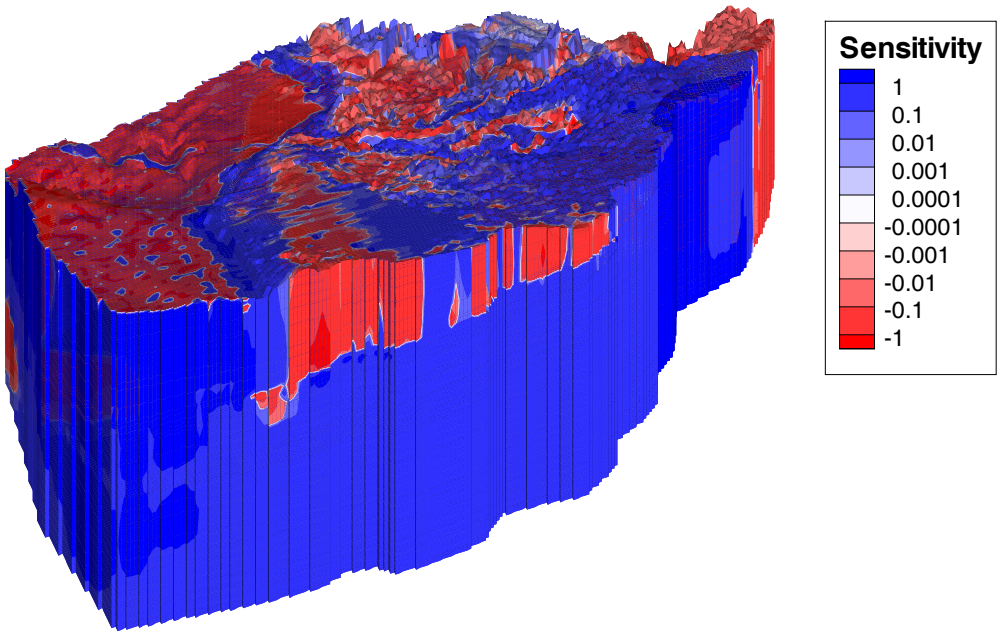

Figure 5.45: Sensitvity coefficients for non-density dependent Cobourg permeability.

Table 5.1: Calculated sensitivity coefficients

Scenario	Mean Life Expectancy (years)	Sensitivity Coefficient
Base-case	1.59×10^6	0.0
Queenston	1.93×10^6	0.290 53
Georgian Bay	1.59×10^6	−0.002 973 12
Collingwood	1.63×10^6	0.033 159
Cobourg	1.65×10^6	0.044 434 8
Base-case no density	1.3×10^6	0.0
Cobourg no density	1.18×10^6	−0.152 611

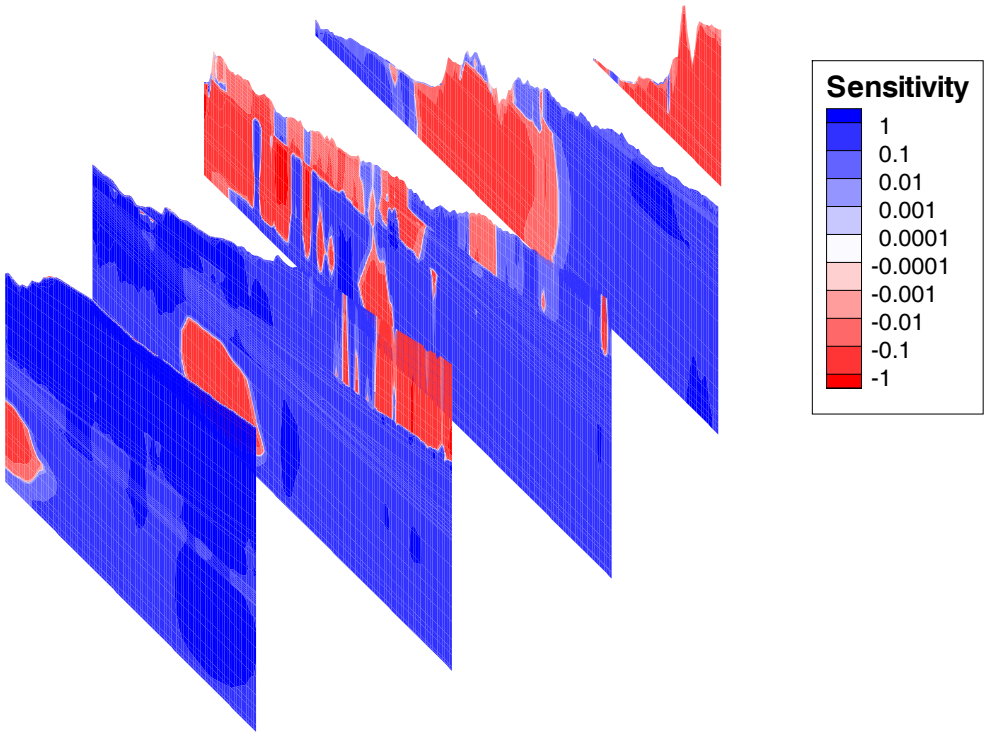

Figure 5.46: Fence diagram of sensitvity coefficients for non-density dependent Cobourg permeability.

Chapter 6

Conclusions

The geologic model for the regional-scale analysis of the Bruce Deep Geologic Repository consists of 37 layers, each correlating to a geological formation found at the Bruce site. The geology in the regional domain was modelled using geostatistical analysis methods to develop the correlation structure of the data and to facilitate the interpolation of the punctual data between boreholes. This geostatistical analysis facilitated the creation of a three-dimensional regional-scale geologic model. To ensure that the top of the model conformed to known surface elevations and lake bathymetries, additional data were added to the geologic model from DEMs and bathymetries of Lake Huron and Georgian Bay. The geologic model, with corrections for proper topography and bathymetry, was used as the basis for the regional scale numerical model. The regional scale domain can be divided into two majors zones: the upper groundwater zone and the deep groundwater zone. The upper groundwater zone includes the area above the Salina formations, in the Devonian formations. Groundwater flow in this zone is typically controlled by the topography at the surface. The upper groundwater zone will have much shorter Mean Lifetime Expectancies than the deeper groundwater zone. With low total dissolved solids, the higher groundwater velocities in the shallow zone are dependent on energy gradients that are relatively independent of fluid density. The upper groundwater zone will be dominated by advective flow, as indicated by the Peclet numbers for the zone.

Separating the upper and deep groundwater zones are the units of the Salina. The low-permeability anhydrite and salt beds, where present, isolate the topographically driven shallow flow system from that of the Ordovician shale and limestone formations. The deep groundwa-

ter zone comprises the areas beneath the Salina Formation, including the Ordovician limestones and shales, as well as the Cambrian and Precambrian formations. The deep groundwater zone is expected to have much lower velocities and much larger Mean Lifetime Expectancies (MLE). Since the deep groundwater zone is removed from any topographic effects by the very low hydraulic conductivities of the Salina Formation and the Ordovician shales, the energy gradients in this zone will be very low and are strongly dependent on the density gradients. The only locale within the domain for a gravitational gradient will be at the Niagara Escarpment, where some of the formations in the deep groundwater zone outcrop. The heads from this area, however, will be reduced because of the high salinity in the deep groundwater zone. The deep groundwater zone, because of the low velocities, will be a diffusionally-dominated system. The model estimated velocities in the Ordovician shale and limestone are negligible with Peclet numbers less than 0.01 for the units. The direction of the velocity is generally upward or downward; significant horizontal velocity components were not estimated for the formations in the vicinity of the DGR site. This result validates the selection of a regional-scale domain that is a subset of the Michigan Basin. The domain has topography that ranges from 176 m at Lake Huron and Georgian Bay to more than 500 m at the Niagara Escarpment. The boundary conditions and extent of the domain is sufficient to permit the development of horizontal flow components in the deeper Ordovician formations. However, the estimated velocities are more sensitive to the very low permeability of the units and the dampening impact of density on the energy gradients than they are to either the extent of the regional domain or the boundary conditions of the conceptual model.

The performance measure used in the analysis of the regional-scale is Mean Lifetime Expectancy (MLE). The independent variables for this probabilistic measure are the spatial distribution of the velocities and for the second-order term the dispersivity components. The velocities are density-dependent and hence a fully-coupled transient flow and brine transport analysis is required for their estimation. A pseudo-equilibrium solution was determined at 1 000 000 years after the imposition of an initial total dissolved solids distribution in the regional domain. The boundary conditions for the analysis were time invariant. For the base-case analysis, the MLE in the Cobourg formation in the vicinity of the proposed repository was more than 1 600 000 years. The sensitivity of the mean life expectancy to the assigned permeabilities for the Ordovician shale and limestone formations is related to the occurrence of divide points in the units that separate zones of upward flow from downward flow. The shift of the divide point could significantly

alter the flow path and the estimate of the time for migration of fluid to a domain boundary. The occurrence of the divide points is related to changes in the topography and the height and density of the fluid column above the point. The MLE is also sensitive to the fluid density gradient. A density-independent analysis that used the base-case parameters and the same boundary conditions as the density-dependent analyses yielded an estimated MLE at the horizon of the DGR of 1 300 000 years. The permeabilities used in the base-case analysis have been constrained by the use of measurement bounds. The pore structure of the deep Silurian and Ordovician formations, based on field and core observation is such that it is highly likely that the permeabilities used in this study have been overestimated. As a result, the estimated Mean Life Expectancies are likely lower bound estimates. A reduction of the dispersivities used in the estimation of the MLE will result in longer times for the deeper formations.

Bibliography

Bear, J. (1988), *Dynamics of Fluids in Porous Media*, Dover ed., Dover Publications Inc.

Cornaton, F., and P. Perrochet (2006), Groundwater age, life expectancy and transit time distributions in advective–dispersive systems: 1. Generalized reservoir theory, *Advances in Water Resources*, *29*(9), 1267–1291.

Ellis, G. D. (1969), Architecture of the Michigan Basin., in *Studies of the Precambrian of the Michigan Basin, Michigan Basin Geological Society Annual Field Excursion Guidebook*, pp. 60–80.

Golder Associates Ltd (2003), LLW geotechnical feasibility study, western waste management facility, Bruce Site, Tiverton, Ontario. report to Municipality of Kincardine and Ontario Power Generation, *Tech. rep.*, Golder Associates Ltd.

Intera Ltd. (1988), Inventory and assessment of hydrogeologic conditions of underground openings in sedimentary rocks. report to ontario hydro, *Tech. rep.*

Intera Ltd. (2006), Geoscientific site characterization plan, OPG's deep repository for low and intermediate level radioactive waste, *Tech. Rep. OPG 00216-PLAN-00120-00002-R00*, Ontario Power Generation.

Jensen, M. (2007), Personal communication.

Mazurek, M. (2004), Long-term used nuclear fuel waste management- geoscientific review of the sedimentary sequence in southern ontario, *Tech. rep.*, Institute of Geological Sciences, Univeristy of Bern, Switzerland.

Mazurek, P. F. J. V. G. B. H., M. (2003), Fepcat project: Features, events and processes evaluation catalogue for argillaceous media., *Tech. rep.*, OECD/NEA.

Novakowsi, K., and P. Lapcevic (1988), Regional hydrogeology of the silurian and ordovician sedimentary rocks underlying niagara falls, ontario canada, *Journal of Hydrogeology*, *104*, 211–236.

Peltier, W. R. (2002), A design basis glacier scenario, *Tech. Rep. 06819-REP-01200-10069-R00*, Ontario Power Generation, Nuclear Waste Management Division, Toronto, Canada.

Peltier, W. R. (2003), Long-term climate change – glaciation, *Tech. Rep. 06189-REP-01200-10113-R00*, Ontario Power Generation, Nuclear Waste Management Division, Toronto, Canada.

Raven, K., K. Novakowski, R. Yager, and R. Heystee (1992), Supernormal fluid pressuresin sedimentary rocks of southern ontario - western new york state., *Canadian Geotechnical Journal*, *29*, 80–93.

Sanford, B. V. (1961), Subsurface stratigraphy of Ordovician rocks in southwestern Ontario, *Geological Survey of Canada Paper*, *60*, 26.

Sanford, B. V., F. J. Thompson, and G. H. McFall (1985), Plate tectonics - a possible controlling mechanism in the development of hydrocarbon traps in southwestern Ontario, *Bulletin of Canadian Petroleum Geology*, *33*(1), 52–71.

Stonehouse, H. (1969), The precambrian around and under the michigan basin, in studies of the precambrian of the michigan basin, *Michigan Basin Geologic Society Annual Field Excursion Guidebook*, pp. 60–80.

Therrien, R., E. A. Sudicky, and R. G. McLaren (2004), *FRAC3DVS: An Efficient Simulator for Three-dimensional, Saturated-Unsaturated Groundwater Flow and Density-dependent, Chain-Decay Solute Transport in Porous, Discretely-Fractured Porous or Dual-porosity Formations. User's Guide*, Groundwater Simulations Group, University of Waterloo, Waterloo, Ontario, Canada.

Toth, J. (1963), A theoretical analysis of groundwater flow in small drainage basins., *Journal of Geophysical Research*, *68 no. 10*, 4795–4812.

Winder, C. G., and B. V. Sanford (1972), Stratigraphy and paleontology of Paleozioc rocks of southern Ontario, in *24th session International Geological Congress*.

Yates, S., and M. Yates (1989), *Geostatistics for waste management: A User's manual for the GEOPACK Geostatistical Software System.*, USDA Salinity Lab, Riverside, CA.